

**Sequence Stratigraphy and Stratigraphic Architecture of the
upper Mississippian lower Hinton Formation: Appalachian
Basin, West Virginia, USA**

Tyson Smith

A thesis submitted to the faculty of the University of North Carolina
at Chapel Hill in partial fulfillment of requirements for the degree of
Master's of Geological Sciences in the Department of Geological
Sciences

Chapel Hill
2009

Approved by:

Dr. Louis R. Bartek
Dr. Stephen R. Meyers
Dr. Kevin G. Stewart

© 2009
Tyson Smith
ALL RIGHTS RESERVED

ABSTRACT

Tyson Smith

Sequence stratigraphy and stratigraphic architecture of the upper Mississippian lower Hinton Formation: Appalachian Basin, West Virginia, USA

Cyclothems are a characteristic feature of Pennsylvanian Appalachian basin stratigraphy. These high frequency transgressive-regressive cycles have been attributed to glacioeustatic fluctuation, but comparatively little work has been done until recent with regards to identification of similar cycles in the upper Mississippian despite the presence of continental ice sheets during that time.

This study provides evidence for the presence of high frequency, transgressive-regressive cycles during the late Mississippian, similar to Pennsylvanian cyclothems. The eight transgressive-regressive episodes identified within the study interval occurred over a roughly 3 to 3.5 million year span in the late Mississippian. Assuming that these are cyclic in nature, they exhibit a fourth order periodicity of ~400 thousand years. The character of these cycles appears to be modulated by a third order lowstand and transgressive trend. This study documents how multiple controls on relative sea level, which operate on different timescales, influence sedimentation and subsequently shape the sedimentary record.

ACKNOWLEDGEMENTS

Many thanks to my advisor, Louis Bartek, and my committee members, Kevin Stewart and Stephen Meyers for all of their support and guidance throughout the entirety of this project. Brian Coffey and Brian Horn also provided invaluable technical support as they were always willing to offer their guidance. I would also like to thank the Scott Bennett, Audrey Loth, Kristen Larkins, Russ Mapes, and Karen Bossenbroek for their technical support during critical periods of this project.

I would like to thank the West Virginia Geological and Economic Survey for the data, assistance, and funding provided, without which, this project would not have been possible. Katherine Lee Avary and Mitch Blake were especially helpful. Also, Stephen Greb of the Kentucky Geological Survey, and Jack Beuthin of the University of Pittsburg-Johnstown were especially helpful during the formative stage of this project.

I would like to thank fiancé, Jessica Tinfo, for her unwavering support and for enduring the many nights that I spent away, laboring at this project. I would also like to thank my parents, Jeff and Dawn, and brother, Brett for all of their love and support in all of my endeavors, which has enabled me to be the person that I am today.

TABLE OF CONTENTS

LIST OF TABLES.....	viii
LIST OF FIGURES.....	ix
Chapter I. Sequence stratigraphy and stratigraphic architecture of the upper Mississippian lower Hinton Formation: Appalachian Basin, West Virginia, USA.	
Introduction.....	1
Background.....	2
Gross depositional environment and tectonic setting.....	2
Climate.....	2
Previous sequence stratigraphic interpretation and biostratigraphic constraints.....	3
Focus of study.....	4
Methods.....	5
Data.....	5
Well logs.....	5
Outcrops.....	5
Cuttings.....	6
Approach.....	6
Sequence boundaries.....	6
Flooding surfaces.....	8

Correlation and analyses.....	9
The lower Hinton Formation.....	9
Depositional systems.....	10
Coastal plain facies association.....	11
High energy facies association.....	12
Proximal marginal marine facies association.....	13
Distal marginal marine facies association.....	15
Marine facies association.....	16
Sedimentary architecture of outcrops.....	17
Cyclic packages.....	18
Paleosol.....	19
Discussion.....	19
Logistics.....	19
High frequency cycles (fourth order).....	20
Cyclothem comparison.....	22
Third order trend.....	23
Experimental study comparison.....	26
Second order trend.....	27
Interaction of cycles.....	28
Climate.....	28
Implications for long-term carbon cycling.....	29
Conclusions.....	30
References.....	54

Appendix A: Point data location table.....	59
Appendix B: Cuttings observation tables.....	61
B-1: McDowell Co., Permit #189.....	61
B-2: McDowell Co., Permit #216.....	67
B-3: Raleigh Co., Permit #15.....	73
B-4: Raleigh Co., Permit #305.....	81
B-5: Raleigh Co., Permit #489.....	88
B-6: Wyoming Co., Permit #714.....	92
Appendix C: Facies distribution map of cycle F.....	97
Appendix D: Paleoshoreline map of cycle F.....	98
Appendix E: Observed and interpreted cuttings lithologies (digital file: description).....	99
Appendix F: Measured sections (digital file).....	99
F-1: Outcrop A (description).....	99
F-2: Outcrop B (description).....	99
F-3: Outcrop C (description).....	99
F-4: Outcrop D (description).....	99
Appendix G: Cross-sections with data (digital file).....	100
G-1: Cross-section 11 (description).....	100
G-2: Cross-section 12 (description).....	100
G-3: Cross-section 21 (description).....	100
G-4: Cross-section 22 (description).....	100

LIST OF TABLES

Table 1: Lithologic description of cuttings.....32

Table 2: Paleosol criteria.....34

LIST OF FIGURES

Figure 1: Lithostratigraphy stratigraphy of study interval.....	35
Figure 2: Paleogeographic map.....	36
Figure 3: Sequence stratigraphy of study interval.....	37
Figure 4: Study area map.....	38
Figure 5: Cuttings: observed to interpreted lithology.....	39
Figure 6: Isopach of study interval	40
Figure 7: Cross-section 11.....	41
Figure 8: Cross-section 12.....	42
Figure 9: Cross-section 21.....	43
Figure 10: Cross-section 22.....	44
Figure 11: Depositional model.....	45
Figure 12: Facies association model.....	46
Figure 13: Examples of coastal plain facies association.....	47
Figure 14: Examples of high energy facies association.....	48
Figure 15: Examples of proximal marginal marine facies association.....	49
Figure 16: Examples of distal marginal marine facies association.....	50
Figure 17: Photograph of paleovertisol.....	51
Figure 18: Comparison of study interval with Wright and Marriott's model.....	52
Figure 19: Comparison of paleovalley architecture	53

INTRODUCTION

Cyclothems are a characteristic feature of Carboniferous coal bearing strata of North America. Glacioeustasy has been suggested by many researchers (Walness and Shepard, 1936, Busch and Rollins, 1984, Veevers and Powell, 1987, Chestnut, 1994, Aitken and Flint, 1995) as the forcing mechanism for these Pennsylvanian age, high frequency, transgressive-regressive cycles. However, despite the presence of massive continental ice sheets during late Chesterian time (Veevers and Powell, 1987, Rygel et al., 2008) comparatively little work has been done with regard to similar cycles potentially present during the upper Mississippian.

In recent years researchers have begun to document fourth order (200 to 500 ky) cyclicity in earlier Carboniferous strata of North America. Al-Tawil and Read (2003) identified high frequency, transgressive-regressive depositional sequences in early Chesterian carbonates of the Appalachian and Illinois basins. Maynard and others (2006) applied sequence stratigraphy to the scarcely documented Bluefield Formation in southern WV and western VA, and generated a depositional model that illustrates sequence stratigraphic hierarchy within strata. Miller and Eriksson (2000) investigated the Appalachian basin's Mauch Chunk Group, and identified multiple fourth order sequences packaged into third order composite sequences. Glacioeustasy has been suggested by all of these authors as the forcing mechanism of the high frequency cycles.

This study demonstrates the potential yield from combing wire-line logs, borehole cuttings, and limited outcrop exposure from an ancient basin with limited data by

constructing 4 regional cross sections through the lower Hinton interval in southern West Virginia. Correlation of sequence stratigraphic surfaces allows for the study interval to be sliced into time significant segments in an effort to increase our understanding of controlling mechanisms on stratigraphic architecture of the late Chesterian Appalachian basin. This study documents fluctuations in relative sea level at multiple scales (i.e. second, third, and fourth-order) within the stratigraphic architecture of the lower Hinton. Furthermore, this research provides evidence that long term cycles (i.e. second and third-order) modulate the character of high frequency cycles (third and fourth-order).

GEOLOGIC BACKGROUND

Gross depositional environment and tectonic setting

The Hinton Formation is part of the late Mississippian Mauch Chunk Group (Figure 1). In southern West Virginia, the Hinton is a lithologic record of coastal plain (in outcrop) to estuarine marginal marine (in the subsurface) environments that were intermittently inundated by marine sedimentation during the late Chesterian. The coastal plain on which these sediments were deposited existed along the northeastern shore of the Appalachian basin during the late Mississippian (Donaldson and Shumaker, 1981, Beuthin, 1994). This foreland basin formed as a consequence of isostatic loading by thrust sheets associated with multiple orogenic events (Hatcher, 1989). Tectonics created large-scale accommodation and consequently facilitated preservation of sediments representing a diverse suite of depositional environments during the Mississippian period.

Climate

Much like today, during the Carboniferous a landmass located in the southern polar region supported large continental ice sheets (Crowley and Baum, 1991, Frakes et al., 1992,

Rygel et al., 2008). Influence of growth and decay continental glaciers during late Chesterian time contributed to as much as 100 meters (Rygel et al., 2008) of rapid glacioeustatic fluctuations. Icehouse conditions that existed during the late Mississippian coupled with the relatively flat topography of the Appalachian basin at the time (Stewart, et al. 2002) created a situation in which high frequency changes of high magnitude in sea level were recorded over a vast area. Fluctuations in glacioeustasy driven by late Mississippian icehouse conditions, most likely exerted control on sedimentation in this system (Cecil, 1990; Crowley, 1991; Maynard and et al., 2006, Rygel et al., 2008).

Latitudinal migration of the North American plate positioned the Appalachian basin at a latitude of about 15 degrees south of the equator (Figure 2) (Scotese et. al, 1990). By the early Pennsylvanian the Appalachian basin existed under an ever wet climate regime as a result of its proximity to the equator (Cecil, 1990, Glonka et al., 1994). This geographic migration of tectonic plates is hypothesized to be the primary cause of climate change affecting the basin (Cecil, 1990).

Previous sequence stratigraphic interpretation and biostratigraphic constraints

The Mauch Chunk Group has been interpreted to represent a second order high-stand systems tract within the Mississippian supersequence, the top of which is marked by the Mississippian-Pennsylvanian unconformity (Al-Tawil and Read, 2003). Miller and Eriksson (2000) observed up to seventeen fourth order sequences within the Mauch Chunk Group, seven of which were assigned to the lower Hinton Formation. That study also interpreted the Hinton Formation as a third order composite sequence bounded by unconformable contacts at the base of the Stony Gap Sandstone and Princeton Sandstone. The Little Stone Gap Limestone member, located between the two unconformities, represents a maximum flooding

event. In outcrop, the Little Stony Gap is a marine limestone containing filter feeding organisms (Simonsen, 1981), and is juxtaposed above a thick succession of terrestrial red beds, suggesting a rapid transgression.

Biostratigraphic constraints place Hinton deposition in the lower portion of the lower Namurian (Jones, 1996, Miller and Eriksson, 2000, Maynard et al., 2006). The implication of this age correlation in the context of the most recent global stratigraphic scale (Menning et al., 2006) is that the span of time between the bounding unconformity at the base of the Stony Gap sandstone and the maximum flooding event corresponding to the Little Stone Gap limestone represents between 3 and 3.5 million years (Figure 3).

Focus of study

This study focuses on the application of high-resolution sequence stratigraphy to the lower portion of the Hinton Formation. Within the study interval, the lower Hinton transitions from the alluvial plain dominated facies along the outcrop belt into predominantly marginal marine facies in the subsurface. The presence of this suite of depositional environments provides a proxy for detecting fluctuations in allocyclic controlling mechanisms. Therefore, location and timing of the study interval place the lower Hinton Formation in a unique position to record the regional tectonics and climate of the late Chesterian Appalachian basin, while also providing a record of eustatic fluctuations. Moreover, this research tests the hypothesis that sedimentary architecture of the late Mississippian Appalachian basin strata records high frequency cyclic behavior.

METHODS

Data

Three different forms of data were analyzed and correlated in this project. By combining well logs, borehole cuttings, and outcrop measurements four cross-sections were constructed throughout the study area (Figure 4)

Well logs

Over 60 geophysical logs were correlated throughout the study area, and constitute the majority of the data used in this project. Natural gamma ray wire-line logs are the most abundant throughout the Appalachian Basin and were therefore the primary type of log correlated. Bulk density logs, especially within the study interval, are not nearly as common, but were also utilized where available. The logs were gathered from the West Virginia Geologic and Economic Survey's website and are available for public use for no cost. The logs were downloaded into the Kingdom Suite program where sequence stratigraphic surfaces were identified and correlated both within the study interval and below to the 'Little Lime' (Figure 1).

Outcrops

Outcrop measurements were taken where significant intervals of the lower Hinton are exposed, and offer the highest resolution data. The lithologic composition of the study interval coupled with the climate of West Virginia does not lend itself to large outcrop exposures, the most complete of which exist along road cuts. Four sections in total were

included in this project, three along I-64 north of the New River, and one along Rt-20 outside the town of Hinton, WV.

Cuttings

Six sections of borehole cuttings were analyzed within the study area. Cuttings are seldom utilized in subsurface correlation, but provide excellent real rock data to tie into geophysical logs (Coffey and Read, 2002). The cuttings were provided by the West Virginia Geologic and Economic Survey and analyzed with a binocular microscope. Borehole cuttings are typically collected and stored in ten foot increments so that each increment should represent an averaged ten feet of lithology. Lithologies were grouped (Table 1) and percentages noted to produce a lithologic column. The observed lithology is then matched against the geophysical log (where available) to produce an interpreted lithologic column (Figure 5).

Approach

Sequence stratigraphic analysis of sedimentary units requires the identification of chronostratigraphically significant surfaces that cut across time transgressive, lithologic boundaries. The two sequence stratigraphic surfaces used in this study, which allow a sedimentary unit to be sliced into parasequences and sequences, are flooding surfaces and sequences boundaries, respectively.

Sequence boundaries

Sequence boundaries are composed of an unconformity up dip and a correlative conformity down dip (Van Wagoner et al., 1990). In siliciclastic systems the down dip correlative conformity is commonly identified as a shallowing shift in facies. The up dip

unconformity typically manifests as an incised valley or as a mature paleosol developed on the interfluves. Zaitlin and others (1994) define incised valley systems as fluvial-eroded troughs that are typically larger than a single channel within the system. This study uses the quantitative definition of an incised valley defined by Strong and Paola (2008), which states that an incised valley is an elongate trough with a total depth greater than twice the depth of a typical fluvial channel within a given system. Typical fluvial channels observed in outcrop ranged between three to five meters.

A decrease in sediment load, an increase in discharge, or a drop in base level are the primary drivers of stream incision. During periods of incision, interfluvial sediments experience extensive levels of pedogenesis, resulting in well developed paleosols.

Deposition within the valley, during this time, is typically controlled by fluvial systems with high levels of sediment supply in comparison to lower rates of relative sea level rise. As a consequence, fluvial channels amalgamate, resulting in multi-story channel-sandstone architecture recorded in the strata. When relative sea level rise outpaces sediment supply the incised valley can be filled by lower energy, estuarine sediments. This commonly occurs during the later stages of valley fill. Experimental studies show that valley widening occurs even during rapid base level rise (Strong and Paola, 2006, 2008). The following are the criteria used in this study to identify sequence boundaries *in outcrop*:

- 1.) Sharp based sandstones exhibiting significant difference in character (i.e. grain-size, structure, color, etc.) from typical coastal plain fluvial, which are defined as hematite stained, argillaceous, fine to very fine grained sandstones to wackes. Incised valley fills are indicative of deposition under a higher energy environment, and are therefore coarser grained, quartz-rich arenites.

- 2.) Paleovalley fills are transgressive in nature, with fluvial facies at the base transitioning into deepening estuarine facies above (Howell and Flint 2003) and potentially capped by marine mudstone (Shanley and McCabe, 1993).
- 3.) Incised valleys are at least twice as deep as other fluvial channels within the system (Strong and Paola, 2008).
- 4.) Paleosols that represent soils developed on interfluves during long periods of incision are highly matured, and exhibit extremely well developed pedogenic structures (Wright, and Marriott, 1993).

-in well logs:

- 1.) Sharp based sand bodies that are at least twice as thick as other fluvial channels within the system (Strong and Paola, 2008).
- 2.) Sharp based sand bodies that exhibit limited lateral continuity and have mappable margins (Howell and Flint 2003).
- 3.) Correlative conformities were identified by down dip coarsening upward packages associated with up dip sharp-based sandstone bodies.

Flooding surfaces

Flooding surfaces are defined by Van Wagoner (1995) as ‘a surface separating younger from older strata across which there is evidence of an abrupt increase in water depth.’ This occurs when the rate of accommodation outpaces the rate of sediment supply. Identification of flooding surfaces in up dip areas can be difficult because the marine incursion does not necessarily directly affect depositional processes inland. Instead, depositional systems may react to the indirect effects of the flooding events. This could mean a change in fluvial style and floodplain architecture (Wright and Marriott, 1993).

Depending on the gradient and profile of the shore and coastal plain, fluvial systems may become less energetic as a response. In many cases a period of rise in base level will manifest in a rise of the water table yielding coastal lakes and mires (Davies et al, 2006).

The following are criteria used for identification of flooding surfaces *in outcrop*:

- 1.) Abrupt shift from normal floodplain facies (paleosols, channel sandstone, etc.) into organic rich shale or carbonate lacustrine facies.
- 2.) Presence of thin, marine mudstones (Shanley and McCabe, 1993) or limestones.
- 3.) Change in stratigraphic architecture manifesting in a higher ratio of floodplain to fluvial channel facies (Wright and Marriott, 1993).

-in well logs and cuttings

- 1.) Regionally correlatable abrupt gamma ray increase above coarsening upward packages.
- 2.) Regionally correlatable spikes or zones of higher gamma ray emission.
- 3.) Regionally correlatable deepening shifts in facies.

CORRELATION & ANALYSES

The lower Hinton Formation

Cross sections within the study area indicate that the lower portion of the Hinton Formation exhibits a wedge-shaped geometry that thins to the northwest. The thickness of the study interval ranges from 780 ft (240 m) in southern McDowell County to 330 ft (100 m) in northeastern Raleigh County, WV (Figure 6). The basal member of this study interval, the Stony Gap Sandstone, lies unconformably on top of the Bluefield Formation and defines the base of the Hinton Formation. The Little Stone Gap Limestone Member sharply overlies the heterogeneous red beds of the lower Hinton, the base of which defines the top of the study interval.

Four cross-section lines (11, 12, 21, and 22) were correlated by interpreting sequence stratigraphic surfaces and facies associations, and utilizing a database of over 60 well logs, six borehole cuttings, and four measured sections (Figure 4). Cross-section lines 11 (Figure 7) and 12 (Figure 8) are oriented perpendicular to Mauch Chunk isopach lines, and 21 (Figure 9) and 22 (Figure 10) are oriented parallel. All four cross-sections exhibit a long term progradation of depositional environments into the basin throughout the window of time covered by the study interval. This progradation was then followed by a rapid transgression, as indicated by the presence of the Little Stone Gap Limestone.

Depositional dip within the study interval appears to have two directional components. One component exhibits a depositional trend in the direction of stratigraphic thinning, SE to NW, presumably a product of the shedding of sediment by the orogenic belt to the east. The other runs roughly perpendicular to stratigraphic thinning and is oriented parallel to the axis of the basin. This axial trend is noted in previous works (Englund and Thomas, 1990), and is attributed to northern highlands created by earlier Appalachian collision events.

Depositional systems

The lower Hinton Formation is a predominately siliciclastic sedimentary succession interspersed with few carbonates. The Little Stone Gap Limestone represents the final major departure from this siliciclastic dominated Mauch Chunk system for the rest of the Mississippian. The three-dimensional depositional model developed for this project was generated by interpretation of lithologic associations, geographic distribution, and reference to the Bluefield Formation depositional model by Maynard and others (2006) (Figure 11). This depositional model can be broadly divided into five major zones; coastal plain, high

energy, proximal marginal marine, distal marginal marine, and marine (Figure 12). These five major zones were correlated in cross-section and described as facies associations. These zones, which are correlated in cross-section, are obviously interpretations, but for the purpose of organization, sedimentary attributes observed within that zone will be discussed in the format of their facies association.

Outcrops measured in this study expose predominately coastal plain facies, a significant proportion of high energy facies, and limited exposure of marginal marine and marine facies. The subsurface is primarily marginal marine facies, but contains significant proportions of others. The geographic relationship of predominant facies in outcrop versus those in the subsurface illustrates the spatial relationship of up dip and down dip environments within the study area.

Coastal plain facies association

Coastal plain facies association consists of a heterogeneous suite of lithologies, and constitutes a significant portion of the subsurface and is the predominate facies in outcrop (Figure 13). The most striking and pervasive characteristic of the coastal plain facies is the reddish brown coloring that a majority of lithologies exhibit. The red coloring is due to the presence of hematite and is found in both sandstones and mudstones. The gamma ray signature of coastal plain facies is ubiquitously irregular. The grain size of these strata is overwhelmingly mud, but ranges from clay to sand. The majority of rock composed of clay and silt sized terrigenous constituent parts exhibit blocky pedogenic fabric, reduced root haloes, caliche nodules, and pedogenic slickesides. Commonly the sandstones are either tabular in form or have a concave-up base and consist of very fine to fine grained argillaceous lithic sandstone or wacke. Cross-beds, ripple laminations, flute casts, and

inclined heterolithic beds are relatively common in these sandstones. In cuttings and well logs this type of sandstone is occasionally associated with a 'dirtying upward' trend in gamma ray emission. Several thin limestone units were identified in outcrop, typically associated with red/brown mudstones above and below. The carbonates exhibit a yellow to gray coloring and are micritic. This study did not recognize any fossils in these carbonate beds, but other research (Englund, 1979, Miller and Eriksson, 2000) identified sparse ostracod, pelecypod, and bivalve fossils hand sample and thin section.

Interpretation

These mudstones are interpreted as paleosols developed in an alternating wet and dry climate, and have been identified as paleoverisols in previous research (Beuthin, 1997, Miller and Eriksson, 2000). On the basis of sedimentary structures, coloring, and association of sandstones found in this facies association are interpreted to represent low energy fluvial channels and crevasse splays. The interpretation of limestones is that they represent deposition by lacustrine systems on the Hinton coastal plain that may have been occasionally influenced by brief periods of marine inundation.

High energy facies association

The primary purpose of distinguishing high energy facies from other facies is to identify deposits within incised valleys. Therefore, the facies association of the high energy system illustrated in figure 12 does not exemplify the majority of that facies interpreted in cross-section. Incised valley fills in cross-section are significantly larger in both thickness and lateral extent than the proximal deltaic high energy facies in figure 12.

In outcrop, the best example of the facies association designated as high energy is the Stony Gap Sandstone. The Stony Gap Sandstone can be traced for tens of kilometers and can

be as thick as 50 meters in certain locations and yet absent in others. Outcrop observations reveal medium to coarse grained quartz arenite with trough and planar cross-beds and locally containing mudstone rip-up clasts. The top of the Stony Gap exhibits ripple laminations and flaser bedding, which transition into wavy bedding and in some locations inclined heterolithic beds (the latter is considered proximal marginal marine facies association). In the subsurface, it exhibits a sharp based, low gamma ray and low bulk density signature. Other intervals interpreted as high energy facies have similar outcrop or subsurface characteristics to the Stony Gap Sandstone (Figure 14). However, a few sections within cuttings intervals that are designated as high energy facies are slightly different in grain size and exhibit fine to medium, quartz rich lithologies.

Interpretation

The Stony Gap Sandstone has been interpreted as marine bar deposits (Englund, 1979), but Miller and Eriksson (2000) cite the lack of marine fossils and association of facies as evidence to suggest braided river to estuarine deposition. This study concurs with the Miller and Eriksson (2000) interpretation citing the same criteria seen in both outcrop and cuttings data. The association, geometry, and lithology of the Stony Gap Sandstone suggests braided river to proximal estuarine deposition within paleovalleys. Sections exhibiting analogous characteristics to those attributed to the Stony Gap Sandstone are interpreted in a similar manner.

Proximal marginal marine facies association

More than half of the study interval within the subsurface is interpreted as marginal marine, a significant portion of which is designated as proximal marginal marine. This facies association commonly has very fine to fine grained, grayish white sandstones associated with

silty, gray mudstones (Figure 15). Borehole cuttings reveal tightly cemented, fine grained, quartz-rich sandstones. In cutting fragments greater than 1 mm, mudstone drapes and mudstone occasionally containing coaly debris and exhibiting parallel laminations have been observed. In measured section D proximal marginal marine facies are exposed at the top and base of the outcrop. Very fine to fine grained sandstones, exhibiting ripple laminations and scour and fill casts, and gray mudstones containing vertical burrows and parallel laminations are interbedded in outcrop. A 'cleaning upward' pattern in the gamma ray signature suggests a progradational characteristic the depositional system. The gamma ray signature can also be irregular, and without the aid of cuttings, would be extremely difficult to distinguish from coastal plain facies. This difficulty is a product of the two different facies associations consisting of similar materials (i.e. sands and muds).

Interpretation

Cleaning upward trends in gamma logs (i.e. decreasing trend in mud content) and coarsening upward trend noted in outcrop coupled with intercalated fine grained sands and gray mudstones suggest a deltaic/estuarine environment (Maguregui and Tyler, 1991). Grain size, mud content and sedimentary structures suggest a low energy shoreline, influenced by tidal and riverine processes (Darlymple et al., 1992). In many sections of cuttings red mudstones are overlain by thick successions of gray mudstones and calcareous shales, which suggest a flooding episode with no evidence of a high energy environment. This type of transition is interpreted to represent a transgressive episode along the coast in locations with minimal fluvial input. The rock record suggests that much of the interface between coastal plain and marine sedimentation during the deposition of the Hinton existed under a regime of minimal wave energy.

Distal marginal marine facies association

The distal marginal marine facies association accounts for a significant portion of interpreted facies in the subsurface and is most easily recognizable in cuttings (Figure 16). The two most common lithologies found within this facies association are gray mudstone and calcareous mudstone. In many cases, the lithologies are visually indistinguishable. They share similar grain size, color, and lack any suggestion of sedimentary structure. In these situations the only discernable characteristic between the two is a weak to moderate reaction to HCl. The calcareous mudstone occasionally contains fossils that are typically replaced by sparry calcite, and are commonly bivalves, ostracods, and crinoid stems. Two other lithologies associated with the distal marginal marine facies are very fine-grained quartz sand and skeletal limestone. These are much less common than the previously mentioned lithologies, and when occasionally found within the cuttings typically constitute no greater than 10% of a bin. The skeletal limestone is grain supported, comprised of fragmented shells (bivalves?), and exhibits a white coloring. The gamma ray signature of these facies can be irregular, but typically emits higher levels of gamma radiation due to high clay content.

Interpretation

The predominance of gray mudstones and calcareous mudstones within this facies indicates a lower energy environment that is sufficiently distal to terrigenous input allowing for carbonate-production (Maynard et al. 2006). The occasional presence of marine fauna indicates a connection to the enclosed continental seaway of the Appalachian basin. This facies association is interpreted to represent a shallow water mixed siliciclastic-carbonate depositional environment that experienced minimal wave energy. The quartz rich sand and skeletal limestone represent thin, discontinuous shoals that form under mild wave action, the

composition of which is determined by the materials that are readily available. Shoals that are created close enough to a terrigenous input, form through the process of winnowing away clays and silts, and leaving behind exceptionally well sorted lenses of fine to very fine grained sand. In areas that experience slight wave energy, but lack adequate terrestrial input, thin, discontinuous shoals of skeletal material are formed. The formation mechanism of these shoals could be either fair weather or storm wave processes (Vera and Molina, 2008).

Marine facies association

Very little of the study interval is interpreted as marine facies. The Little Stone Gap Limestone is an end member of the marine facies association, but serves as an excellent example. It is composed primarily of fossiliferous micritic limestone intercalated with thin beds of calcareous mudstone. The limestone is texturally classified as fossiliferous lime mudstone/wackestone with occasional packstone beds. The base of the Little Stone Gap Limestone is marked in outcrop by a sharp based argillaceous micrite, transitioning quickly into clean carbonate facies, and then grades into calcareous shales. The most abundant fossils are bryozoans, crinoids, bivalves, pelecypods, gastropods, brachiopods, and ostracods (Englund, 1979, Gordon and Henry, 1981, Miller and Eriksson, 2000).

Interpretation

The Little Stone Gap is interpreted to represent carbonate dominated, shallow shelf sedimentation in relatively quite water. Background sedimentation was dominated by lime muds with occasional terrigenous influence. The thin packstone beds represent brief departures from the low-energy background sedimentation to higher-energy, winnowing events (Dattilo, 2008). The interpretation of this depositional environment is a shallow shelf

occasionally affected by storms, and far enough away from clastic input to facilitate carbonate sedimentation, and support filter-feeding organisms (Simonsen, 1981).

Sedimentary architecture of outcrops

Measured sections along the outcrop belt primarily expose lower portions of the study interval, and offer the highest resolution data. The Stony Gap Sandstone is a quartz-rich arenite that contains meter scale cross-beds and was deposited by a high energy system (i.e. braided river) under a regime of relatively low accommodation. Sediments become finer grained and more clay-rich towards the top of the Stony Gap, and sedimentary structures are suggestive of tidally dominated estuarine sedimentation. A portion of this estuarine package is removed at outcrop A, and is replaced by a few meter thick fluvial channel sandstone (argillaceous lithic sandstone to lithic wacke). The rest of the measurable sections are largely dominated by fluvial/coastal plain sedimentation, and contain many well developed paleosols, crevasse splays, channel sandstones, and thin lacustrine carbonates. The exception to this is the sharp based quartz arenite found at both outcrops A and B, towards the top of the measured sections. This sandstone bears a striking resemblance to the Stony Gap Sandstone in both character and sedimentary structures, but is several meters thick as opposed to over 30. This sandstone transitions into a thin interval of greenish gray shale before returning to fluvial coastal plain sedimentation at both locations. Most of the study interval above this point is not well exposed until the Little Stony Gap Limestone Member.

Data provided by Miller and Eriksson (2000) also lacks measured sections from this interval. The lack of exposure suggests high clay content in the composition of strata. With consideration to the predictability of outcrop exposure within the study interval there are three separate architectural components: (1.) the lower most component consisting of the

ridge-forming, quartz-rich, fluvial to estuarine facies of the Stony Gap Sandstone, (2.) the middle; argillaceous sandstone/ fluvial channel and mudstone/floodplain dominated interval, and (3.) the uppermost component, which lacks much of any outcrop exposure, consisting of primarily clay-rich sediment, presumably flood plain deposits up to the base of the Little Stone Gap Limestone.

The architecture of the sedimentary fill of paleovalleys changes within the study interval as well, but has only been noted in well logs. Towards the base of the Hinton, valley fills consist almost entirely of sand (cycles A and C), which suggest deposition by a high energy system, whereas paleovalley fill later within the study interval contains much larger proportion of finer grained sediments (cycle H) suggesting deposition by much lower energy systems.

Cyclic packages

Including the unconformity at the base of the Stony Gap Sandstone, and the flooding surface at the base of the Little Stone Gap Limestone, eight regionally correlatable cycles were identified within the study interval. These cycles are defined at the top and bottom by flooding surfaces* and labeled A through H (Figure 3).

Only four of the eight cycles (A, C, E, and H) exhibited evidence of significant periods of incision (i.e. sequences boundaries). The methods section of this paper outlines the criteria used to identify sequences boundaries. The sequence boundary at the base of the Stony Gap Sandstone, as well as the sequence boundaries identified in cycle C, E, and H, is associated with extensive incision. Within the study area cycles B, D, F, and G reveal no indications of regionally significant incision, normal regressive phases within those

*Cycle A is defined at the base by the Stony Gap unconformity, and not a flooding surface.

cycles, or incision outside the study area.

Paleosols

In outcrop, paleosols are ubiquitous within the Hinton Formation. The character and development of paleosols within the study interval were noted and used as a proxy for late Chesterian climate. Criteria used in the study (Table 2) show no major change in paleosols. Pedogenic structures such as slickenlines, caliche, occasional mottling, and blocky ped structure existed, in varying levels of maturity, in most of the paleosols observed (Figure 17). The maturity of paleosols was rated on the basis of pedogenic development, which is outlined by Retallack (1988, 1997). The paleosols observed within the study interval are interpreted in this study, as well as others (Beuthin, 1997, Miller and Eriksson, 2000) to be the B horizon of vertisols. Thin layers of organic rich shale were noted above paleosols in some locations, indicating poorly developed O horizons. This interpretation is supported by the suite of pedogenic structures and features present in the strata. From several meters above the Stony Gap Sandstone, to meters below the Little Stone Gap Limestone, the character of these vertisols was consistent with varying levels of maturity.

DISCUSSION

Logistics

The Hinton Formation is not exposed well in the outcrop, and though gamma ray and bulk density logs provide a good proxy of lithology, an inherent lack of high quality suites of wire-line logs, and a scarcity of data within the study interval present significant challenges to high-resolution interpretation. For these reasons, the Hinton Formation originally lumped together as a lithologic group of variegated shales, sandstones, and limestones (Campbell and

Mendenhall, 1896, Wilpolt and Marden, 1959, Englund, 1979), has received little in depth analyses until recent (Beuthin, 1997, 2002, Miller and Eriksson, 2000). Borehole cuttings proved to be an invaluable resource for this study in that they allow real rock data to be tied into geophysical logs where cores are not available. Other research (Coffey and Read, 2002, Wynn and Read, 2006) have demonstrated the value of well cuttings in reconstructing high resolution vertical facies successions in carbonate dominated stratigraphy, but this project applies a similar approach for the first time in a siliciclastic dominated rocks within the Appalachian basin. This study demonstrates that analyses of limited outcrop exposure, gamma ray and bulk density wire-line logs, and borehole cuttings can be applied in tandem to generate a high resolution, sequence stratigraphic framework and depositional model within logistically difficult intervals.

High frequency cycles (fourth order)

Miller and Eriksson identified seven sequence bounded cycles within the lower Hinton. This study identified eight regional cycles, but only four of them were found to exhibit significant levels of incision during their regressive phases. The eight regionally correlatable cycles that were identified, occurred over a time period of between 3 and 3.5 my (Figure 3). Assuming that the packages are cyclic in nature, the transgressive-regressive episodes exhibit a $\sim 400 \pm 30$ ky periodicity, which indicates fourth order control on stratigraphy. This suggests that high frequency cycles are in fact preserved within the Appalachian basin during the late Mississippian. The correlation of these cycles across an area of over 350 km² suggests that they are allogenic in origin, as opposed to autogenic.

Potential causes of these allogenic cycles are tectonics, climate, or eustasy. The possibility of tectonics as the forcing mechanism for these cycles is not likely. Based upon

the short time scale at which these fluctuations occur, basin scale subsidence and other tectonically driven factors do not offer a satisfying explanation (Paola et al., 1992, Blum and Tornqvist, 2000).

A seasonally wet-dry climate provides the optimal conditions for clastic sediment production (Cecil, 1990). Climate during the late Chesterian in the Appalachian basin is interpreted to be semi-arid/seasonally wet (Beuthin, 1997, Kahman and Driese, 2008), which suggests close to maximum clastic sediment yield. Climate could potentially cause cyclic changes in deposition by controlling sediment supply. This outcome would be reached if the climate either became wetter or dryer. If so, evidence of drastic climate changes should exist. Sediment would decrease if a.) climate became very dry, limiting erosion via a lack of precipitation, or b.) climate became very wet, limiting erosion through increased ground cover by vegetation. The consistent presence of pedogenic structures such as slicken lines, reduced root haloes, and blocky ped structures indicate a relatively steady climate of semi-arid/seasonally wet conditions (Retallack, 1997) throughout the study interval. The character of paleosols throughout the study interval remains constant, which suggests a relatively steady climate regime.

Eustasy may have been the dominant control of high frequency cyclicity observed within the lower Hinton Formation. Glacioeustasy is characterized by high frequency, high magnitude fluctuations which can operate on a fourth order time scale. Documented fourth order cyclicity within the Greenbrier Group of the Mississippian (Al-Tawil et al., 2003) and in the Breathitt Group of the Pennsylvanian (Aitken and Flint, 1995) has been attributed to glacioeustatic mechanisms. Miller and Eriksson (2000) suggested a similar forcing mechanism for the fourth order sequences that they observed within the Mauch Chunk

Group. Moreover, many supporting lines of evidence support the existence of continental ice sheets on polar regions of Gondwana during the late Mississippian (Crowley et al., 1991, Rygel, 2008).

Cyclothem comparison

Sedimentary rhythms, known as cyclothem, have been noted in the Carboniferous coal-bearing strata of North America for close to a century (Emery and Myers, 2006). These high frequency, transgressive-regressive cycles of the Pennsylvanian have been observed in the fluvial to marginal marine deposits of the Kentucky (Aitken and Flint, 1995). As previously mentioned, the fourth order cyclicity and a glacioeustatic forcing mechanism has been noted in the Mauch Chunk Group and compared to the cyclicity of the Pennsylvanian cyclothem (Miller and Eriksson, 2000).

High amplitude, glacioeustatic fluctuations during the Pennsylvanian (Goldhammer et al., 1991, Rygel, 2008) caused drastic changes in facies within cyclothem intervals.

Cyclothem of the Pennsylvanian Appalachian basin typically contain a thick succession of quartz-rich fluvial to deltaic sandstone, capped by a regionally extensive coal, and overlain by dark organic-rich shale of shallow marine origin.

The character and magnitude of the paleovalley fills in the lower portion of the study interval are quartz-rich and similar to the fluvial/deltaic facies of the Pennsylvanian.

Moreover, the juxtaposition of the Little Stone Gap Limestone above continental red beds in much of the basin suggests, high amplitude fluctuation in sea level. Though cycles within the lower Hinton are more difficult to recognize, the estimated periodicity of cycles identified in this study is similar to that of Pennsylvanian cyclothem. The lack of more ordered cyclicity, like that noted in cyclothem, could be a result of a difference in the amount and

character of sediment supplied to the basin during the late Mississippian versus the Pennsylvanian (which is primarily a function of climate and tectonics). Another possibility is that glacioeustasy had not yet gained the momentum that was present during the Pennsylvanian, and therefore the eustatic signal was dampened by other competing influences (autogenic phenomenon, tectonics, etc.).

Third order trend

As documented by Miller and Eriksson (2000), the unconformity at the base of the Stony Gap Sandstone and the flooding event associated with the deposition of the Little Stone Gap Limestone represent a sequence boundary and maximum flooding surface of a third order (2 to 4 my) composite sequence. According to Miller and Eriksson (2000) this trend exhibits an internal stacking pattern comprised of seven fourth order component sequences that lay the framework for retrogradational, aggradational, and progradational sequence sets. They suggest a glacioeustatic or global tectonic eustatic forcing mechanism, citing the coincidence with the sea level curve from Swann (1964) and onlap curve by Ross and Ross (1988).

A trend of increasing accommodation is noted throughout the study interval. As a result of documenting the alluvial architecture in outcrop, the nature of the regressive phases of high frequency cycles and the nature of sequence boundaries and the subsequent fill of their paleovalleys, a trend of an increasing rate of accommodation throughout the study interval is noted. This third order trend is best illustrated by comparison with the Wright and Marriott (1993) fluvial model. The alluvial architecture of the study interval exhibits similar characteristics to those outlined in the model (Wright and Marriott, 1993) with regard to

architectural and pedogenic development within a fluvial environment during a third order sequence (Figure 18).

In general, stratigraphic architecture of the study interval is dominated by finer grained sediments and low energy fluvial systems. As noted in the correlation and analyses section, the Hinton exposed in outcrop may be divided into three separate components. Each of these components corresponds with characteristics of third order systems tracks explained in Wright and Marriott's (1993) model.

Lowstand Systems Tract (LST)-High energy facies with abundant coarse grained, quartz-rich sediments.

Early Transgressive Systems Tract (ETST)- Well developed soils, relatively abundant channel sandstones, and higher frequency cycles have a greater chance of initiating incision.

Late Transgressive Systems Tract (LTST)- Floodplain dominated (composition is primarily fine grained supported by the complete lack of exposure at the surface); higher frequency cycles have a lower probability of initiating sequence boundaries during the regressive phase.

There is a notable pattern in the regressive components of each of the higher frequency cycles. The internal structure of higher frequency cycles suggests that this third order trend is, partially modulating the character of the fourth order signal.

This is supported by the pattern of change in the regressive phases of cycles throughout the interval. Ergo, the trend of decreasing magnitude of incision, and the shift from incised sequence boundaries to normal regressions (or sequence boundaries characterized by minimal incision) going from the base of the Stony Gap to cycle G.

The exception to the observed trend would be the interpreted sequence boundary below the Little Stone Gap Limestone (cycle H). Outcrops, as well as much of the

subsurface observations indicate that vast areas experienced paleosol development immediately before the deposition of the Little Stone Gap Limestone. The level of pedogenesis indicates a prolonged period of exposure, suggesting the presence of a sequence boundary. The incision fill associated with this sequence boundary and subsequent lowstand and transgression contains a heterogeneous suite of sediments (i.e. high energy, proximal marginal marine, and distal marginal marine facies associations). This is in stark contrast to the high energy facies of the Stony Gap Sandstone paleovalley fill. The sedimentary fill of the paleovalleys within cycle H are more difficult to identify in many locations due to the greater amount of fine grained sediments present (figure 19). In updip locations paleovalley fills most likely preserve poorly developed paleosols as well as fluvial sandstones, which would also indicate greater levels of accommodation during episodes of valley filling.

The maximum flooding surface in the Wright and Marriott model is marked by the presence of a hydromorphic soil. In contrast, many outcrop locations show the maximum flooding event of the Little Stony Gap Limestone is denoted by the juxtaposition of marine limestone directly above terrigenous red mudstones. This is a significant difference in magnitude of flooding events when comparing the Wright and Marriott (1993) model and the sedimentary record present in the lower Hinton. Departure from this model, accompanied by the unique nature of paleovalley fill beneath the Little Stone Gap, suggests an anomalous, high magnitude marine incursion. This anomalous event could either be the result of a single, rapid, high magnitude forcing mechanism, or the coincidence, and hence coupling of two or more drivers of relative sea level rise, resulting in a single marine marker bed.

The architecture of the paleovalley in cycle H and the anomalous juxtaposition of facies above and below the Little Stony Gap flooding event indicate a rapid rate of relative

sea level rise or a drastic decrease in sediment supply. A drastic decrease in sediment supply would most likely be caused by a sudden change in climate. Due to the relatively consistent nature of paleosols, that is not a very likely scenario. The coincidence of the Menard Limestone of the Illinois Basin tied into the Ross and Ross (1987) eustatic curve (Miller and Eriksson, 2000) (Figure 3), and the Little Stone Gap Limestone of the Appalachian basin suggest a global sea-level event. The presence of continental glaciers during the late Chesterian provides a glacioeustatic mechanism for high frequency, high magnitude fluctuations in global sea level. Rygel and others (2008) have shown that up to 100 meter glacioeustatic fluctuations occurred during late Chesterian time. The magnitude of these changes can account for the observed depth of incision and subsequent flooding, which led to the deposition of the Little Stone Gap Limestone. Cross-section line 22 (Figure 10) displays the thickest portion of the Stony Gap Sandstone within the study area, and therefore the location of the greatest incision. At this location the Stony Gap sandstone cuts deepest into the underlying stratigraphy at 50 meters, yielding a minimum fall in base level of 50 meters. Many of the other cycles exhibit base level fluctuation on the order of 10's of meters.

Experimental study comparison

The presence of multiple incision events and an increase in quantity of well developed soils around regressive phases of cycles observed in outcrop support model observations by Strong and Paola (2006, 2008), which state that stochastic fluvial down-cutting is coupled with allocyclic driven incision during periods of base level fall. This is also in keeping with the alluvial architectural model of Wright and Marriott (1993), as explained in the third order trend portion of this paper. Observations of this phenomenon include the presence of amalgamated channels and multiple horizons of well developed

paleosols in interpreted regressive zones of cycles. This indicates that as base level fell there was not a single episode of incision, but rather a period in time in which allocyclically induced low accommodation facilitated multiple autocyclically driven incisions.

Second order trend

The siliciclastic dominated Mauch Chunk Group marks a departure from the carbonate ramp system of the Greenbrier Group. Al-Tawil and Read (2003) and Maynard and others (2006) have suggest that this long term change in depositional modes represents the transgression and highstand systems tracts within a second order Mississippian super sequence.

The overall progradation of depositional environments into the basin noted in this study support the placement of the lower Hinton Formation in this long term, early highstand trend. This cycle has been noted in both the Appalachian and Illinois basins (Al-Tawil et al., 2003), and suggests that early onset of Gondwanan glaciation could potentially serve as the forcing mechanism.

Al-Tawil and Read (2003) suggest long term glacioeustasy as the driving mechanism of this second order trend. Another major contributing factor is the early onset of the Alleghanian Orogeny. Paleoseismite occurrence (Stewart, et al., 2002) and ages of metamorphism in the Appalachians associated with Alleghanian onset (Goldberg and Dallmeyer, 1997, Worthman, et al., 1998) support the coincidence of early Alleghanian collision and the timing of Hinton deposition. As uplift to the east associated with early Alleghanian collision occurred, a steadily increasing supply of terrigenous sediment was delivered to the basin from the newly rejuvenated and growing Appalachians to the east. This increase in siliciclastics eventually shut down carbonate systems and provided a

mechanism for progradation of depositional environments into the basin. Ultimately, this collision resulted in the regional unconformity at the base of Appalachian basin Pennsylvanian strata.

Interaction of cycles

This study illustrates the nature of interaction between independently operating scales of control on the sedimentary architecture and cycle development of the lower Hinton Formation. The second order trend noted within this study interval appears to control the general spatial geometries and character (i.e. carbonate versus siliciclastic) of depositional environments. Superimposed over that trend is the third order scale of operations, which appears to modulate the character and magnitude of higher frequency cycles (fourth order). As previously explained, the modulation of fourth order cycles by the third order trend within the lower Hinton Formation is architecturally similar to Wright and Marriott's (1993) sequence stratigraphic fluvial model. The broader implication is that in foreland basins, which have similar boundary conditions (i.e. continental glaciation, local climate, and orogenic influence); higher frequency cyclicity is modulated by longer term trends. Furthermore, architecture of sedimentary successions can be subdivided into architectural units based upon comparison of lithologic components within the time constraints of sequence stratigraphy, to aid in the identification of patterns in accommodation.

Climate

This study utilized paleosol characteristics as a proxy for climate change during the deposition of the lower Hinton. Paleosols throughout the entire interval shared similar soil features which all suggest pedogenesis under extended periods of aridity, punctuated by

shorter periods of rain. This is supported by paleosol observations of the upper Hinton Formation (Beuthin, 1997). The absence of significant climate change within the study interval suggests that the 'dry to wet' transition within the Appalachian basin of the Mississippian to the Pennsylvanian occurred later in the Mississippian. This also supports the theory the primary cause of climate change during this time was due to longer term tectonic migration of the Appalachian basin into equatorial regions (Cecil, 1990).

Implications for long-term carbon cycling

Architectural unit three discussed earlier in the discussion corresponds with the late transgressive systems tract of Wright and Marriott's model, outcrop exposure of which is very limited to nonexistent. The reasoning given in this paper for the lack of exposure is the mudstone rich lithology, which constitute poorly developed paleosols. The higher percentage of muds comprising the flood plain during that time of deposition is not due to an increase in clays and silts transported within the system. Most likely, there are similar quantities of mud being transported by the fluvial systems on the coastal plain, but the floodplain captures a greater percentage due to the higher levels of accommodation.

Storage of particulate and dissolved organic matter in floodplains represents a significant sink in terms of biogeochemical cycling on all time scales (Metivier and Gaudemer, 1999, Malmon et al. 2002). Alluvial plains serve as a first-order catchment for material transported from the hinterland into the basin. Residence time of materials in floodplains is a function of the complex interactions of fluvial system dynamics (McKee, 2003). There are two factors that created the situation in which the Hinton coastal plain was preserved; foreland basin subsidence and eustatic accommodation created by late stage third order transgression. The latter condition alone facilitated residence times of millions of

years. This is potentially significant for carbon cycling if the forcing mechanism that increases floodplain accommodation is in fact global. This would result in floodplains on a global scale experiencing increased rates of carbon sequestration.

During the Pennsylvanian the earth was cooler (Ross and Ross, 1988) and the Appalachian basin existed under equatorial regime (Scotese, 1990) of an ever-wet climate (Cecil, 1990). The ubiquitous coal measures within the Pennsylvanian stratigraphy exemplify the optimal climatic conditions, tectonic regime, and eustatic cyclicity that facilitate sequestration of organic carbon in large quantities.

As stated earlier in this paper, during the time of Hinton deposition, the Appalachian basin existed under a semi-arid/seasonally wet climate, and most likely did not support extensively vegetated regions. This is also evidenced by thin, poorly developed O horizons occasionally observed in outcrop. Therefore, despite the high levels of floodplain preservation, comparatively little organic rich material was preserved. If the Appalachian basin climate was different during that time, potentially significant quantities of organic material would be preserved. Therefore, when the appropriate conditions exist, alluvial plains in coastal regions serve major carbon sinks. This factor potentially plays a significant role in paleoclimate modeling of long-term carbon cycling.

CONCLUSIONS

1.) In ancient sedimentary basins that offer limited outcrop exposure and lack high-quality suites of wire-line logs, borehole cuttings can be applied in combination with these limited data to generate a depositional model and high resolution, sequence stratigraphic framework.

2.) The lower Hinton Formation of southern WV preserves a record of high frequency, high magnitude transgressive regressive cycles. There is evidence for up to 50 meters of base level fall. These cycles are comparable to cyclothems of the Pennsylvanian. There are eight transgressive-regressive, fourth order cycles identified in the lower Hinton interval of this study.

3.) The lower Hinton Formation also records the lowstand and transgressive system tracts of a third order cycle. This third order trend appears to modulate the character of higher frequency cycles and is comparable to the third order alluvial architectural model generated by Wright and Marriott (1993).

4.) Though the lower Hinton Formation is only a small portion of the Mississippian super sequence outlined by Al-Tawil and Read (2003), the second order highstand trend appears to be preserved. This is evidenced by the progradation of the coastal plain into the basin, and shows that lower frequency trends control the general location of depositional environments.

5.) Paleosols maintain a relatively consistent character throughout the study interval. They also serve as excellent paleoclimate indicators, and therefore consistency in character suggests that climate through out the period of time represented by the lower Hinton Formation existed under a steady regime of semi-arid/seasonally wet conditions.

6.) During late stage, third order transgressions flood plains experience increased rates of accommodation. In basins with appropriate climatic conditions, large amounts of organic carbon are removed via burial. In contrast to this study interval, Pennsylvanian stratigraphy exemplifies these optimal conditions. This has implications in paleoclimate modeling of long-term carbon cycling.

Table 1.

Cuttings data: Observed lithologies

Key for frequency of occurrence:

- ub-ubiquitous
- c-common
- uc-uncommon
- r-rare
- vr-very rare

Number	Name	Comp.	Color	Fossils	Grain size	Structures	Sorting	Rxn w/ HCl	Notes
1	Red mudstone	quartz clay lithics	pale red to mod. brown	OC fragments r	vf-sand to clay	slicks c mottling c root haloes u	poor	none to moderate	mica present c
2	Lithic/Qtz sandstone	quartz lithics clay	dull red to mod. brown	none	m-sand to clay sand; sub-ang to sub-round	none	moderate to poor	none	hemtite staining
3	Gray/white sandstone	quartz lithics clay	light gray to white	OC fragments r	f- to vf-sand sand; round	parallel lam u	moderate	none	clay drapes c
4	White sandstone	quartz lithics	white	OC fragments r	med- to f-sand sand; sv round to round	none	moderate to well	none c or CaCO3 cemented r	gravel size grains vr
5	Gray mudstone	clay quartz	light gray to dark gray	OC fragments c	silt to clay	parallel lam r	poor	none	pyrite c , black spherical concretions (~1mm) r
6	Calcareous mudstone	clay quartz calcite	light gray to dark gray	sparry calcite replaced shell fragments and crinoid stems r	silt to clay	none	poor	weak to moderate	difficult to discern from gray mudstone in some cases
7	Brown quartz sandstone	quartz lithics	white to brown	none	med- to f-sand sand; sub ang to sub round	none	moderate	none	brown coloring appears to be staining on quartz grains (hemtite?)

Table 1 (cont.).

	8 White skeletal limestone	calcite quartz (?)	white	sparry calcite replaced shell fragments ub	silt to sand	none	moderate	vigorous	occurrence of white skeletal limestone was not very common
	9 Calcic lithic sandstone	lithics quartz clay calcite	dull white	none	med-sand to clay sand; sub ang to sub round	none	poor	vigorous	poorly indurated
	10 Glauconitic sandstone	quartz glauconite	light greenish gray to white	none	med- to f-sand sand; sub round to round	none	moderate to well	none	
	11 Yellow siltstone	quartz clay	orangish yellow	none	clay to vf-sand sand; round	none	poor	none	yellow coloring appears to be limonite, highly friable
	12 Purple calcareous siltstone	quartz calcite	pale pink to pale purple	sparry calcite replaced shell fragments ub	silt to clay	none	poor to moderate	vigorous	produces bright yellow residue during rxn with HCl
	13 Quartz sand	quartz	white	none	vf-sand	n/a	very well	none	non-indurated, very mature sand.
	14 Micrite	calcite	medium to dark gray	none to sparry calcite replaced shell fragments ub	clay	none	poor (?)	vigorous	
	15 Bituminous coal	organic carbon	black	entirely OC		none		none	occurrence of coal in cuttings samples was extremely rare

Table 2.

Climate	Color	Texture	Structures	Peds	OM present	Chemical precipitation	Type
wet/dry (seasonal)	pale brown to palered	silt/clay	slickensides root haloes none to mod. mottling	platy (weakly dev.) angular blocky (well dev.)	little to none	calcareous rhizoconcretions caliche nodules calcrete	vertisol
wet	mod. red to grayish yellow	silt/clay	no slickensides heavily rooted heavily mottled	platy (weakly dev.) granular or crumb (well dev.)	*coaly O horizon if not eroded *abundant (utisol) *none (deeper oxisol horizons)	non calcareous ferruginous deposits siderite nodules	oxisol utisol

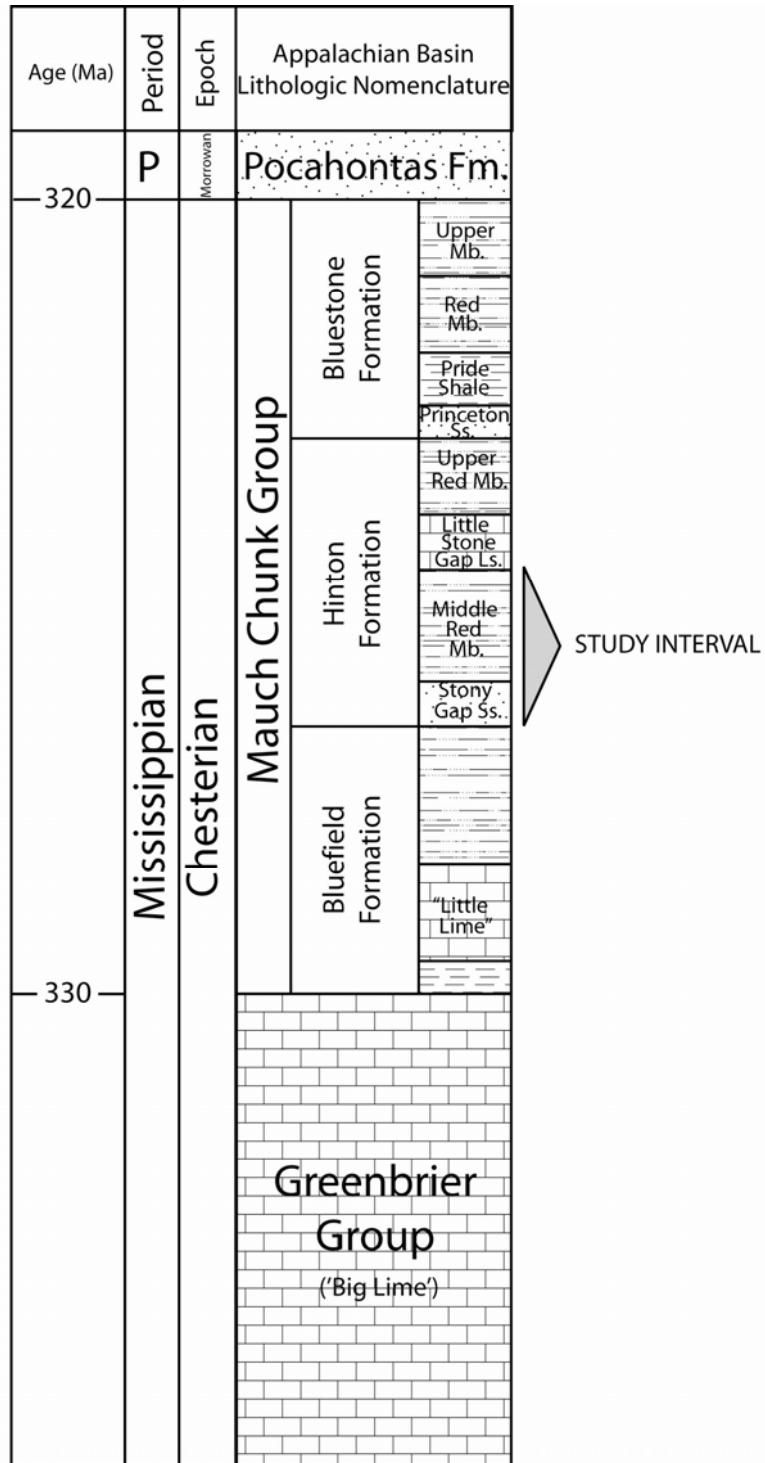


Figure 1.

Study interval within the context of Mississippian lithostratigraphy adapted from Kahmann & Driese (2008) and geochronology adapted from Menning and others (2006).

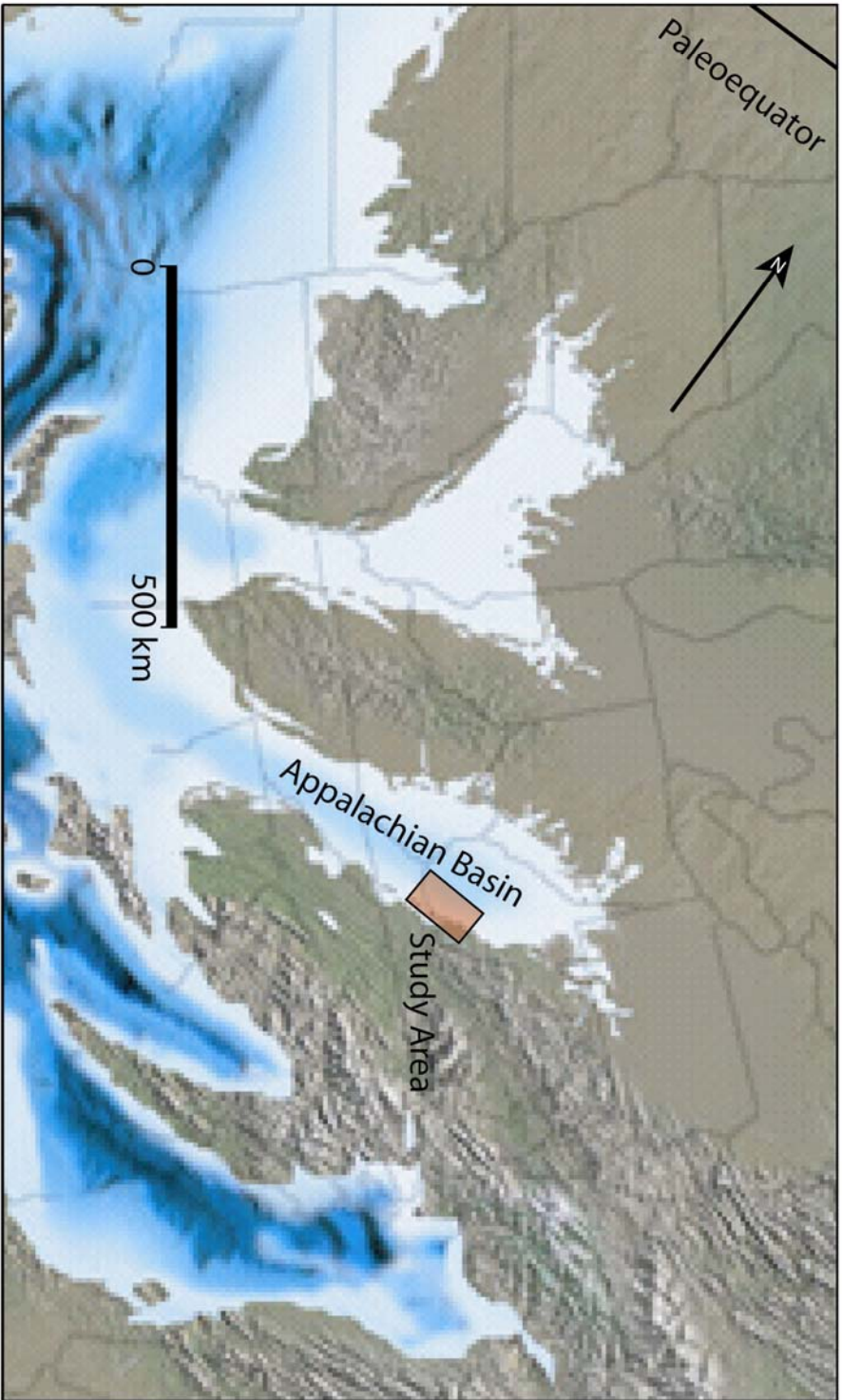


Figure 2.

Paleogeographic reconstruction of the North American plate during the Late Mississippian period (~325 Ma) with location of study area. Paleogeographic image modified from <http://jan.ucc.edu/~rcb7/>

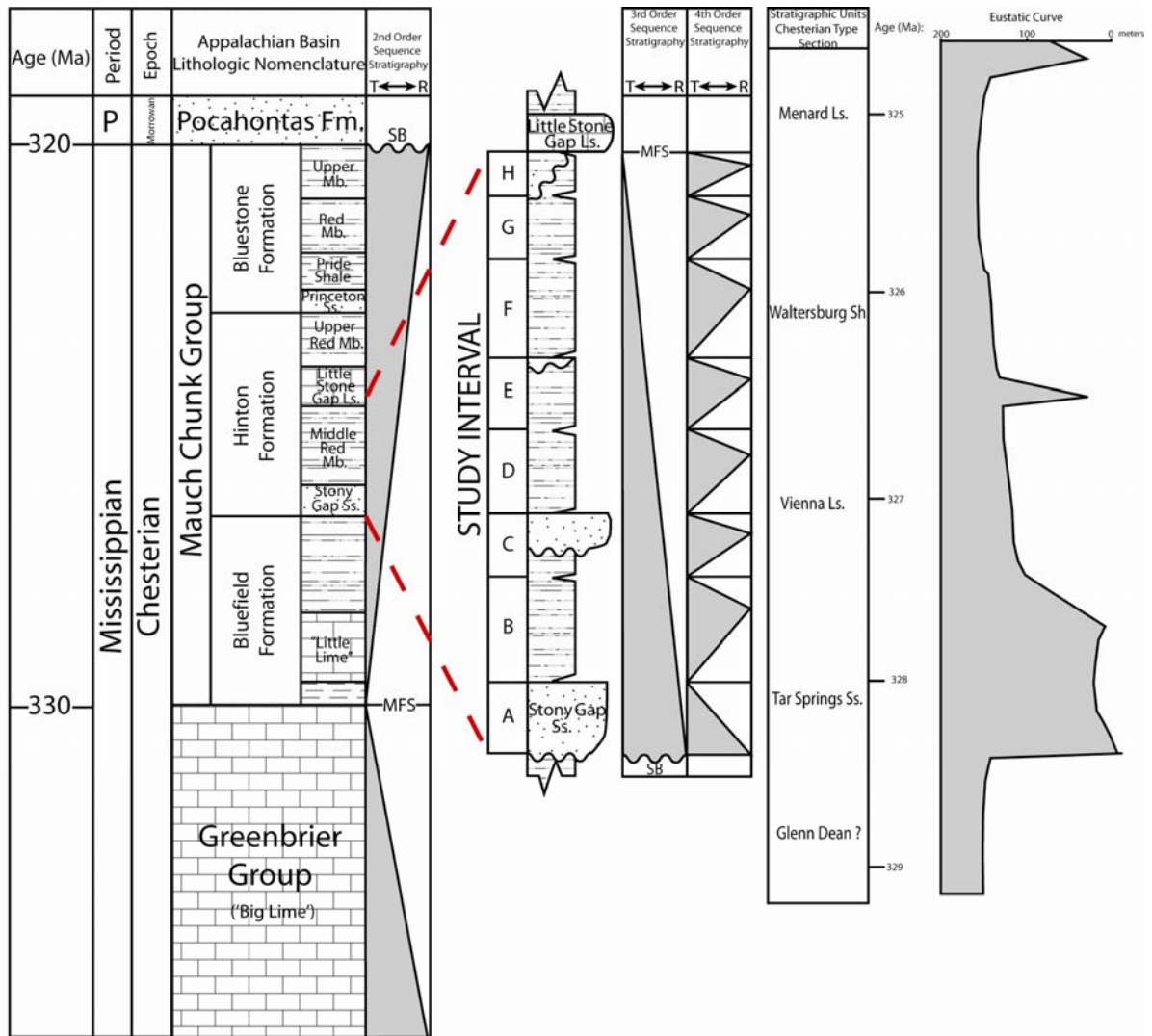


Figure 3.

Schematic of Mississippian lithostratigraphy (Kahmann & Driese, 2008), geochronology (Menning et al., 2006), second order (Al-Tawil & Read, 2003, Maynard & Eriksson, 2006) and third order (Miller & Eriksson, 2000) sequence stratigraphy, and sea level trends (Ross & Ross, 1987) gathered from information documented in other publications and fourth order sequence stratigraphy generated in this study.

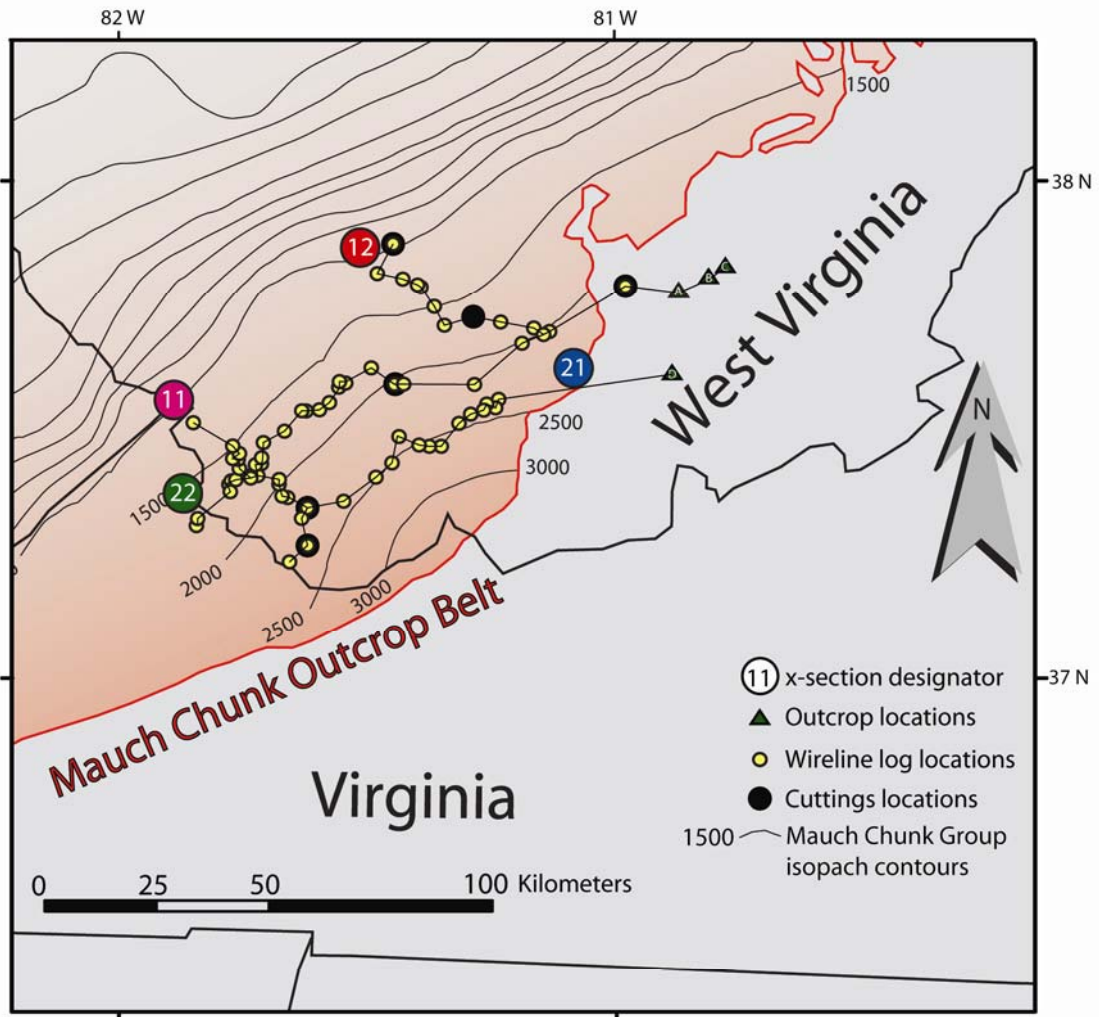


Figure 4.

Study area map with data locations and cross-sections. Mauch Chunk Group isopach contours in feet and modified after Barlow (1996).

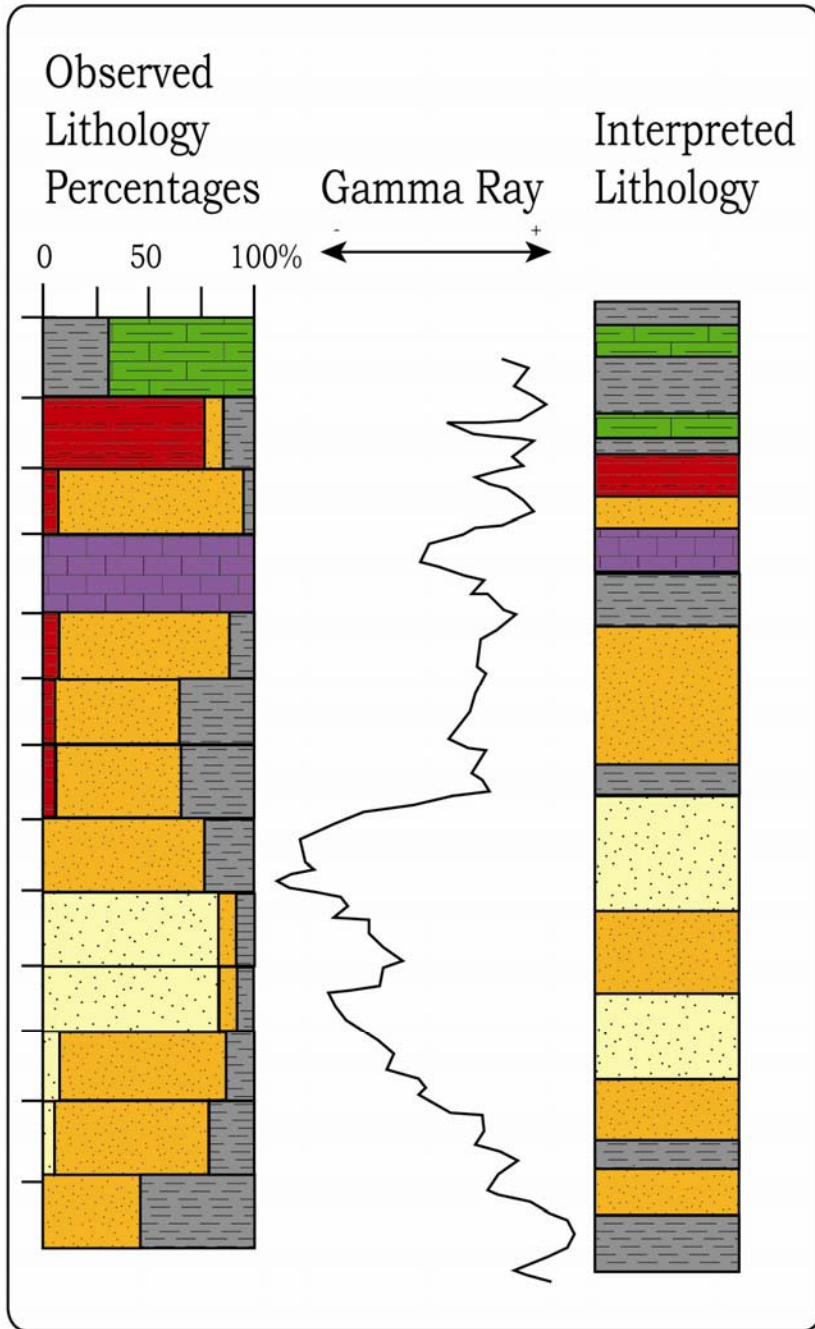


Figure 5.

Explanation of method used to note observed lithology percentages with well cuttings, and how interpreted lithologic columns were generated. In this process it is most important to weight the data provided by the geophysical log above that of the cuttings due to the many caveats inherent in the cuttings process (i.e. down-hole mixing processes and potential inaccuracies in the mud-logging technique).

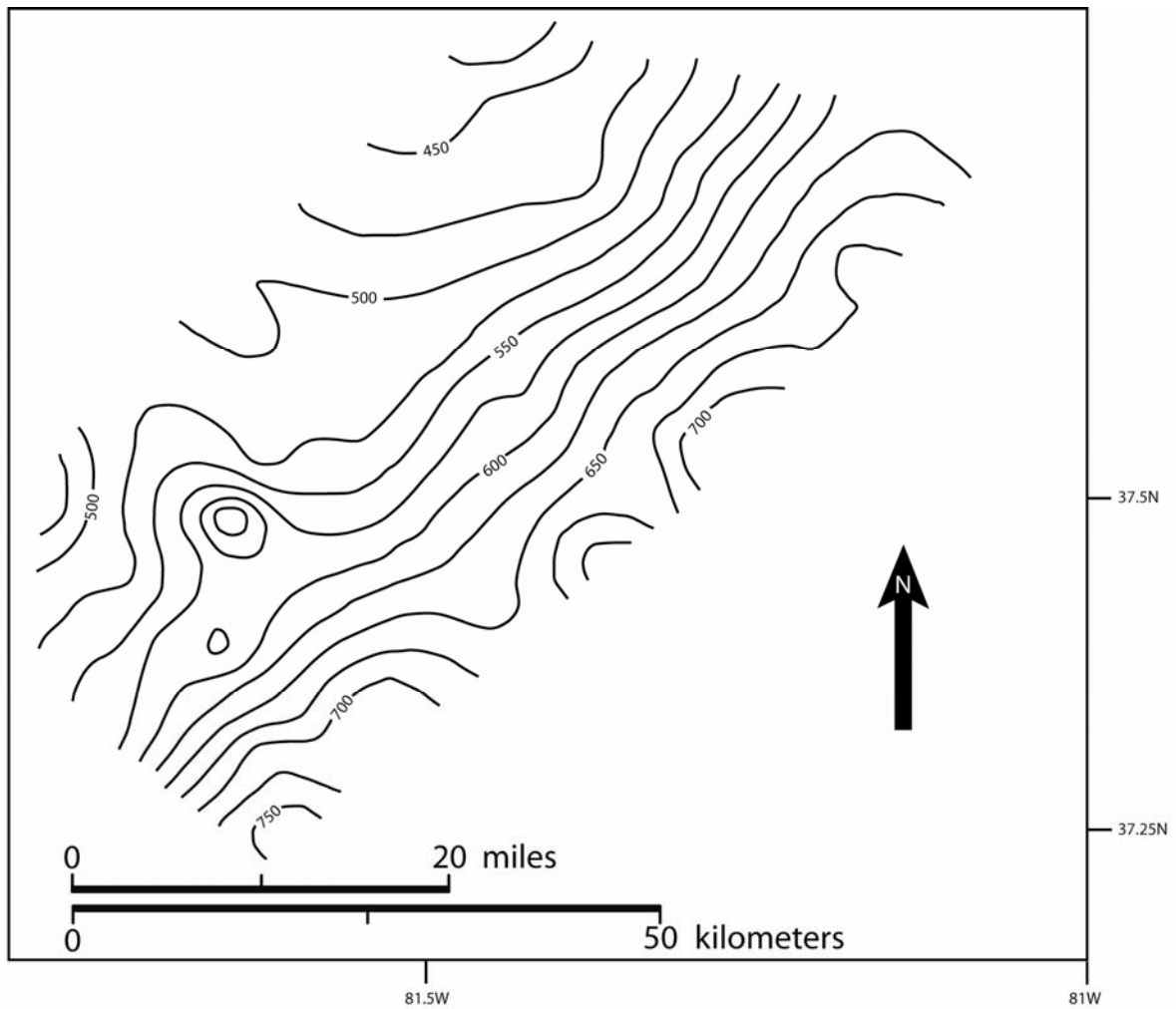


Figure 6.

Isopach map of strata, in feet, between the sequence boundary at the base of the Stony Gap Sandstone and the base of the Little Stone Gap Limestone within the study interval.

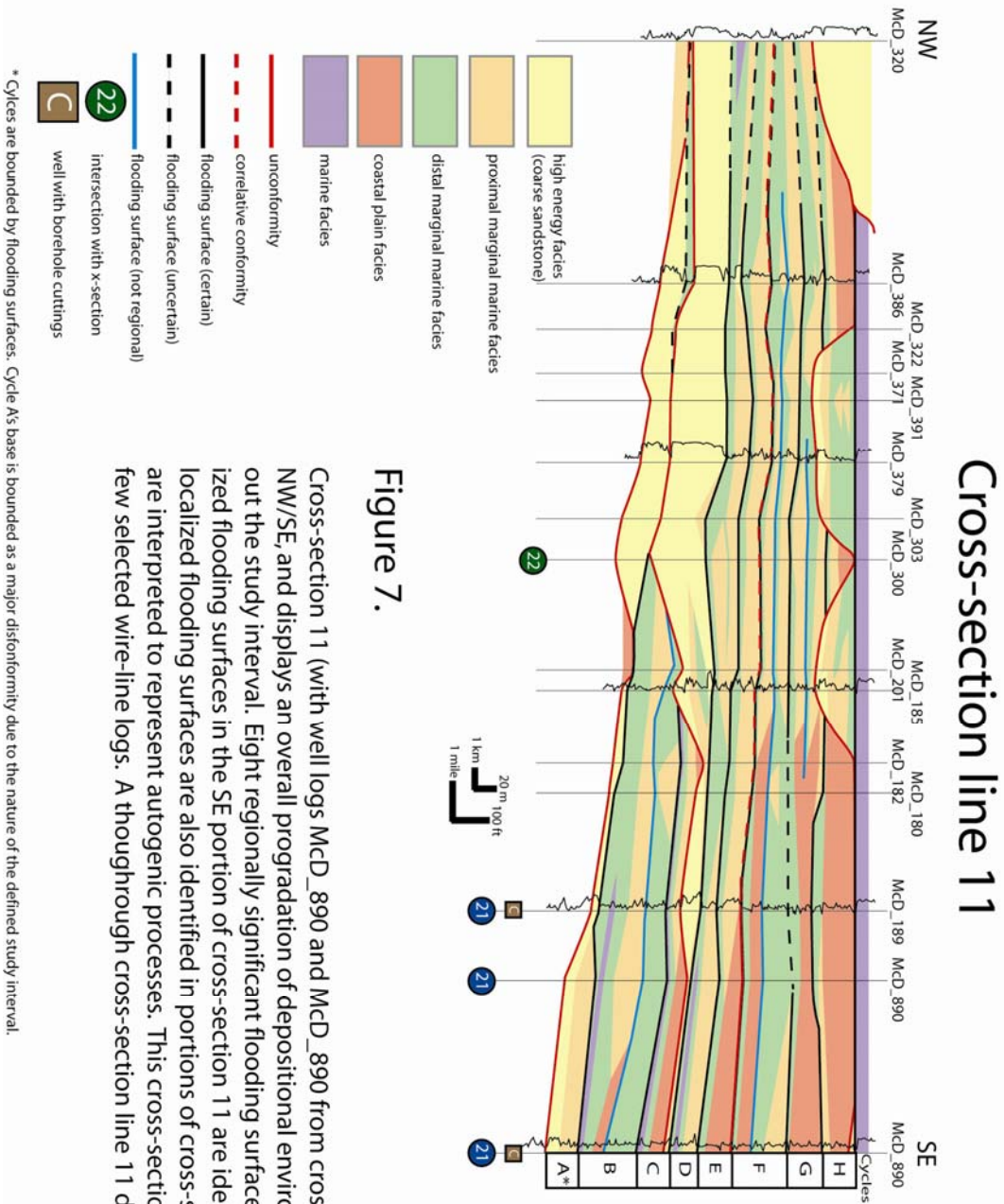


Figure 7.

Cross-section 11 (with well logs MCD_890 and MCD_890 from cross-section 22) trends NW/SE, and displays an overall progradation of depositional environments throughout the study interval. Eight regionally significant flooding surfaces and three localized flooding surfaces in the SE portion of cross-section 11 are identified. Two of the localized flooding surfaces are also identified in portions of cross-section line 22, and are interpreted to represent autogenic processes. This cross-section only displays a few selected wire-line logs. A throughline cross-section line 11 displaying all wire-

* Cycles are bounded by flooding surfaces. Cycle A's base is bounded as a major disconformity due to the nature of the defined study interval.

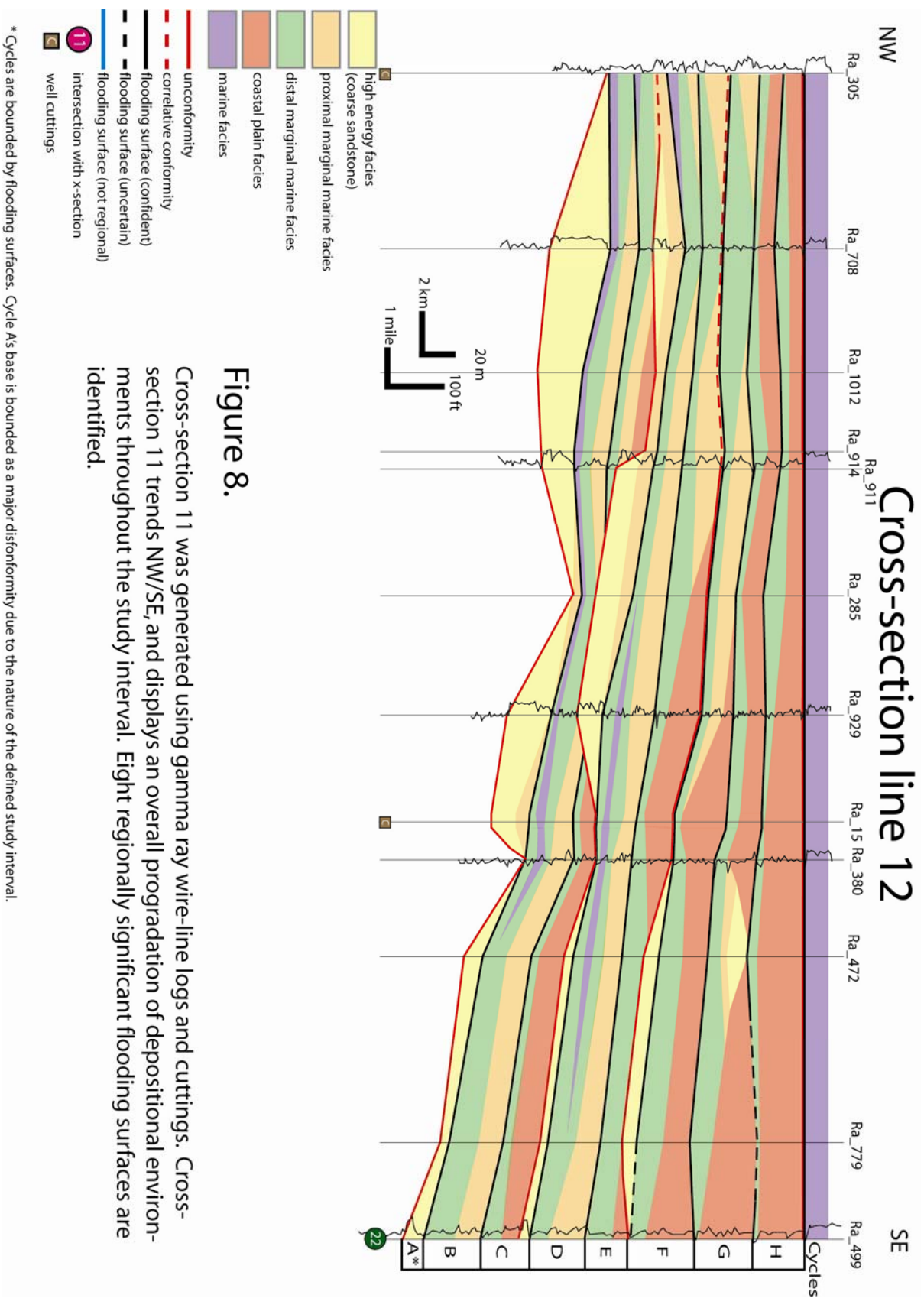


Figure 8.

Cross-section 11 was generated using gamma ray wire-line logs and cuttings. Cross-section 11 trends NW/SE, and displays an overall progradation of depositional environments throughout the study interval. Eight regionally significant flooding surfaces are identified.

*Cycles are bounded by flooding surfaces. Cycle A's base is bounded as a major disconformity due to the nature of the defined study interval.

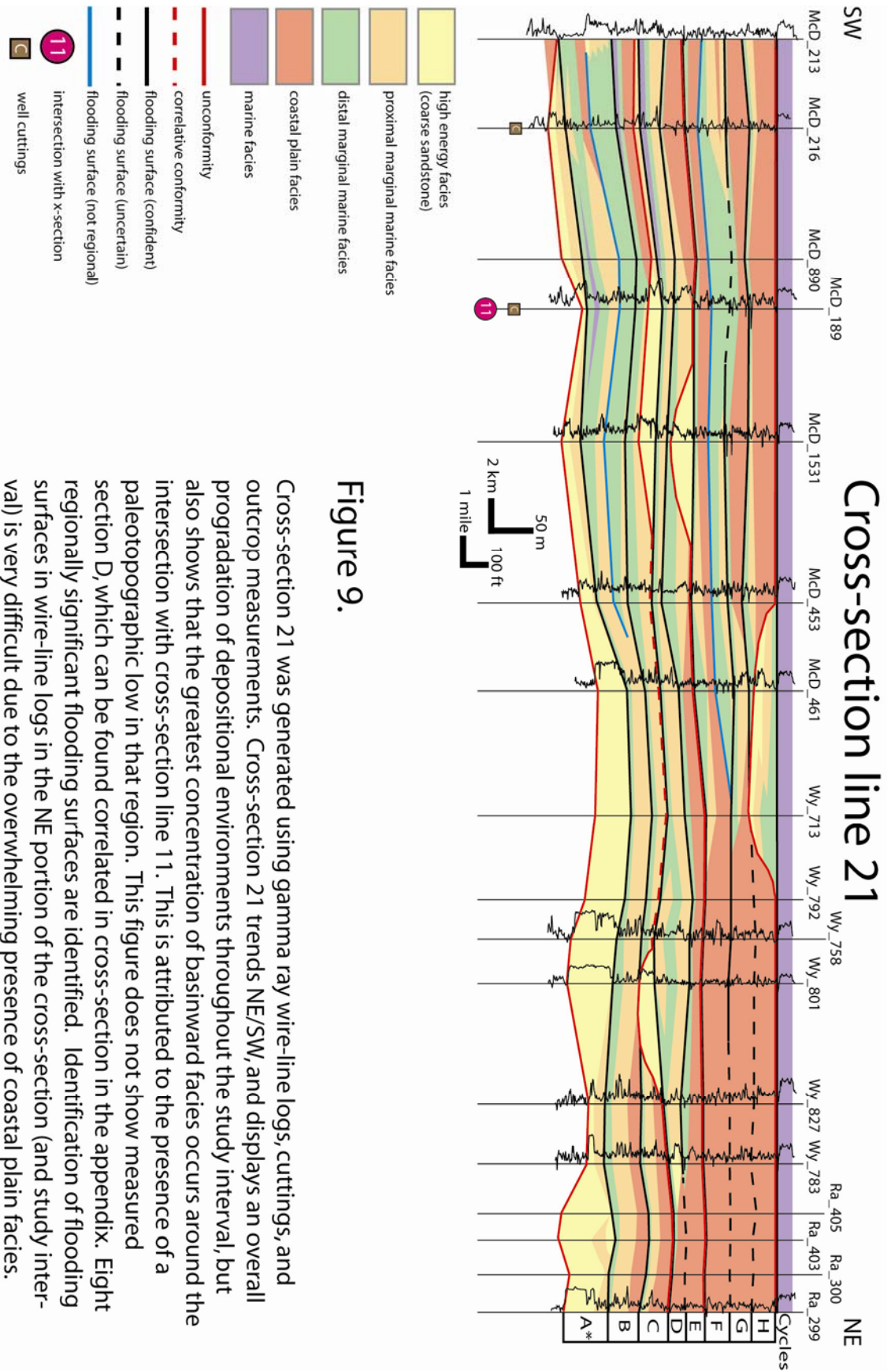


Figure 9.

Cross-section 21 was generated using gamma ray wire-line logs, cuttings, and outcrop measurements. Cross-section 21 trends NE/SW, and displays an overall progradation of depositional environments throughout the study interval, but also shows that the greatest concentration of basinward facies occurs around the intersection with cross-section line 11. This is attributed to the presence of a paleotopographic low in that region. This figure does not show measured section D, which can be found correlated in cross-section in the appendix. Eight regionally significant flooding surfaces are identified. Identification of flooding surfaces in wire-line logs in the NE portion of the cross-section (and study interval) is very difficult due to the overwhelming presence of coastal plain facies.

* Cycles are bounded by flooding surfaces. Cycle A's base is bounded as a major disconformity due to the nature of the defined study interval.

Cross-section line 22

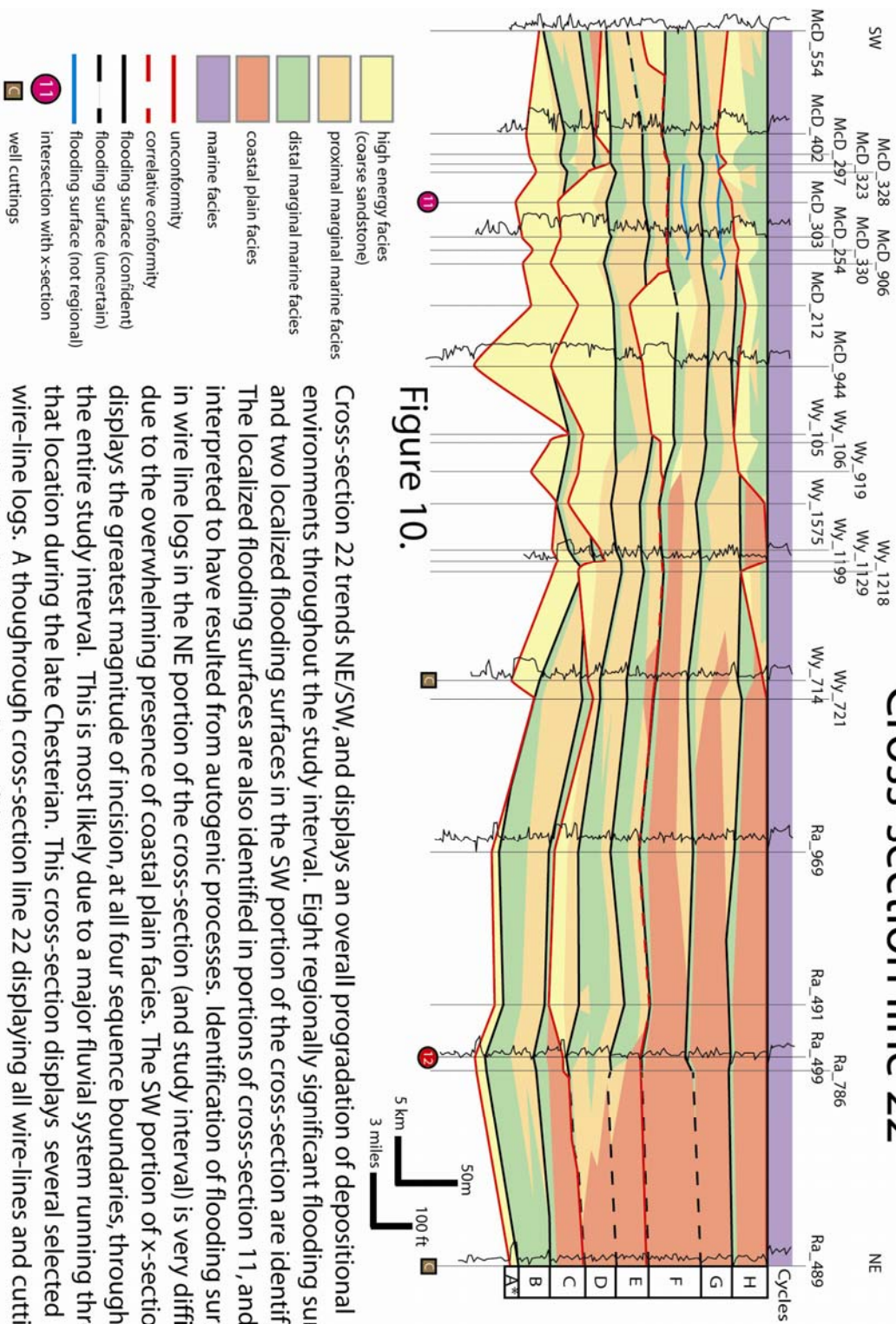


Figure 10.

Cross-section 22 trends NE/SW, and displays an overall progradation of depositional environments throughout the study interval. Eight regionally significant flooding surfaces and two localized flooding surfaces in the SW portion of the cross-section are identified. The localized flooding surfaces are also identified in portions of cross-section 11, and are interpreted to have resulted from autogenic processes. Identification of flooding surfaces in wire line logs in the NE portion of the cross-section (and study interval) is very difficult due to the overwhelming presence of coastal plain facies. The SW portion of x-section 22 displays the greatest magnitude of incision, at all four sequence boundaries, throughout the entire study interval. This is most likely due to a major fluvial system running through that location during the late Chesterian. This cross-section displays several selected wire-line logs. A thorough cross-section line 22 displaying all wire-lines and cuttings data is included in the appendices of this paper.

* Cycles are bounded by flooding surfaces. Cycle A's base is bounded as a major disconformity due to the nature of the defined study interval.

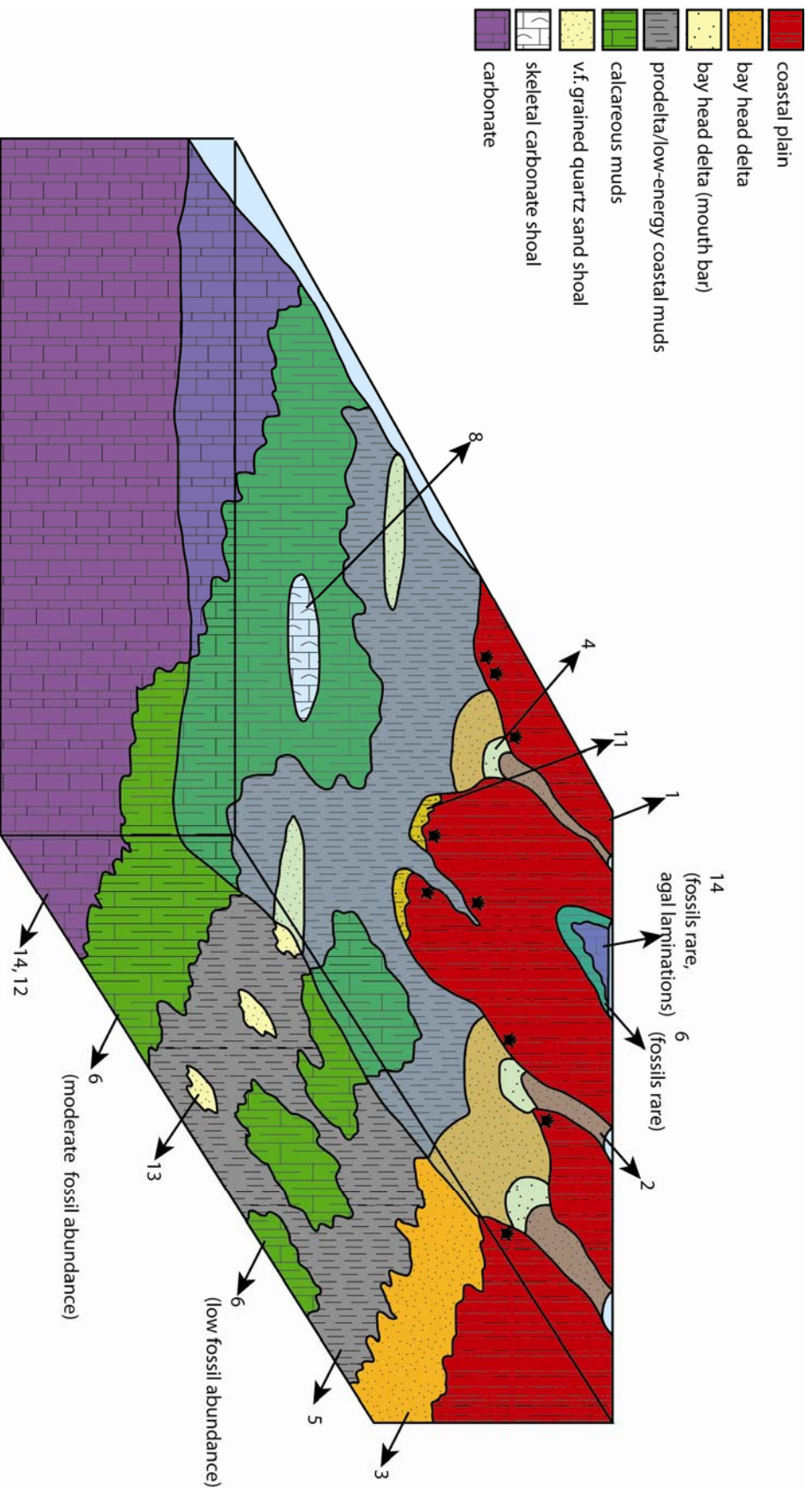


Figure 11.

Three-dimensional depositional model developed for this study. Key explains simplified environments, but table 1 contains detailed descriptions of lithologies matching the appropriate numbers. No vertical or horizontal scale implied.

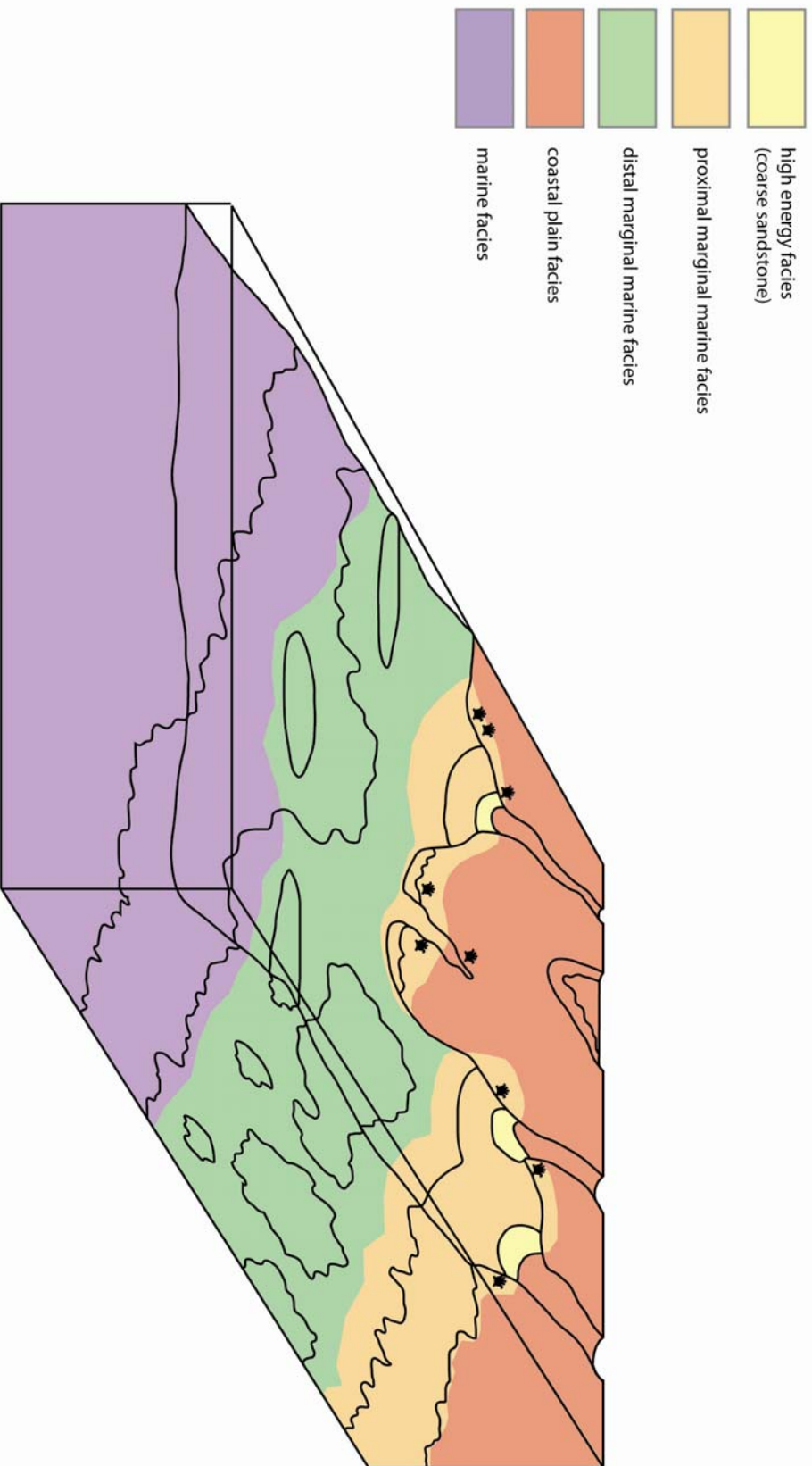


Figure 12.

Facies associations assigned to depositional environment model in figure 9. Note that the high energy facies shown in this model does not account for the deposition of that facies within incised valleys, which are pre-
sumably deposited by confined fluvial systems.

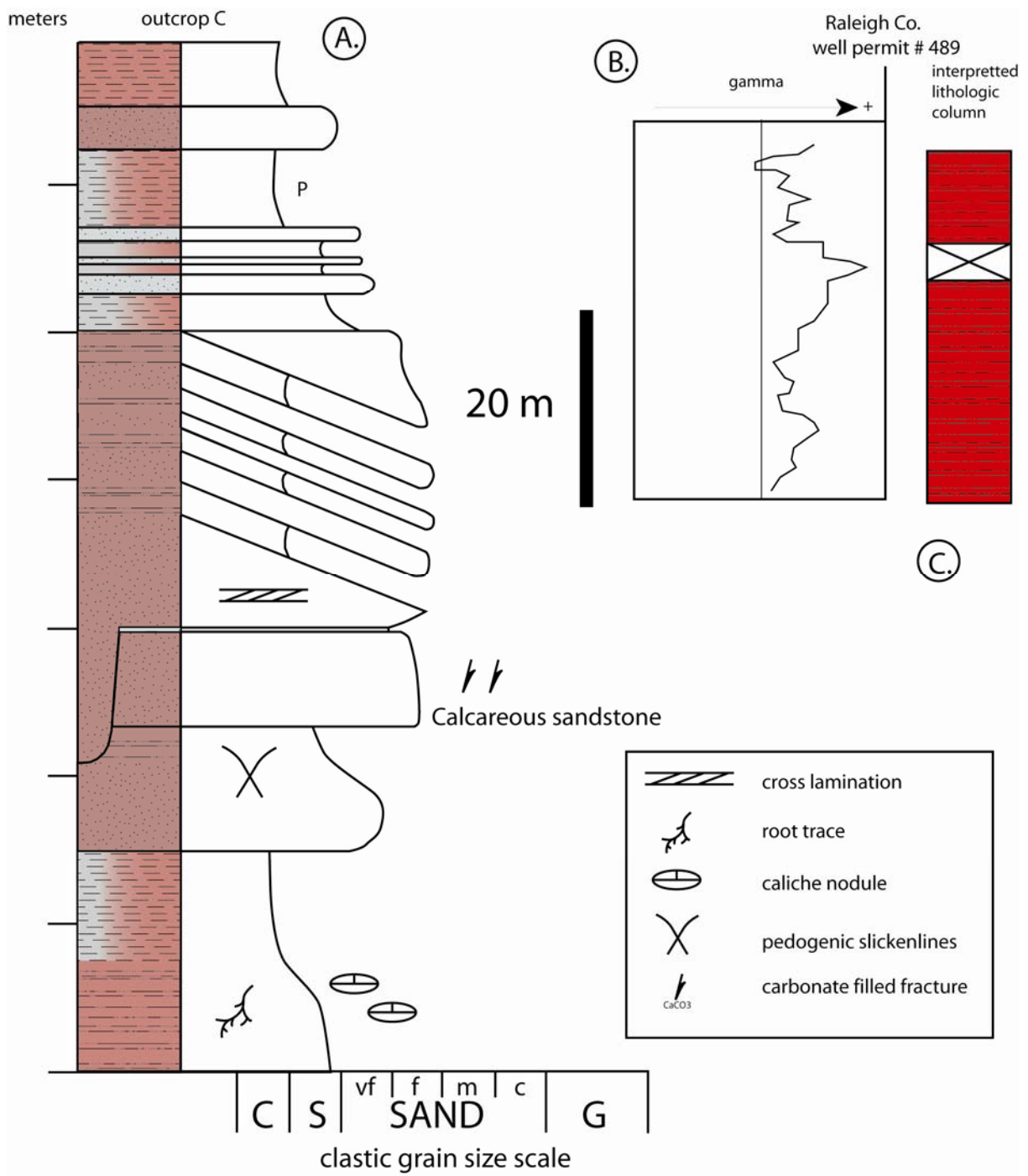


Figure 13.

Examples of coastal plain facies association in outcrop (A.), gamma ray wireline log (B.), and lithologic column interpreted (C.) from borehole cuttings.

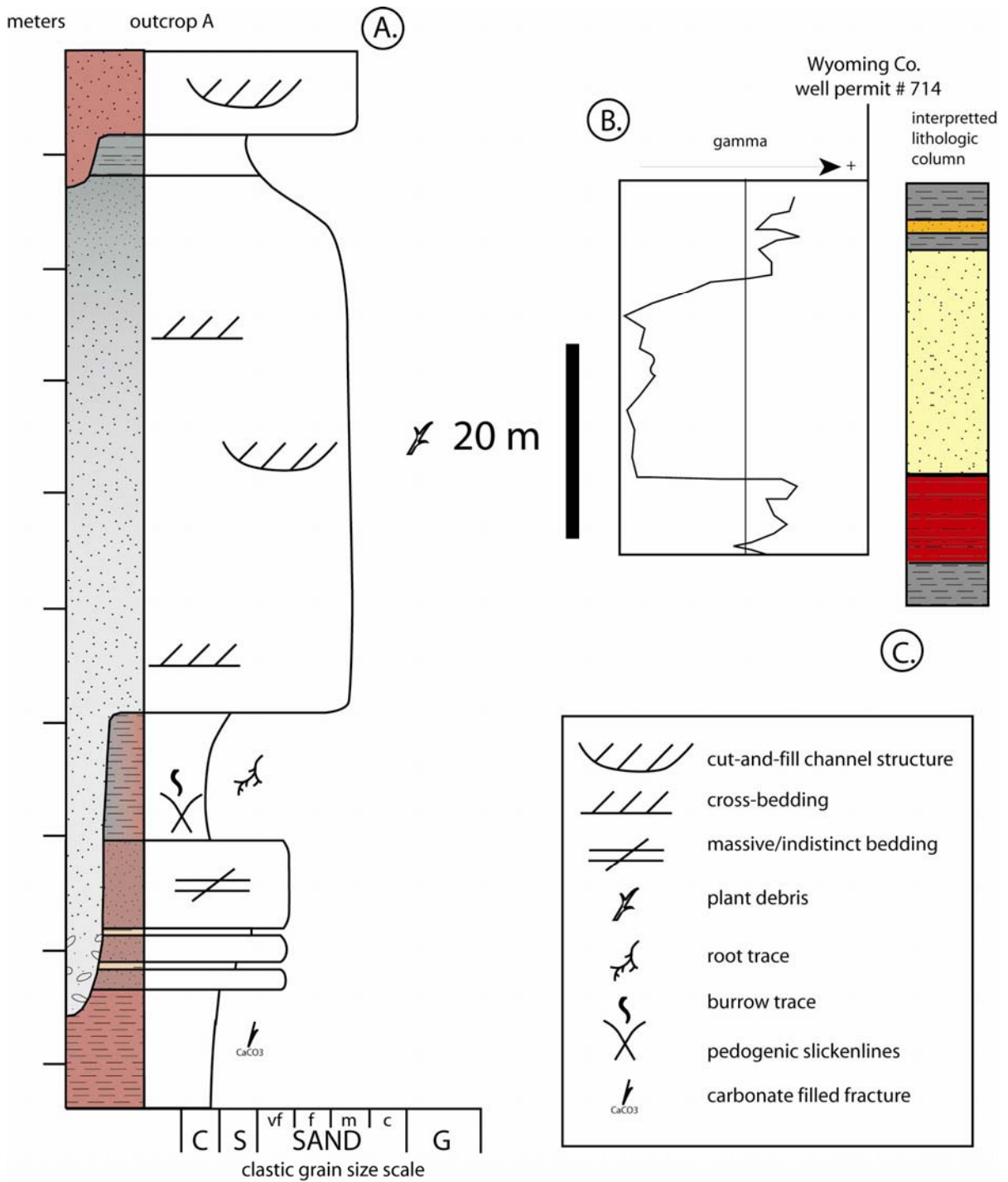


Figure 14.

Examples of high energy facies association in outcrop (A.), gamma ray wireline log (B.), and lithologic column interpreted (C.) from borehole cuttings.

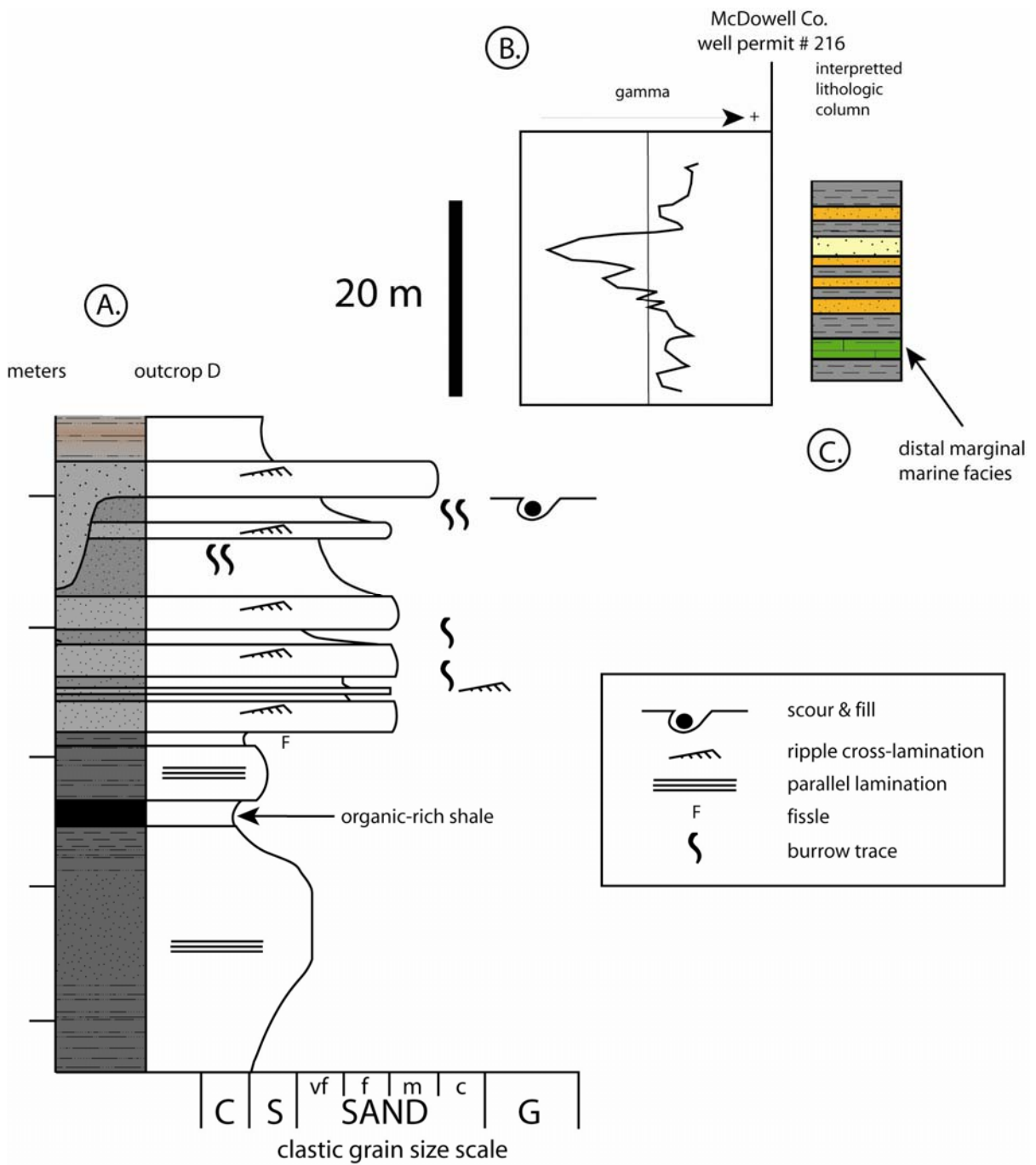


Figure 15.

Examples of proximal marginal marine facies association in outcrop (A.), gamma ray wireline log (B.), and lithologic column interpreted (C.) from borehole cuttings.

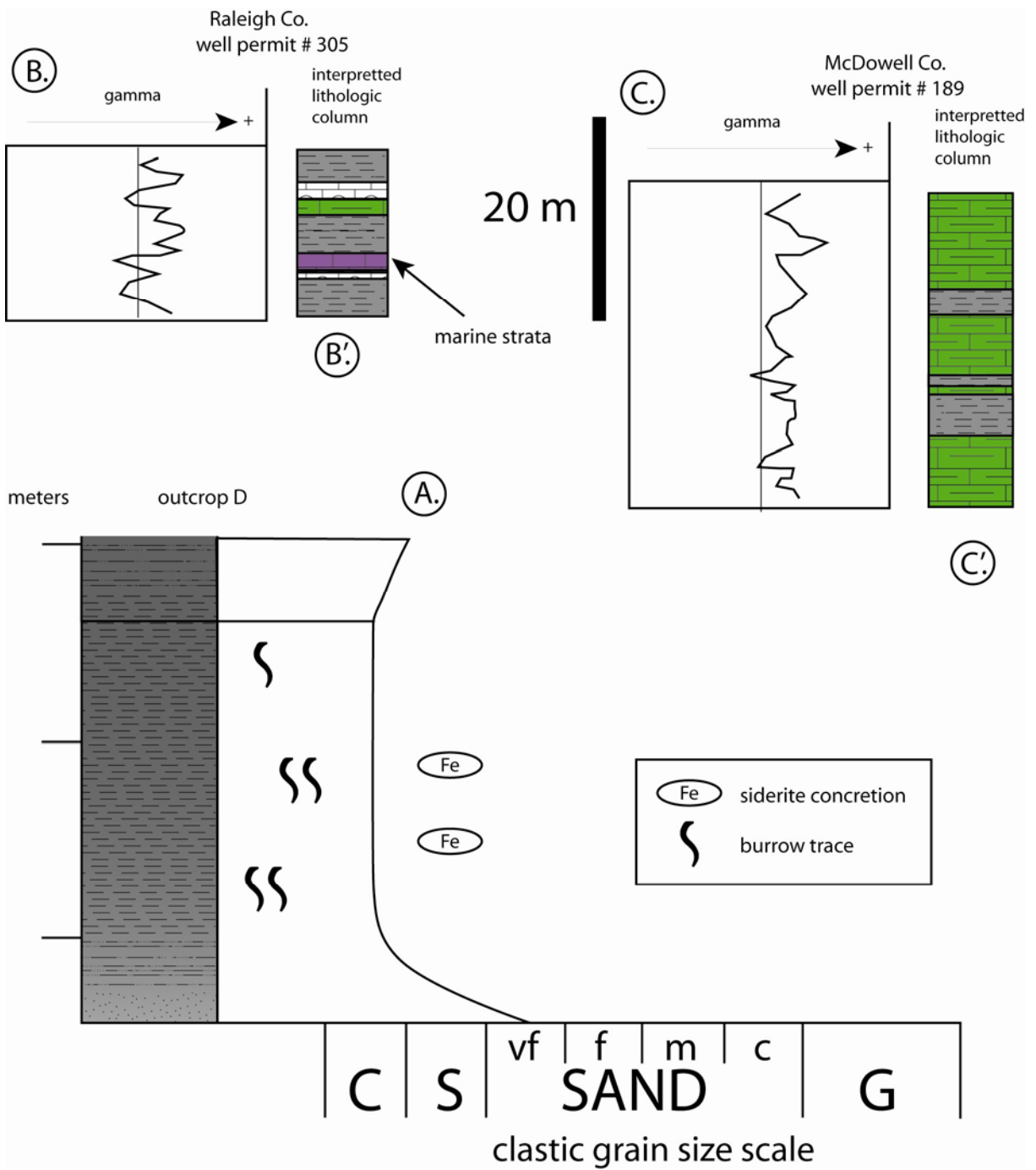


Figure 16.

Examples of distal marginal marine facies association in outcrop (A.), gamma ray wireline log (B. and C.), and lithologic column interpreted (B'. and C'.) from borehole cuttings.



Figure 17.

Photograph of paleovertisol in the lower Hinton Formation exhibiting mottling, caliche nodules, and blocky peds.

Alluvial architecture model (Wright & Marriott, 1993)

Study Interval

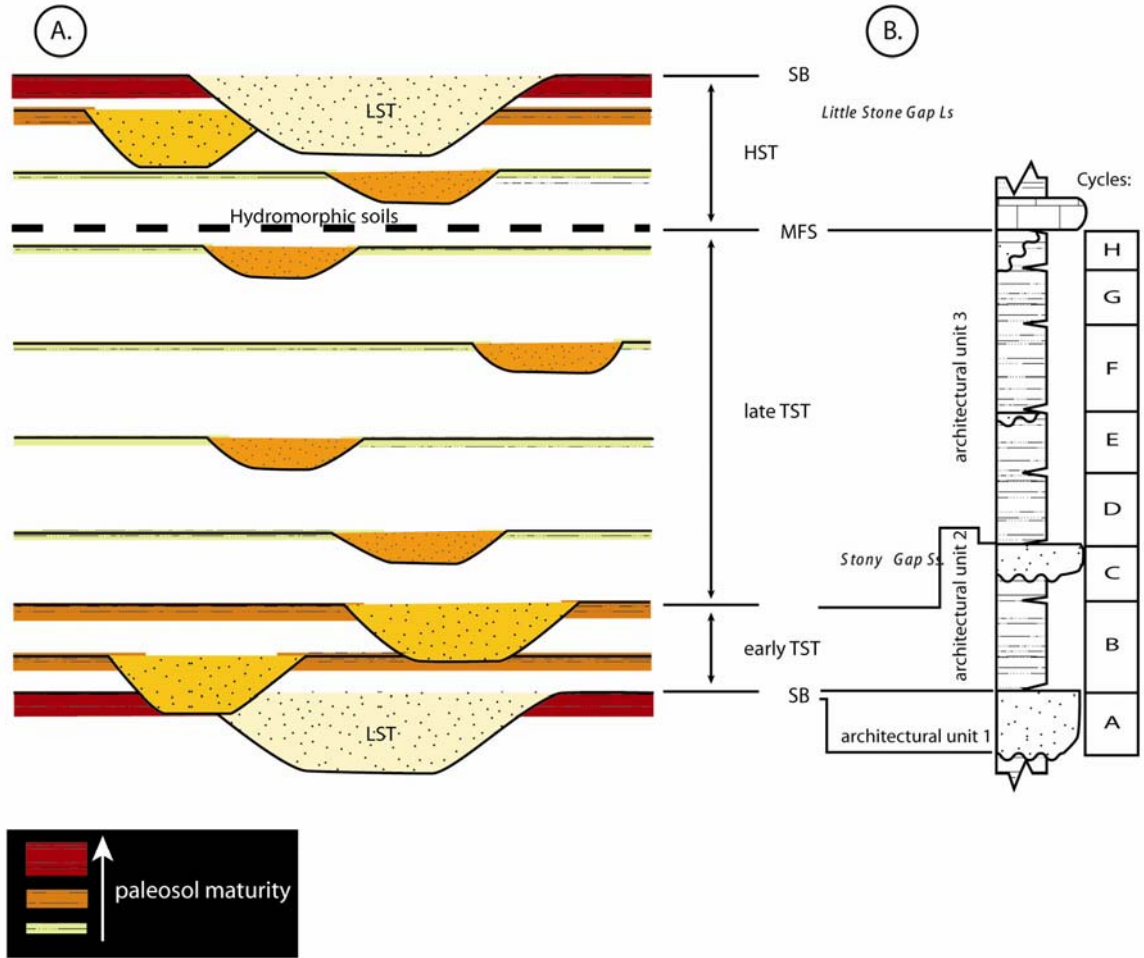


Figure 18.

Comparison between Wright and Marriott's alluvial architecture model (A.) and the stratigraphic architecture recognized in this study (B.) as described in the third order cycle section of the discussion. Architectural units correspond with those described in the sedimentary architecture of outcrops section of correlation and analyses. Model modified from Cateanu's (2006) adaptation of Wright and Marriott (1993).

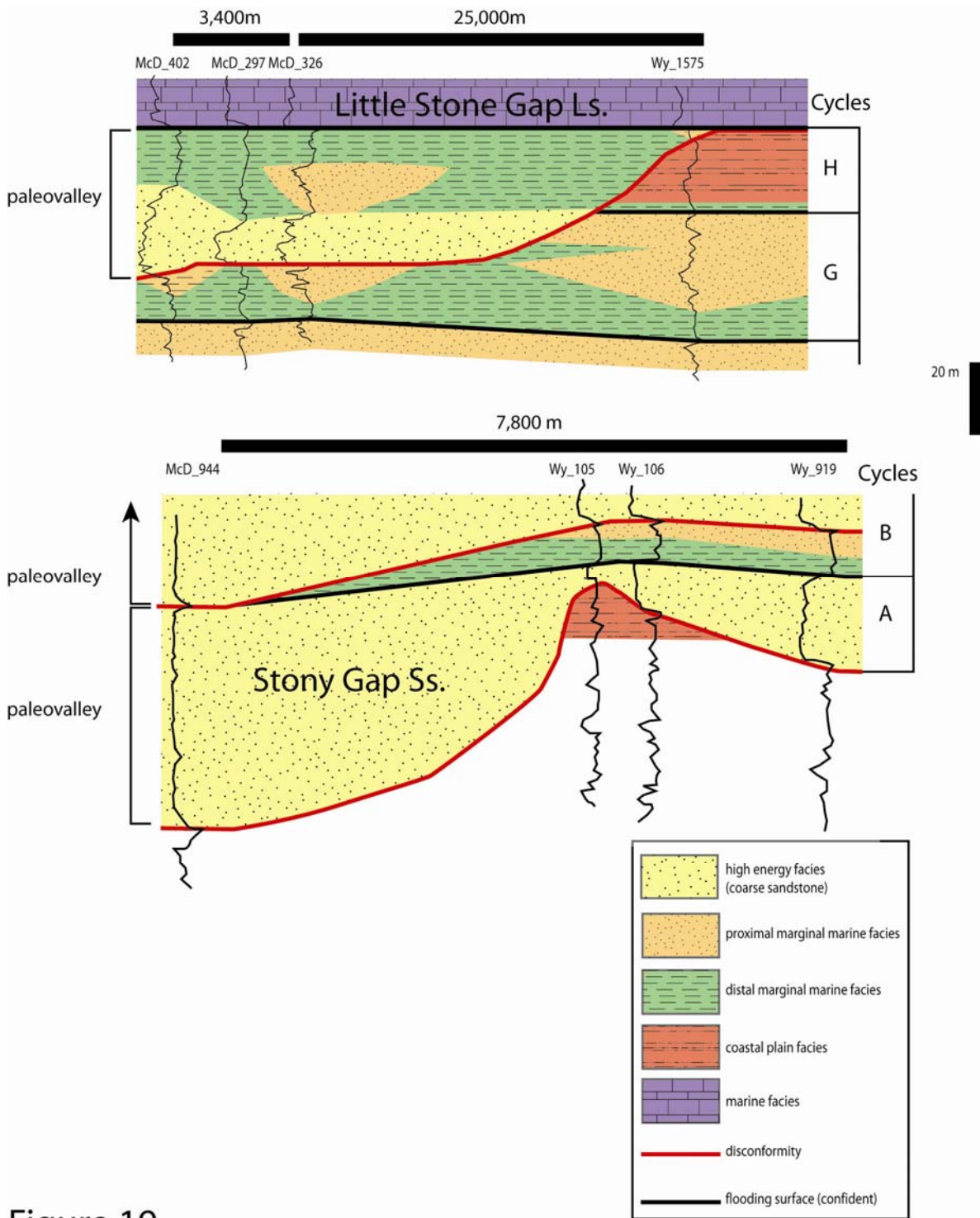


Figure 19.

Comparison of paleovalley fills between cycle A and cycle H. Note the diversity of valley fill in cycle H suggesting that relative rise in sea level outpaced sediment supply. The valley fill in cycle A consists almost entirely of high energy facies suggesting that relative rise in sea level was outpaced by sediment supply.

REFERENCES

- Aitken, J.F., and Flint, S. S.** 2001. Sequence Stratigraphic Analysis of Transgressive-Regressive Cycles in the Upper Hinton Formation (Upper Mississippian), Central Appalachian Basin. *Geologic Society of America*.
- Aitken, J.F., and Flint, Stephen S.** 1995. The application of high-resolution sequence stratigraphy to fluvial systems: a case study from the Upper Carboniferous Breathitt Group, eastern Kentucky, USA. *Sedimentology*, **42**: 3-30.
- Al-Tawil, A., and Read, J. Fred** 2003a. *Late Mississippian (Late Meramecian-Chesterian) glacio-eustatic sequence development on an active distal foreland ramp, Kentucky U.S.A.* SEPM special publication, **78**.
- Al-Tawil, A., Wynn, Thomas C., and Read, J. Fred** 2003b. *Sequence Response of a Distal-to-Proximal Foreland Ramp to Glacioeustasy and Tectonics: Mississippian, Appalachian Basin, West Virginia-Virginia, U.S.A.* SEPM Special Publication, **78**, 11-34 pp.
- Barlow, C., A.** 1996. *Play Mmc: Upper Mississippian Mauch Chunk Group and equivalent strata.* The atlas of major Appalachian gas plays. The Appalachian Oil and Natural Gas Consortium, 31-36 pp.
- Beuthin, J.D.** 1994. *A sub-Pennsylvanian paleovalley system in the central Appalachian basin and its implications for tectonic and eustatic controls on the origin of regional Mississippian-Pennsylvanian unconformity.* Tectonic and eustatic controls on sedimentary cycles, **4**, 107-120 pp.
- Beuthin, J.D.** 1997. Paleopedological Evidence for a Eustatic Mississippian-Pennsylvanian (Mid-Carboniferous) Unconformity in Southern West Virginia. *Southern Geology*, **37**: 25-37.
- Beuthin, J.D., and Bascombe, B.M., Jr.** 2002. Scrutiny of a Global Climate Model for Upper Mississippian Depositional Sequences in the Central Appalachian Foreland Basin, U.S.A. *The Journal of Geology*, **110**: 739-747.
- Blum, M.D., and Tornqvist, Torbjorne E.** 2000. Fluvial response to climate and sea-level change: A review. *Sedimentology*, **47**: 2-48.
- Busch, R.M., and Rollins, H.B.** 1984. Correlation of Carboniferous strata using a hierarchy of transgressive-regressive units. *Geology*, **12**: 802-805.
- Campbell, M.R., and Mendenhall, W.C.** 1896. Geologic section along the New and Kanawha rivers in West Virginia. *U.S.G.S Annual Report*, **17**: 473-511.
- Catuneanu, O.** 2006. *Principles of Sequence Stratigraphy.* Elsevier, Oxford.
- Cecil, C.B.** 1990. Paleoclimate Controls on Stratigraphic Repetition of Chemical and Siliciclastic Rocks. *Geology*, **18**: 533-536.

- Chestnut, D.R., Jr.** 1994. *Eustatic and tectonic controls of deposition of Lower and Middle Pennsylvanian strata of the Appalachian basin*. Tectonic and eustatic controls on sedimentary cycles: SEPM Concepts in Sedimentology and Paleontology, **A66**. 58-70 pp.
- Coffey, B.P., and Read, J. Fred** 2002. High-resolution sequence stratigraphy in Tertiary carbonate-rich sections by thin-sectioned well cuttings. *AAPG Bulletin*, **86**: 1407-1415.
- Crowley, T.J., and Baum, S.K.** 1991. Estimating Carboniferous sea-level fluctuations from Gondwanan ice extent. *Geology*, **19**: 975-977.
- Dalrymple, R.W., Zaitlin, B.A., and Boyd, R.** 1992. Estuarine facies models: Conceptual basis and stratigraphic implications. *Journal of Sedimentary Petrology*, **62**: 1130-1146.
- Dattilo, B.F., Brett, Carlton E., Tsujita, Cameron J., and Fairhurst, Robert** 2008. Sediment supply versus storm winnowing in the development of muddy and shelly interbeds from the Upper Ordovician of the Cincinnati region, U.S.A. *Canadian Journal of Earth Science*, **45**: 243-265.
- Davies, R., Howell, John, Boyd, Ron, Flint, Stephen, and Diessel, Claus** 2006. High-resolution sequence-stratigraphic correlation between shallow-marine and terrestrial strata: Examples from the Sunnyside Member of the Cretaceous Blackhawk Formation, Book Cliffs, eastern Utah. *AAPG Bulletin*, **90**: 1121-1140.
- Davydov, V., Wardlaw, B.R., and Gradstein, F.M.** 2004. *The Carboniferous Period*. A Geologic Time Scale. Cambridge University Press, 222-248 pp.
- Emery, D., and Myers, Keith J.** 2006. *Sequence Stratigraphy*. Blackwell Publishing, 6 pp.
- Englund, K.J.** 1979. Mississippian System and lower series of the Pennsylvanian System in the proposed Pennsylvanian System stratotype area. *AGI Selected Guidebook Series* 69.
- Englund, K.J., and Thomas, R.E.** 1990. Late Paleozoic depositional trends in the central Appalachian basin. *U.S. Geological Survey Bulletin*, **1839-F**.
- Frakes, L.A., Francis, J.E., and Syktu, J.I.** 1992. *Climate modes of the Phanerozoic*. Cambridge University Press, 274 pp.
- Goldberg, S.A., and Dallmeyer, R.D.** 1997. Chronology of Paleozoic metamorphism and deformation in the Blue Ridge thrust complex, North Carolina and Tennessee. *American Journal of Science*, **297**: 488-526.
- Goldhammer, R.K., Oswald, E.J., and Dunn, P.A.** 1991. *Hierarchy of the stratigraphic forcing: example from Middle Pennsylvanian shelf carbonates of the Paradox basin*. Sedimentary Modeling: Computer Simulations and Methods for Improved Parameter Definition. Kansas Geological Survey, Lawrence, 361-414 pp.

- Golonka, J., Ross, M.I., and Scotese, C.R.** 1994. Phanerozoic paleogeographic and paleoclimatic modeling maps: Pangaea: global environments and resources. *Canadian Society of Petroleum Geologists Memoir*, **17**: 1-47.
- Gordon, M.J., and Henry, T.W.** 1981. *Late Mississippian and Early Pennsylvanian invertebrate faunas. east-central Appalachians-a preliminary report*. Geological Society of America Cincinnati '81 field trip guidebooks, **1**. American Geological Institute.
- Hatcher, R.D.** 1989. *The Alleghanian orogen*. The Appalachian-Ouachita orogen in the United States, **F-2**. GSA Inc., 233-318 pp.
- Howell, J.A., and Flint, S.** 2003. *Sedimentology and sequence stratigraphy of the Book Cliffs*. The sedimentary record of sea-level change. Cambridge University Press, Cambridge, 135-208 pp.
- Kahman, J.A., and Driese, Steven G.** 2008. Paleopedology and geochemistry of Late Mississippian (Chesterian) Pennington Formation paleosols at Pound Gap, Kentucky, USA: Implications for high-frequency climate variations. *Palaeogeography, Palaeoclimatology, Palaeoecology*, **259**: 357-381.
- Maguregui, J.A.T., N.** 1991. *Evolution of Middle Eocene tide-dominated deltaic sandstones, Lagunillas Field, Maracaibo Basin, Western Venezuela*. Three Dimensional facies Architecture of Terrigenous Clastic Sediments and its Implications for Hydrocarbon Discovery and Recovery, **3**, 233-244 pp.
- Malmon, D.V., Dunne, T., and Reneau, S.L.** 2002. Predicting the fate of sediment and pollutants in river floodplains. *Environmental Science and Technology*, **36**: 2026-2032.
- Maynard, J.P., Eriksson, K.A., and Law, R.D.** 2006. The upper Mississippian Bluefield Formation in the Central Appalachian Basin: A hierarchical sequence-stratigraphic record of a greenhouse to icehouse transition. *Sedimentary Geology* 99-122.
- McKee, B.A.** 2003. RiOMar: The Transport, Transformation, and Fate of Carbon in River-Dominated Ocean Margins. *Report of the RiOMar Workshop*.
- Menning, M., Alekseev, A.S., Chuvashov, B.I., Davydov, V.I., Devuyt, F.-X., Forke, H.C., Grunt, T.A., Hance, L., Heckel, P.H., Izokh, Jin, Y.-G., Jones, P.J., Kotlyar, G.V., Kozar, H.W., Nemyrovska, T.I., Schneider, J.W., Wang, X., -D., Weddige, K., Weyer, D., and Work, D.M.** 2006. Global time scale and regional stratigraphic reference scales of Central and West Europe, East Europe, Tethys, South China, and North America as used in the Devonian-Carboniferous-Permian Correlation Chart 2003 (DCP 2003). *Palaeogeography, Palaeoclimatology, Palaeoecology*, **240**: 318-372.
- Metivier, F., and Gaudemer, Y.** 1999. Stability of output fluxes of large rivers in South and East Asia during the last 2 million years: implications on floodplain processes. *Basin Research*, **11**: 293-303.

- Miller, D.J., and Eriksson, K.A.** 2000. Sequence Stratigraphy of Upper Mississippian Strata in the Central Appalachians: A Record of Glacioeustacy and Tectonoeustasy in a Foreland Basin Setting. *AAPG Bulletin*, **84**: 210-233.
- Paola, C., Hellaer, P.L., and Angevine, C.L.** 1992. The large-scale dynamics of grain size variation in alluvial basins: 1, Theory. *Basin Research*, **4**: 73-90.
- Retallack, G.J.** 1988. *Field recognition of paleosols*. Paleosols and weathering through geologic time: Geological Society of America Special Paper, **216**, 1-20 pp.
- Retallack, G.J.** 1997. *A colour guide to paleosols*. New York: John Wiley, Chichester.
- Ross, C.A., and Ross, J.R.P.** 1987. *Late Paleozoic sea levels and depositional sequences*. Timing and Depositional History of Eustatic Sequences: Constraints on Seismic Stratigraphy, **24**. Cushman Foundation for Foraminiferal Research, Special Publication, 137-149 pp.
- Ross, C.A., and Ross, J.R.P.** 1988. Late Paleozoic Transgressive-Regressive Deposition. *SEPM Special Publication* 227-247.
- Rygel, M.C., Fielding, Christopher R., Tracy D. Frank, and Birgenheier, Lauren P.** 2008. The magnitude of Late Paleozoic Glacioeustatic Fluctuations: A Synthesis. *Journal of Sedimentary Research*, **78**: 500-511.
- Scotese, C.R., and Barrett, S.F.** 1990. *Gondwana's movement over the South Pole during the Paleozoic: Evidence from lithological indicators of climate*. Paleozoic Paleogeography and Biogeography. Geological Society London Memoir, **12**, 75-85 pp.
- Shanely, K.W., and McCabe, P.J.** 1993. *Alluvial architecture in a sequence stratigraphic framework: a case study from the Upper Cretaceous of southern Utah, USA*. The Geological Modeling of Hydrocarbon Reservoirs and Outcrop Analogues, **Special Publication 15**. International Association of Sedimentology, 21-55 pp.
- Simonsen, A.H.** 1981. Paleoecology of fenstrate dryozoans in the Wymps Gap Limestone of southwestern Pennsylvanian. *Pennsylvania geology*, **12**: 11.
- Stewart, K.G., Dennison, John M., and Bartholomew, Mervin J.** 2002. Late Mississippian paleoseismites from southern West Virginia and southwestern Virginia. *Geological Society of America Special Paper*, **359**: 127-144.
- Strong, N., and Paola, C.** 2006. Fluvial landscapes and stratigraphy in a flume. *The Sedimentary Record*, **4**: 5-8.
- Strong, N., and Paola, Chris** 2008. Valleys that never were: time surfaces versus stratigraphic surfaces. *Journal of Sedimentary Research*, **78**: 579-593.
- Swann, D.H.** 1964. Late Mississippian rhythmic sediments of Mississippi Valley. *AAPG Bulletin*, **48**: 637-658.

- Van Wagnor, J.C.** 1995. *Overview of sequence stratigraphy of foreland basin deposits: Terminology, summary of papers, and glossary of sequence stratigraphy*. Sequence Stratigraphy of Foreland Basin Deposits. American Association Petroleum Geologists Memoir, **64**, 1-13 pp.
- Van Wagoner, J.C., Mitchum, R.M., Jr., Campion, K.M., and Rahmanian, V.D.** 1990. *Siliciclastic Sequence Stratigraphy in Well Logs, Cores, and Outcrop: Concepts for High Resolution Correlation of Time and Facies*, **7**. American Association of Petroleum Geologists Methods in Exploration Series, Tulsa.
- Veevers, J.J., and Powell, C. M.** 1987. Late Paleozoic Episodes in Gondwanaland Reflected in Transgressive-Regressive Depositional sequences in Eur-America. *Geologic Society of America*, **98**: 475-487.
- Vera, J.A., and Molina, J.M.** 1998. Shallowing-upward cycles in pelagic troughs (Upper Jurassic, Subbetic, Southern). *Sedimentary Geology*, **119**: 103-121.
- Walness, J.R., and Shepard, F.P.** 1936. Sea level and climatic changes related to Late Paleozoic cycles. *Geological Society of America Bulletin*, **47**: 1177-1206.
- Wilpolt, R.H., and Marden, Douglas W.** 1959. Geology and oil and gas possibilities of Upper Mississippian rocks of southwestern Virginia, southern West Virginia and eastern Kentucky. *Geological Society of America Bulletin*, **1072-K**: 587-656.
- Wortman, G.L., Samson, S.D., and Hibbard, J.P.** 1998. Precise timing constraints on the kinematic development of the Hyco shear zone: Implications for the central Piedmont shear zone, Southern Appalachian orogen. *American Journal of Science*, **298**: 108-130.
- Wright, V.P., and Marriott, S.B.** 1993. The sequence stratigraphy of fluvial depositional systems: The role of floodplain sediment storage. *Sedimentary Geology*, **86**: 203-210.
- Wynn, T.C., and Read, J. Fred** 2006. Sequence-stratigraphic analysis using well cuttings, Mississippian Greenbrier Group, West Virginia. *AAPG Bulletin*, **90**: 1869-1882.
- Zaitlin, B.A., Dalrymple R.W., and Boyd, R.** 1994. *The stratigraphic organization of incised-valley systems associated with relative sea level change*. Incised-Valley Systems: Origin and Sedimentary Sequences, **51**, 45-60 pp.

Appendix A.

Point data location table:

County	Permit # or ID	Data Type	Latitude	Longitude
McDowell	180	wire line	37.363099	-81.658779
McDowell	182	wire line	37.366727	-81.670662
McDowell	185	wire line	37.389961	-81.67649
McDowell	189	wire line, cuttings	37.342065	-81.619352
McDowell	201	wire line	37.397073	-81.677763
McDowell	212	wire line	37.472714	-81.707961
McDowell	213	wire line	37.23476	-81.655132
McDowell	216	wire line, cuttings	37.264683	-81.621835
McDowell	254	wire line	37.427274	-81.722341
McDowell	297	wire line	37.38909	-81.776377
McDowell	300	wire line	37.407813	-81.720158
McDowell	303	wire line	37.404475	-81.73653
McDowell	320	wire line	37.513219	-81.848093
McDowell	322	wire line	37.450508	-81.75764
McDowell	323	wire line	37.39446	-81.771284
McDowell	326	wire line	37.398089	-81.76328
McDowell	330	wire line	37.430902	-81.711244
McDowell	371	wire line	37.440348	-81.768191
McDowell	379	wire line	37.419013	-81.755457
McDowell	386	wire line	37.464586	-81.770192
McDowell	391	wire line	37.435982	-81.75855
McDowell	402	wire line	37.374722	-81.774012
McDowell	453	wire line	37.403314	-81.482346
McDowell	461	wire line	37.432208	-81.449593
McDowell	554	wire line	37.3194	-81.838782
McDowell	754	wire line	37.320706	-81.807207
McDowell	814	wire line	37.307208	-81.842051
McDowell	890	wire line	37.321432	-81.630085
McDowell	906	wire line	37.441352	-81.711426
McDowell	938	wire line	37.498549	-81.679582
McDowell	944	wire line	37.495646	-81.666476
McDowell	1531	wire line	37.354535	-81.547297
Raleigh	15	cuttings	37.715602	-81.29842
Raleigh	285	wire line	37.747097	-81.365092
Raleigh	294	wire line	37.704415	-81.231878
Raleigh	299	wire line	37.558079	-81.236394
Raleigh	305	wire line, cuttings	37.871952	-81.44793
Raleigh	380	wire line	37.726342	-81.289059
Raleigh	472	wire line	37.710232	-81.231513
Raleigh	489	wire line,	37.787179	-80.994186

		cuttings		
Raleigh	499	wire line	37.68874	-81.144347
Raleigh	708	wire line	37.813159	-81.479541
Raleigh	779	wire line	37.703399	-81.164972
Raleigh	911	wire line	37.784845	-81.392917
Raleigh	914	wire line	37.78949	-81.397488
Raleigh	929	wire line	37.709361	-81.344285
Raleigh	1012	wire line	37.802709	-81.427636
				-
Summers	A	outcrop	37.7824	80.89346667
Summers	B	outcrop	37.80875	-80.81615
Summers	C	outcrop	37.83083333	-80.7817
Summers	D	outcrop	37.641425	-80.888601
Wyoming	105	wire line	37.536877	-81.631378
Wyoming	106	wire line	37.536151	-81.623785
Wyoming	713	wire line	37.485486	-81.435222
Wyoming	714	wire line, cuttings	37.589441	-81.44327
Wyoming	721	wire line	37.589731	-81.42596
Wyoming	758	wire line	37.465167	-81.3739
Wyoming	783	wire line	37.529475	-81.291181
Wyoming	790	wire line	37.638365	-81.47549
Wyoming	792	wire line	37.465892	-81.395192
Wyoming	801	wire line	37.465457	-81.349342
Wyoming	827	wire line	37.511623	-81.315537
Wyoming	919	wire line	37.537603	-81.596999
Wyoming	1086	wire line	37.622678	-81.490768
Wyoming	1199	wire line	37.584651	-81.556973
Wyoming	1218	wire line	37.592053	-81.5444
Wyoming	1575	wire line	37.553435	-81.575012

Appendix B-1.

Cuttings observations table:

McDowell 189

depth	composition (%)	notes
1850-1860	red mudstone: 80% lith. ss.: 15% micrite: 5%	
1860-1870	red mudstone: 90% micrite: 10%	
1870-1880	red mudstone: 80% lith. ss.: 5% micrite: 15%	
1880-1890	red mudstone: 100%	
1890-1900	red mudstone: 5% calc. mudstone: 95%	
1900-1910	red mudstone: 5% calc. mudstone: 95%	
1910-1920	calc. mudstone: 100%	
1920-1930	red mudstone: 5% calc. mudstone: 95%	
1930-1940	gray mudstone: 20% calc. mudstone: 80%	
1940-1950	gray mudstone: 20% calc. mudstone: 80%	
1950-1960	gray mudstone: 50% calc. mudstone: 50%	
1960-1970	gray mudstone: 80% calc. mudstone: 20%	
1970-1980	calc. mudstone: 100%	
1980-1990	calc. mudstone: 100%	
1990-2000	calc. mudstone: 100%	
2000-2010	red mudstone: 100%	
2010-2020	red mudstone: 95% calc. mudstone: 5%	
2020-2030	red mudstone: 95% calc. mudstone: <5%	
2030-2040	red mudstone: <5% gray mudstone: 95%	
2040-2050	gray mudstone: 100%	

2050-2060	red mudstone: 90% gray mudstone: 10%	
2060-2070	red mudstone: 95% gray mudstone: <5%	
2070-2080	lith. ss.: 10% lg/wh. ss.: 90%	mottling present in r.m.
2080-2090	lith. ss.: 5% lg/wh. ss.: 95%	
2090-2100	lith. ss.: 5% lg/wh. ss.: 85% gray mudstone: 10%	
2100-2110	lith. ss.: <5% wh. ss.: 90% gray mudstone: <5%	mottling present in r.m. and calcareous
2110-2120	wh. ss.: 95% gray mudstone: <5%	black debris and pyrite present in c.m.
2120-2130	red mudstone: <5% wh. ss.: <5% gray mudstone: 95%	black debris and pyrite present in c.m.
2130-2140	wh. ss.: 10% lg/wh. ss.: 85% gray mudstone: 5%	black debris, pyrite, and fossils(?) present in c.m.
2140-2150	lg/wh. ss.: 85% gray mudstone: 15%	black debris, pyrite, and fossils(?) present in c.m.
2150-2160	lg/wh. ss.: 85% gray mudstone: 15%	black debris, pyrite, and fossils(?) present in c.m.
2160-2170	wh. ss.: 80% lg/wh. ss.: 15% gray mudstone: 5%	black debris, pyrite, and fossils(?) present in c.m.
2170-2180	wh. ss.: 80% lg/wh. ss.: 15% gray mudstone: 5%	black debris, pyrite, and fossils(?) present in c.m.
2180-2190	wh. ss.: 80% lg/wh. ss.: 15% gray mudstone: 5%	black debris, pyrite, and fossils(?) present in c.m.
2190-2200	wh. ss.: 95% gray mudstone: 5%	black debris present in c.m. and very silty
2200-2210	wh. ss.: 90% lg/wh. ss.: 5% gray mudstone: 5%	black debris present in c.m. and very silty
2210-2220	wh. ss.: 95% gray mudstone: 5%	black debris present in c.m. and very silty
2220-2230	wh. ss.: 95% gray mudstone: 5%	very silty
2230-2240	red mudstone: <5% wh. ss.: <5% gray mudstone: 95%	
2240-2250	wh. ss.: <5% gray mudstone: 95%	
2250-2260	gray mudstone: 100%	

2260-2270	red mudstone: <5% gray mudstone: 95%	
2270-2280	red mudstone: <5% gray mudstone: 95%	
2280-2290	gray mudstone: 100%	
2290-2300	gray mudstone: 100%	
2300-2310	red mudstone: <5% lg/wh. ss.: <5% gray mudstone: 95%	shale drapes present in lg/wh. ss.
2310-2320	lg/wh. ss.: <5% gray mudstone: 85% calc.mudstone: 10%	shale drapes present in lg/wh. ss.
2320-2330	gray mudstone: 10% calc.mudstone: 90%	
2330-2340	wh. ss.: <5% gray mudstone: 10% calc.mudstone: 85%	sand to gravel sized lithic clasts in wh. ss.
2340-2350	gray mudstone: 100%	
2350-2360	gray mudstone: 30% calc.mudstone: 70%	
2360-2370	red mudstone: 15% gray mudstone: 85%	
2370-2380	red mudstone: 10% lg/wh. ss.: 85% gray mudstone: <5%	
2380-2390	micrite:100%	
2390-2400	red mudstone: <5% lg/wh. ss.: 75% gray mudstone: 20%	
2400-2410	red mudstone: <5% lg/wh. ss.: 55% gray mudstone: 40%	
2410-2420	red mudstone: <5% lg/wh. ss.: 55% gray mudstone: 40%	
2420-2430	lg/wh. ss.: 85% gray mudstone: 15%	
2430-2440	wh. ss.: 10% lg/wh. ss.: 85% gray mudstone: 5%	
2440-2450	wh. ss.: 10% lg/wh. ss.: 85% gray mudstone: 5%	
2450-2460	wh. ss.: 10% lg/wh. ss.: 85% gray mudstone: <5%	

2460-	wh. ss.: <5%	
2470	lg/wh. ss.: 80%	
	gray mudstone: 15%	
2470-	lg/wh. ss.: 40%	
2480	gray mudstone: 60%	
2480-	lg/wh. ss.: 40%	
2490	gray mudstone: 60%	
2490-	red mudstone: 95%	pyrite present
2500	lg/wh. ss.: 5%	
2500-	red mudstone: <5%	black debris and plant fragment
2510	gray mudstone: 95%	impressions present in g.m.
2510-	red mudstone: <5%	
2520	wh. ss.: 40%	
	lg/wh. ss.: 50%	
	gray mudstone: <5%	
2520-	lg/wh. ss.: <5%	
2530	gray mudstone: 95%	
2530-	red mudstone: <5%	
2540	calc. mudstone: 95%	
2540-	calc. mudstone:	
2550	100%	
2550-	red mudstone: <5%	
2560	gray mudstone: 95%	
2560-	red mudstone: <5%	
2570	wh. ss.: 5%	
	lg/wh. ss.: 80%	
	gray mudstone: 10%	
2570-	red mudstone: <5%	
2580	wh. ss.: <5%	
	lg/wh. ss.: 75%	
	gray mudstone: 15%	
2580-	lg/wh. ss.: 20%	
2590	gray mudstone: 80%	
2590-	red mudstone: <5%	
2600	lg/wh. ss.: 5%	
	gray mudstone: 90%	
2600-	gray mudstone:	
2610	100%	
2610-	lg/wh. ss.: 95%	
2620	gray mudstone: 5%	
2620-	lg/wh. ss.: 100%	
2630		
2630-	lg/wh. ss.: 85%	
2640	gray mudstone: 15%	
2640-	lg/wh. ss.: 85%	
2650	gray mudstone: 15%	
2650-	lg/wh. ss.: 50%	shale drapes present in lg/wh. ss.
2660	gray mudstone: 50%	
2660-	red mudstone: <5%	
2670	lg/wh. ss.: 20%	
	gray mudstone: 75%	

2670- 2680	gray mudstone: 100%	shale drapes present in lg/wh. ss.
2680- 2690	wh. ss.: <5% gray mudstone: 80% calc.mudstone: 15%	
2690- 2700	wh. ss.: <5% gray mudstone: 95%	
2700- 2710	gray mudstone: 100%	
2710- 2720	gray mudstone: 100%	
2720- 2730	wh. ss.: <5% gray mudstone: 95%	
2730- 2740	wh. ss.: 90% gray mudstone: 10%	
2740- 2750	wh. ss.: 85% gray mudstone: 15%	
2750- 2760	gray mudstone: 100%	black debris and plant fragment impressions present in c.m.
2760- 2770	gray mudstone: 100%	fossils present
2770- 2780	gray mudstone: 100%	
2780- 2790	gray mudstone: 100%	
2790- 2800	red mudstone: <5% gray mudstone: 95%	shale drapes present in lg/wh. ss. and wh. ss.
2800- 2810	red mudstone: 5% gray mudstone: 95%	
2810- 2820	gray mudstone: 100%	
2820- 2830	red mudstone: <5% gray mudstone: 95%	
2830- 2840	red mudstone: <5% gray mudstone: 95%	shale drapes present in lg/wh. ss.
2840- 2850	gray mudstone: 100%	shale drapes present in lg/wh. ss.
2850- 2860	gray mudstone: 5% calc. mudstone: 15% micrite: 80%	pyrite present
2860- 2870	gray mudstone: 20% calc. mudstone: 40% micrite: 40%	
2870- 2880	gray mudstone: 40% calc. mudstone: 30% micrite: 30%	
2880- 2890	micrite:100%	
2890- 2900	micrite:100%	
2900- 2910	calc. mudstone: 10% micrite:90%	

2910-
2920

micrite:100%

Appendix B-2.

Cuttings observations table:

McDowell 216

depth	composition (%)	notes
1270-1280	gray mudstone: 90% micrite: 10%	
1280-1290	lg/wh. ss.: 20% gray mudstone: 50% micrite: 30%	lg/wh. ss. is vf and light gray
1290-1300	lg/wh. ss.: 10% gray mudstone: 50% calc. mudstone: 20% micrite: 30%	pyrite flakes present
1300-1310	gray mudstone: 15% micrite: 85%	
1310-1320	gray mudstone: 70% calc. mudstone: 15% micrite: 15%	
1320-1330	red mudstone: 5% gray mudstone: 70% calc. mudstone: 15% micrite: 15%	
1330-1340	lg/wh. ss.: 55% gray mudstone: 35% calc. mudstone: 10%	
1340-1350	lg/wh. ss.: 85% gray mudstone: 15%	
1350-1360	red mudstone: 90% gray mudstone: 10%	
1360-1370	red mudstone: 80% lith. ss.: 15% gray mudstone: 5%	mottling present in r.m.
1370-1380	red mudstone: 80% lith. ss.: 15% gray mudstone: 5%	
1380-1390	red mudstone: 95% gray mudstone: <5%	
1390-1400	red mudstone: 70% lg/wh. ss.: 20% gray mudstone: 10%	black spherical objects (vf-sized) in g.m.
1400-1410	red mudstone: 80% lith. ss.: 5% lg/wh. ss.: 10% gray mudstone: 5%	

1410- 1420	red mudstone: 65% lith. ss.: 20% lg/wh. ss.: 10% gray mudstone: <5%	black debris present in lg/wh. ss. (oc)
1420- 1430	red mudstone: 80% lith. ss.: 15% gray mudstone: 5%	mottling present in r.m.
1430- 1440	red mudstone: 90% lg/wh. ss.: <5% gray mudstone: <5%	r.m. is very clay rich
1440- 1450	red mudstone: 95% lg/wh. ss.: <5%	
1450- 1460	red mudstone: 80% lith. ss.: 15% lg/wh. ss.: 5%	
1460- 1470	red mudstone: 90% lg/wh. ss.: <5% gray mudstone: <5%	
1470- 1480	red mudstone: 90% lg/wh. ss.: 10%	
1480- 1490	red mudstone: 95% lg/wh. ss.: <5%	
1490- 1500	red mudstone: 95% lg/wh. ss.: 5%	
1500- 1510	red mudstone: 90% lg/wh. ss.: <5% gray mudstone: <5%	
1510- 1520	red mudstone: 90% lg/wh. ss.: <5% gray mudstone: <5%	r.m. is more brown/maroon than red
1520- 1530	red mudstone: 5% lith. ss.: 15% lg/wh. ss.: 10% gray mudstone: 70%	pyrite veins present in g.m.
1530- 1540	red mudstone: 10% lith. ss.: 30% lg/wh. ss.: <5% gray mudstone: 55%	lighter gray pieces of g.m. have significant amounts of black debris (oc)
1540- 1550	red mudstone: 65% lg/wh. ss.: 30% gray mudstone: 5%	shale drapes present in lg/wh. ss. black spherical objects (vf-sized) in g.m.
1550- 1560	red mudstone: 15% lg/wh. ss.: 60% gray mudstone: 25%	black spherical objects (vf-sized) in g.m. r.m. is bright red and mottled
1560- 1570	red mudstone: 10% lg/wh. ss.: 50% gray mudstone: 40%	lg/wh. ss. is vf and light gray
1570- 1580	red mudstone: <5% lg/wh. ss.: 10% gray mudstone: 85%	fragments of pyrite present

1580- 1590	red mudstone: <5% lg/wh. ss.: 5% gray mudstone: 45% calc. mudstone: 45%	small cuttings fragment make differentiation between g.m. and c.m. difficult
1590- 1600	red mudstone: <5% gray mudstone: 30% calc. mudstone: 60%	red and dark gray nodules of calcite in some fragments of c.m.
1600- 1610	wh. ss.: <5% gray mudstone: 25% calc. mudstone: 70%	red and dark gray nodules of calcite in some fragments of c.m.
1610- 1620	red mudstone: 70% gray mudstone: 20% calc. mudstone: 10%	r.m. is bright red/orange and may contain burrow casts
1620- 1630	red mudstone: 80% gray mudstone: 20%	
1630- 1640	red mudstone: 95% gray mudstone: <5%	
1640- 1650	red mudstone: 95% gray mudstone: 5%	r.m. may contain root traces
1650- 1660	red mudstone: 95% gray mudstone: 5%	
1660- 1670	red mudstone: 60% lg/wh. ss.: 10% gray mudstone: 30%	
1670- 1680	red mudstone: 95% gray mudstone: <5%	
1680- 1690	red mudstone: 95% gray mudstone: <5%	
1690- 1700	red mudstone: 90% gray mudstone: 10%	
1700- 1710	red mudstone: 90% gray mudstone: 10%	
1710- 1720	red mudstone: <5% lg/wh. ss.: 25% gray mudstone: 70%	lg/wh. ss. is fine grained and light gray g.m. is silty
1720- 1730	red mudstone: <5% lg/wh. ss.: 15% gray mudstone: 80%	black debris present (oc?)
1730- 1740	quartz sand: 100%	
1740- 1750	quartz sand: 90% gray mudstone: 10%	
1750- 1760	red mudstone: <5% lg/wh. ss.: 10% gray mudstone: 85%	
1760- 1770	wh. ss.: 5% lg/wh. ss.: 10% gray mudstone: 85%	pyrite present

1770- 1780	red mudstone: <5% wh. ss.: 5% lg/wh. ss.: 10% gray mudstone: 60% calc. mudstone: 20%	pyrite present
1780- 1790	gray mudstone: 60% calc. mudstone: 35% micrite: 5%	fossils present
1790- 1800	gray mudstone: 30% calc. mudstone: 60% micrite: 10%	fragment of micrite has irregular, wavy laminations (algal?) fossils present in c.m.
1800- 1810	red mudstone: 5% gray mudstone: 35% calc. mudstone: 40% micrite: 20%	
1810- 1820	gray mudstone: 60% calc. mudstone: 40%	
1820- 1830	red mudstone: 15% wh. ss.: <5% lg/wh. ss.: 25% gray mudstone: 40% calc. mudstone: 15%	
1830- 1840	red mudstone: 5% gray mudstone: 80% calc. mudstone: 15%	black spherical objects (vf-sized) in g.m.
1840- 1850	red mudstone: 5% gray mudstone: 90% calc. mudstone: 5%	g.m. is very silty r.m. is mottled
1850- 1860	red mudstone: 50% gray mudstone: 50%	r.m. is heavily mottled and more brown than red
1860- 1870	red mudstone: 50% gray mudstone: 50%	r.m. is heavily mottled and more brown than red
1870- 1880	red mudstone: 15% gray mudstone: 85%	r.m. is heavily mottled
1880- 1890	red mudstone: 5% gray mudstone: 75% calc. mudstone: 20%	
1890- 1900	red mudstone: <5% gray mudstone: 15% calc. mudstone: 80%	
1900- 1910	red mudstone: <5% calc. mudstone: 55% micrite: 40%	sparry replaced fossils in micrite
1910- 1920	red mudstone: 10% gray mudstone: 90%	pyrite present
1920- 1930	red mudstone: <5% gray mudstone: 80% calc. mudstone: 15%	
1930- 1940	red mudstone: <5% gray mudstone: 95%	r.m. is mottled g.m. is silty and light gray

1940-1950	gray mudstone: 80% calc. mudstone: 20%	
1950-1960	red mudstone: <5% gray mudstone: 80% calc. mudstone: 15%	
1960-1970	red mudstone: <5% gray mudstone: 80% calc. mudstone: 15%	
1970-1980	gray mudstone: 90% calc. mudstone: 10%	g.m. exhibits parallel laminations pyrite nodules and black debris present in c.m.
1980-1990	red mudstone: <5% gray mudstone: 95%	g.m. exhibits parallel laminations
1990-2000	red mudstone: 85% gray mudstone: <5%	r.m. is mottled
2000-2010	red mudstone: 85% gray mudstone: <5%	root haloes in r.m.
2010-2020	red mudstone: 20% gray mudstone: 80%	g.m. exhibits parallel laminations black spherical objects (vf-sized) in g.m. pyrite present
2020-2030	red mudstone: 5% gray mudstone: 90% calc. mudstone: 5%	r.m. is bright red and mottled
2030-2040	red mudstone: 10% gray mudstone: 60% calc. mudstone: 30%	g.m. is silty and light gray
2040-2050	red mudstone: 5% gray mudstone: 95%	r.m. is mottled
2050-2060	red mudstone: 85% gray mudstone: 15%	
2060-2070	quartz sand: 60% gray mudstone: 40%	pyrite present
2070-2080	red mudstone: 20% gray mudstone: 80%	
2080-2090	red mudstone: 5% gray mudstone: 95%	
2090-2100	red mudstone: 20% gray mudstone: 80%	
2100-2110	red mudstone: 60% gray mudstone: 40%	
2110-2120	lg/wh. ss.: 100%	
2120-2130	wh. ss.: 100%	
2130-2140	wh. ss.: 40% gray mudstone: 60%	
2140-2150	red mudstone: 5% gray mudstone: 95%	
2150-2160	red mudstone: 60% gray mudstone: 40%	

2160- 2170	red mudstone: 85% gray mudstone: 15%	pyrite present in g.m.
2170- 2180	red mudstone: 60% gray mudstone: 30% calc. mudstone: 10%	
2180- 2190	red mudstone: <5% gray mudstone: 85% calc. mudstone: 10%	
2190- 2200	gray mudstone: 80% calc. mudstone: 20%	
2200- 2210	red mudstone: 5% gray mudstone: 80% calc. mudstone: 15%	
2210- 2220	red mudstone: 10% gray mudstone: 85% calc. mudstone: 5%	
2220- 2230	red mudstone: 60% quartz sand: 10% gray mudstone: 30%	
2230- 2240	quartz sand: 75% gray mudstone: 25%	
2240- 2250	quartz sand: 100%	
2250- 2260	red mudstone: 20% quartz sand: 60% gray mudstone: 20%	
2260- 2270	red mudstone: 50% quartz sand: 30% gray mudstone: 20%	ped structures and slicks in r.m.
2270- 2280	red mudstone: 25% wh. ss.: 15% gray mudstone: 60%	
2280- 2290	red mudstone: 5% quartz sand: 55% gray mudstone: 40%	
2290- 2300	red mudstone: 20% gray mudstone: 80%	coaly, leafy material in g.m.
2300- 2310	red mudstone: 25% wh. ss.: 15% gray mudstone: 60%	
2310- 2320	red mudstone: 5% wh. ss.: 5% gray mudstone: 90%	
2320- 2330	red mudstone: 10% quartz sand: 70% gray mudstone: 20%	
2330- 2340	red mudstone: 30% gray mudstone: 35% calc. mudstone: 35%	calcite filled fractures in fragments of r.m.

2340- 2350	red mudstone: 5% gray mudstone: 45% calc. mudstone: 40%	
2350- 2360	red mudstone: 10% gray mudstone: 50% calc. mudstone: 40%	
2360- 2370	lg/wh. ss.: 85% gray mudstone: 15%	
2370- 2380	red mudstone: 40% gray mudstone: 60%	bituminous coal fragments present sulfur odor from packet
2380- 2390	gray mudstone	bituminous coal fragments present sulfur odor from packet g.m. is a dark gray
2390- 2400	red mudstone: 20% lg/wh. ss.: 40% gray mudstone: 40%	shale drapes present in lg/wh. ss.
2400- 2410	red mudstone: 15% wh. ss.: 5% lg/wh. ss.: 50% gray mudstone: 30%	shale drapes present in lg/wh. ss.
2410- 2420	lg/wh. ss.: 70% gray mudstone: 30%	
2420- 2430	red mudstone: 5% lg/wh. ss.: 60% gray mudstone: 35%	
2430- 2440	red mudstone: 5% wh. ss.: 35% wh/lg. ss.: 20% gray mudstone: 40%	

Appendix B-3.

Cuttings observations table:

Raleigh 15

depth	composition (%)	notes
1345-1355	wh. ss.: <5% micrite:>95%	
1355-1365	calc. mudstone: 30% micrite: 70%	sparry calcite replaced fossils framboidal pyrite present in c.m.
1365-1375	calc. mudstone: 40% micrite: 60%	sparry calcite replaced fossils dark pellets present
1375-1385	red mudstone: 55% wh. ss.: 10% lg/wh ss.: 25% micrite: 10%	sparry calcite replaced fossils pyrite replacement in burrow tubes
1385-1395	red mudstone: 90% hem. st. ss.: 5% gray mudstone: <5%	
1395-1405	red mudstone: 90% gray mudstone: 5% calc. mudstone: <5%	r.m. is calc. and mottling is present pyrite present in c.m. and g.m.
1405-1415	red mudstone: 85% hem. st. ss.: 10% gray mudstone: <5%	r.m. is calc. and mottling is present
1415-1425	red mudstone: 60% hem. st. ss.: 25% lg/wh. ss.: 10% gray mudstone: 5%	r.m. is calc. and mottling is present
1425-1435	red mudstone: 95% lg/wh ss.: <5%	r.m. is calc. and mottling is present
1435-1445	red mudstone: 55% hem. st. ss.: 40% lg/wh. ss.: <5%	r.m. is slightly calc. and mottling is present h.s.s contains large quantity of silt
1445-1455	red mudstone: 70% hem. st. ss.: 20% lg/wh. ss.: 5% micrite: <5%	h.s.s contains large quantity of silt
1455-1465	red mudstone: 75% hem. st. ss.: 25%	
1465-1475	red mudstone: 60% hem. st. ss.: 35% calc. mudstone: <5%	

1475- 1485	red mudstone: 85% hem. st. ss.: 10% lg/wh. ss.: 5%	
1485- 1495	red mudstone: 85% hem. st. ss.: 10% lg/wh. ss.: 5%	lg/wh. ss. has shale partings
1495- 1505	red mudstone: 85% lg/wh. ss.: 5% gray mudstone: 10%	g.m. is entirely clay and light gray with organic debris
1505- 1515	red mudstone: 95% lg/wh ss.: 5%	
1515- 1525	red mudstone: 90% lg/wh ss.: 10%	
1525- 1535	red mudstone: 40% lg/wh. ss.: 5% gray mudstone: 55%	fragments of pyrite present
1535- 1545	red mudstone: 55% gray mudstone: 45%	small portion (5%) of g.m. is black r.m. is mottled
1545- 1555	red mudstone: 60% hem. st. ss.: 35% gray mudstone: <5%	r.m. is mottled
1555- 1565	red mudstone: 95% gray mudstone: <5%	r.m. is mottled
1560- 1575	red mudstone: 95% gray mudstone: <5%	
1575- 1585	red mudstone: 90% lg/wh ss.: 10%	some black debris in the r.m.
1585- 1595	red mudstone: 90% lg/wh ss.: 10%	r.m. is slightly mottled
1595- 1605	red mudstone: 90% gray mudstone: 10%	small portion (5%) of g.m. is black
1605- 1615	red mudstone: 90% lg/wh. ss.: 5% gray mudstone: <5%	
1615- 1625	red mudstone: 65% lg/wh. ss.: 10% gray mudstone: 25%	
1625- 1635	red mudstone: 95% gray mudstone: 5%	r.m. is calc. and mottled
1635- 1645	red mudstone: 85% lg/wh. ss.: 5% gray mudstone: 10%	r.m. is calc. and has slicks much of the lg/wh. ss. is gray and vf grained

1645- 1650	red mudstone: 85% lg/wh. ss.: 10% gray mudstone: <5%	
1650- 1657	red mudstone: 90% lg/wh. ss.: 5% gray mudstone: <5%	r.m. is very silt rich and more brown than red
1657- 1667	red mudstone: 75% lg/wh. ss.: <5% gray mudstone: 20%	
1667- 1677	red mudstone: 65% lg/wh. ss.: 25% gray mudstone: 10%	lg/wh. ss. is vf grained and completely gray, and difficult to discern from coarse gray mudstone
1677- 1687	red mudstone: <5% gray mudstone: 55% calc.mudstone: 40%	g.m. and c.m. are light gray and silty
1687- 1697	red mudstone: <5% gray mudstone: 55% calc.mudstone: 40%	g.m. and c.m. are light gray and silty
1697- 1707	red mudstone: <5% gray mudstone: 25% calc.mudstone: 60% micrite: 10%	sparry replaced fossils present
1707- 1717	red mudstone: 40% lg/wh. ss.: 10% calc.mudstone: 35% micrite: 15%	r.m. is mottled and has root haloes fossil fragments are ubiquitous in micrite
1717- 1727	red mudstone: 40% hem. St. ss.: <5% lg/wh. ss.: 30% calc.mudstone: 20% micrite: 5%	fossil fragments are ubiquitous in micrite
1727- 1737	red mudstone: 85% hem. st. ss.: 10% calc. mudstone: <5%	
1737- 1745	red mudstone: 85% hem. st. ss.: 10% gray mudstone: <5%	
1747- 1757	red mudstone: <5% lg/wh. ss.: 15% gray mudstone: 80%	
1757- 1762	red mudstone: <5% lg/wh. ss.: 15% gray mudstone:	shale partings present in lg/wh. ss.

80%

1762- 1776	red mudstone: 10% wh. Ss.: 50% lg/wh. ss.: 20% gray mudstone: 20%	fragments of pyrite present wh. ss. has black debris
1773- 1780	red mudstone: 25% wh. ss.: 65% gray mudstone: 10%	
1780- 1790	wh. ss.: <5% lg/wh. ss.: 30% gray mudstone: 40%	coaly material present calc. fossils in g.m. and c.m.
1790- 1800	red mudstone: 15% lg/wh. ss.: 40% gray mudstone: 30% calc.mudstone: 15%	
1800- 1810	lg/wh. ss.: 70% gray mudstone: <5% micrite: 15% skel. wh. ls: 10%	lg/wh. ss. may be calc. cement
1810- 1820	calc. mudstone: 85% micrite: 15%	pyrite present in c.m.
1820- 1825	red mudstone: 20% gray mudstone: 5% calc. mudstone: 65% micrite: 5%	
1825- 1832	red mudstone: 80% gray mudstone: 20%	
1832- 1842	red mudstone: 80% gray mudstone: 20%	r.m. is more brown/maroon than red
1842- 1852	red mudstone: 20% lg/wh. ss.: 70% calc.mudstone: <5% micrite: 5%	r.m. is more brown/maroon than red micrite is actually closer to a packstone
1852- 1862	red mudstone: 15% wh. ss.: 45% lg/wh. ss.: 20% gray mudstone: 20%	micrite is actually closer to a packstone
1862- 1869	red mudstone: <5% wh. ss.: 30% lg/wh. ss.: 15% gray mudstone: 50%	wh. ss. ls either partially calcite cemented or has calcite fragments in it larger g.m. chunks appear to be bioturbated

1868- 1872	wh. ss.: 85% gray mudstone: 15%	
1872- 1877	red mudstone: <5% wh. ss.: 90% gray mudstone: 5%	
1877- 1885	wh. ss.: 90% gray mudstone: 10%	Fe-oxide staining ob fragments
1885- 1895	wh. ss.: 95% gray mudstone: <5%	
1895- 1905	wh. ss.: 95% gray mudstone: <5%	
1905- 1915	wh. ss.: 95% gray mudstone: <5%	
1905- 1915	wh. ss.: 95% gray mudstone: <5%	wh. ss. is 100% qtz
1915- 1925	lg/wh. ss.: <5% gray mudstone: 95%	g.m. is very silt rich
1925- 1935	red mudstone: 95% gray mudstone: 5%	
1935- 1945	red mudstone: 95% gray mudstone: 5%	
1945- 1955	red mudstone: 95% gray mudstone: 5%	
1955- 1965	red mudstone: 95% gray mudstone: 5%	
1965- 1975	red mudstone: 75% gray mudstone: 15% skel. wh. ls: 10%	
1975- 1980	red mudstone: 65% gray mudstone: 35%	root haloes present in r.m.
1985- 1995	red mudstone: 60% gray mudstone: 40%	
1995- 2005	red mudstone: 60% gray mudstone: 30% micrite: <5% skel. wh. ls: 5%	
2005- 2015	red mudstone: 60% lg/wh. ss.: 20% gray mudstone: 20%	

2015- 2025	red mudstone: 10% gray mudstone: 35% calc.mudstone: 40% micrite: 10% skel. wh. ls: 5%	pyrite present in g.m.
2020- 2030	micrite: 100%	micrite is actually closer to a packstone <i>perhaps misplaced sample-> lithology doesn't really fit</i>
	red mudstone: 5% gray mudstone: 60% calc.mudstone: 30% skel. wh. ls: <5%	c.m. is dark, with pyrite, and some quartz sand
2035- 2045	red mudstone: 10% gray mudstone: 35% calc.mudstone: 45% micrite: 10%	pyrite present
2045- 2055	red mudstone: 10% gray mudstone: 80% calc. mudstone: 10%	pyrite present
2055- 2065	red mudstone: 15% gray mudstone: 65% calc.mudstone: 10% skel. wh. ls: 10%	
2065- 2075	gray mudstone: 80% calc. mudstone: 20%	
2075- 2085	gray mudstone: 60% calc. mudstone: 40%	
2085- 2095	wh. ss.: 5% gray mudstone: 60%	wh. ss. is calcite cemented
2095- 2105	red mudstone: 30% lg/wh. ss.: 15% gray mudstone: 55%	
2105- 2115	red mudstone: 30% lg/wh. ss.: 15% gray mudstone: 55%	g.m. is primarily silt
2115- 2125	red mudstone: 60% gray mudstone: 40%	g.m. is primarily silt
2125- 2135	red mudstone: 35% gray mudstone: 65%	g.m. is primarily silt

2135- 2145	gray mudstone: 55% calc.mudstone: 40% skel. wh. ls: <5%	dark spherical nodules present in some fragments of silty c.m.
2145- 2155	gray mudstone: 20% calc.mudstone: 80%	dark spherical nodules present in some fragments of silty c.m.
2155- 2160	gray mudstone: 10% calc.mudstone: 60% micrite: 30%	
2165- 2175	lg/wh. ss.: 30% gray mudstone: 40% calc.mudstone: 20% micrite: 10%	
2175- 2185	lg/wh. ss.: 40% gray mudstone: 60%	g.m. very silty
2185- 2195	lg/wh. ss.: 40% gray mudstone: 60%	g.m. very silty parallel laminations present in lg/wh. ss.
2195- 2205	wh. ss.: 10% lg/wh. ss.: 85% gray mudstone: 5%	g.m. very silty parallel laminations present in lg/wh. ss.
2205- 2215	wh. ss.: 10% lg/wh. ss.: 85% gray mudstone: 5%	parallel laminations present in lg/wh. ss.
2215- 2225	wh. ss.: 20% lg/wh. ss.: 75% gray mudstone: 5%	parallel laminations present in lg/wh. ss.
2225- 2235	gray mudstone: 100%	g.m. has parallel laminations of silt rich and clay rich laminations
2235- 2245	gray mudstone: 100%	g.m. has parallel laminations of silt rich and clay rich laminations
2245- 2255	red mudstone: <5% lg/wh. ss.: <5% gray mudstone: 95%	g.m. has parallel laminations of silt rich and clay rich laminations
2255- 2260	red mudstone: <5% lg/wh. ss.: <5% gray mudstone: 95%	g.m. has parallel laminations of silt rich and clay rich laminations
2268- 2275	red mudstone: <5% gray mudstone: 95%	g.m. has parallel laminations of silt rich and clay rich laminations
2275- 2285	gray mudstone: 70% micrite: 30%	micrite is actually closer to a packstone

2285- 2295	gray mudstone: 10% calc. mudstone: 30% micrite: 60%	
2295- 2305	micrite: 100%	fossils present

Appendix B-4.

Cuttings observations table:

Raleigh 305

depth	composition (%)	notes
1420-1430	micrite: 100%	no fossils
1430-1440	wh. ss.: <5% micrite: 95%	pyrite present in some fragments of micrite
1440-1450	red mudstone: 95% micrite: 5%	r.m. slicks present
1450-1460	red mudstone: 90% gray mudstone: 5% micrite: 5%	
1460-1470	red mudstone: 90% calc. mudstone: 10%	
1470-1480	red mudstone: 95% calc. mudstone: 5%	
1480-1490	red mudstone: 95% gray mudstone: 5%	
1490-1500	red mudstone: 20% calc. mudstone: 80%	
1500-1510	red mudstone: 15% glauc. ss.: 75% calc. mudstone: 10%	
1510-1520	red mudstone: 15% glauc. ss.: 70% gray mudstone: 10% calc. mudstone: 5%	bituminous coal fragments present
1520-1530	red mudstone: 5% wh. ss.: 80% glauc. ss.: 10% gray mudstone: 5%	pyrite fragments present wh. ss. has calc. cement and mud drapes present
1530-1540	red mudstone: 10% glauc. ss.: 80% calc. mudstone: 10%	
1540-1550	red mudstone: 5% glauc. ss.: 85% gray mudstone: 10%	glauc ss. has calc. cement

1550- 1560	red mudstone: <5% wh. ss.: 90% gray mudstone: 5% skel. wh. ls: <5%	bituminous coal fragments present pyrite fragments present wh. ss. has coaly fragments
1560- 1570	red mudstone: <5% wh. ss.: 75% lg/wh. ss.: 20	wh. ss. has calc. cement
1570- 1580	red mudstone: 10% wh. ss.: 5% lg/wh. ss.: 70% gray mudstone: 10% calc. mudstone: 5%	wh. ss. has calc. cement
1580- 1590	red mudstone: 95% gray mudstone: 5%	r.m. is calc.
1590- 1600	red mudstone: <5% lg/wh. ss.: 90% gray mudstone: 5%	lg/wh. ss. is vf grained and completely gray, and difficult to discern from coarse gray mudstone
1600- 1610	lg/wh. ss.: 85% gray mudstone: 15%	lg/wh. ss. is vf grained and completely gray, and difficult to discern from coarse gray mudstone
1610- 1620	lg/wh. ss.: 75% gray mudstone: 25%	lg/wh. ss. is vf grained and completely gray, and difficult to discern from coarse gray mudstone
1620- 1630	lg/wh. ss.: 15% gray mudstone: 85%	lg/wh. ss. is vf grained and completely gray, and difficult to discern from coarse gray mudstone
1630- 1640	lg/wh. ss.: 15% gray mudstone: 85%	lg/wh. ss. is vf grained and completely gray, and difficult to discern from coarse gray mudstone
1640- 1650	red mudstone: 5% wh. ss.: 5% lg/wh. ss.: 55% gray mudstone: 35%	
1650- 1660	red mudstone: <5% lg/wh. ss.: 65% gray mudstone: 10% skel. wh. ls: 20%	
1660- 1670	red mudstone: <5% lg/wh. ss.: 5% gray mudstone: 75% skel. wh. ls: 15%	
1670- 1680	red mudstone: 15% glauc. ss.: 70% gray mudstone: 10% calc. mudstone: 5%	sparry calcite replaced fossils in c.m. and g.m.

1680- 1690	red mudstone: 10% wh. ss.: 5 yell_rock.: 70% gray mudstone: 15% micrite: 10%	fragments of highly organic rich shale/lignite present
1690- 1700	red mudstone: 10% yell_rock.: 20% calc. mudstone: 55% skel. wh. ls: 5% micrite: 10%	fragments of highly organic rich shale/lignite present
1690- 1700 <i>?repeat?</i>	red mudstone: 5% yell_rock.: 25% gray mudstone: 30% calc. mudstone: 30% skel. wh. ls: 5% micrite: 5%	sparry calcite replaced fossils in c.m. and g.m.
1700- 1710	red mudstone: 25% wh. ss.: 5% yell_rock.: 20% gray mudstone: 45% calc. mudstone: 5%	r.m. is calc. bituminous coal fragments present
1710- 1720	red mudstone: 35% yell_rock.: 20% gray mudstone: 40% micrite: 5%	shell imprint in micrite
1720- 1730	red mudstone: 15% yell_rock.: 15% gray mudstone: 65% calc. mudstone: 5%	laminations present in y_r
1730- 1740	red mudstone: 5% wh. ss.: 5% lg/wh. ss.: 10% gray mudstone: 55% calc. mudstone: 10% micrite: 15	fossils present in micrite
1740- 1750	red mudstone: 5% wh. ss.: 5% gray mudstone: 75% calc. mudstone: 5% micrite: 10%	
1750- 1760	red mudstone: 10% gray mudstone: 75% calc. mudstone: 10% micrite: 5%	fossils present in micrite
1760- 1770	red mudstone: 5% gray mudstone: 85% calc. mudstone: 10%	

1770- 1780	red mudstone: 5% gray mudstone: 80% calc. mudstone: 15%	
1780- 1790	red mudstone: <5% gray mudstone: 90% calc. mudstone: 5%	g.m. is mostly clay
1790- 1800	red mudstone: <5% gray mudstone: 50% calc. mudstone: 35% micrite: 10%	cm is very fossiliferous
1800- 1810	red mudstone: 65% gray mudstone: 20% calc. mudstone: 15%	
1810- 1820	red mudstone: 95% gray mudstone: 5%	
1820- 1830	red mudstone: 95% gray mudstone: <5%	r.m. is calc.
1830- 1840	red mudstone: 95% gray mudstone: <5%	
1840- 1850	red mudstone: <5% wh. ss.: 5% lg/wh. ss.: 15% gray mudstone: 75%	
1850- 1860	lg/wh. ss.: 5% gray mudstone: 90% calc. mudstone: 5%	
1860- 1870	gray mudstone: 95% calc. mudstone: 5%	coaly debris present in some g.m. pieces fragments of pyrite present
1870- 1880	red mudstone: 65% gray mudstone: 20% calc. mudstone: 15%	g.m. is very silty
1880- 1890	red mudstone: 20% wh. ss.: 7% gray mudstone: 10% calc. mudstone: 5%	wh. ss. has a few red/brown, spherical nodules g.m. has pyrite present
1890- 1900	red mudstone: 5% wh. ss.: 20% gray mudstone: 60% calc. mudstone: 15%	
1900- 1910	red mudstone: 5% wh. ss.: 20% gray mudstone: 60% calc. mudstone: 15%	

1900-1960		missing section
1960-1970	red mudstone: <5% gray mudstone: 10% calc. mudstone: 85%	fossils present in c.m.
1970-1980	wh. ss.: 95% gray mudstone: <5%	
1980-1990	wh. ss.: 90% gray mudstone: 10%	
1990-2000	red mudstone: 10% wh. ss.: 70% lg/wh. ss.: 5% gray mudstone: 15%	
2000-2010	red mudstone: 5% wh. ss.: 90% gray mudstone: 5%	
2010-2020	red mudstone: 5% wh. ss.: 90% gray mudstone: <5%	
2020-2030	wh. ss.: >95% gray mudstone: <5%	
2030-2040	wh. ss.: >95% gray mudstone: <5%	
2040-2050	wh. ss.: >95% gray mudstone: <5%	
2040-2050 <i>?repeat?</i>	red mudstone: 10% hem. st. ss.: 75% gray mudstone: 15%	r.m. is calc.
2050-2060	red mudstone: 10% micrite: 90%	sparse fossils present in micrite
2060-2070	micrite: 100%	sparse fossils present in micrite
2070-2080	micrite: 100%	sparse fossils present in micrite
2080-2090	red mudstone: 10% gray mudstone: 20% micrite: 90% pr. Calc. ls.: 50%	
2090-2100	micrite: 100%	sparse fossils present in micrite
2100-2110	skel. wh. ls: 15% micrite: 85%	micrite is very fossiliferous
2110-2120	skel. wh. ls: 15% micrite: 85%	micrite is very fossiliferous

2120- 2130	gray mudstone: 15% micrite: 85%	micrite is actually sparry bioclastic limestone
2130- 2140	red mudstone: 40% micrite: 60%	r.m. is calc.?
2140- 2150	micrite: 100%	micrite is actually sparry bioclastic limestone
2150- 2160	micrite: 100%	micrite is actually sparry bioclastic limestone

Appendix B-5.

Cuttings observations table:

Raleigh 489

depth	composition (%)	notes
1140-1150	red mudstone: 5% wh. ss.: 10% gray mudstone: 55% micrite: 30%	calc. horizon in a fragment of g.m. with dark fragments in horizon sparry replaced fossils in micrite
1150-1160	red mudstone: 5% wh. ss.: 15% gray mudstone: 60% micrite: 20%	sparry replaced fossils in micrite
1160-1170	red mudstone: 5% wh. ss.: 15% gray mudstone: 60% calc. mudstone: 30% micrite: 20%	sparry replaced fossils in micrite pyrite present in g.m.
1170-1180	co. lith. silts: 100%	
1180-1190	red mudstone: 5% co. lith. silts: 25% gray mudstone: 50% calc. mudstone: 10% micrite: 10%	fragments of bituminous coal present
1190-1200	red mudstone: 85% calc. mudstone: 5% micrite: 10%	
1200-1210		missing section
1210-1220	red mudstone: 95% gray mudstone: 5%	r.m. is calc.
1220-1230	red mudstone: 95% gray mudstone: 5%	r.m. is calc. and mottled
1230-1240	red mudstone: 100%	r.m. is calc. and mottled
1240-1250	red mudstone: 100%	r.m. is calc. and mottled
1250-1260	red mudstone: 100%	r.m. is calc. and mottled
1260-1270	red mudstone: 95% gray mudstone: 5%	r.m. is calc. and mottled
1270-1300		missing section
1300-1310	red mudstone: 90% gray mudstone: 10%	r.m. is calc.

1310-1320	red mudstone: 95% gray mudstone: <5%	
1320-1330	red mudstone: 100%	
1330-1340	red mudstone: 100%	fragments of bituminous coal present
1340-1350	red mudstone: 100%	r.m. is calc., mottled, and has slicks
1350-1360	red mudstone: 100%	r.m. is calc., mottled, and has slicks
1360-1370	red mudstone: 100%	r.m. is calc., mottled, and has slicks
1370-1380	red mudstone: 100%	r.m. is calc., mottled, and has slicks
1380-1390	red mudstone: 100%	r.m. is calc., mottled, and has slicks fragments of bituminous coal present
1390-1470		missing section
1470-1480	red mudstone: 95% micrite: 5%	r.m. is calc., mottled, and has slicks micrite is reddish gray
1480-1490	red mudstone: 100%	r.m. is calc., mottled, and has slicks
1490-1500	red mudstone: 95% micrite: 5%	r.m. is calc., mottled, and has slicks
1500-1510	red mudstone: 100%	r.m. is calc.
1510-1520	red mudstone: 100%	r.m. is calc.
1520-1530	red mudstone: 95% micrite: 5%	r.m. is calc.
1530-1540		missing section
1540-1550	red mudstone: 100%	r.m. is calc.
1550-1630		missing section
1630-1640	red mudstone: 100%	r.m. is calc.
1640-1650	red mudstone: 100%	r.m. is calc.
1650-1660	red mudstone: 100%	r.m. is calc. and has slicks
1660-1670	red mudstone: 100%	
1670-1690		missing section
1690-1700	red mudstone: 100%	
1700-1710	red mudstone: 10% gray mudstone: 90%	fragments of bituminous coal present
1710-1720	red mudstone: 5% gray mudstone: 35% calc.	fragments of bituminous coal present

	mudstone: 60%	
1720-1730	red mudstone: <5% gray mudstone: 25% calc. mudstone: 70%	pyrite present
1730-1740	red mudstone: <5% gray mudstone: 55% calc. mudstone: 40%	g.m. and c.m. are both very silty and light gray->they are difficult to discern from one another
1740-1750	red mudstone: <5% gray mudstone: 55% calc. mudstone: 40%	g.m. and c.m. are both very silty and light gray->they are difficult to discern from one another
1750-1760	red mudstone: <5% gray mudstone: 55% calc. mudstone: 40%	g.m. and c.m. are both very silty and light gray->they are difficult to discern from one another
1760-1820		missing section
1820-1830	red mudstone: 95% calc. mudstone: 5%	
1830-1850		missing section
1840-1850	red mudstone: 30% gray mudstone: 50% calc. mudstone: 20%	
1850-1860	red mudstone: 95% calc. mudstone: 5%	
1860-1880		missing section
1880-1890	red mudstone: 90% calc. mudstone: 10%	r.m. is calc.
1890-1900	red mudstone: 95% calc. mudstone: 5%	fragments of bituminous coal present r.m. is calc.
1900-1910	red mudstone: 85% gray mudstone: 10% calc. mudstone: 5%	g.m. is light gray
1900-1910	red mudstone: 95% calc. mudstone: 5%	g.m. is light gray
1910-1920	red mudstone: 95% gray mudstone: 5%	
1920-1930	red mudstone: 100%	
1930-1940	red mudstone: 100%	
1940-1950	red mudstone: 100%	r.m. is mottled
1950-1960	red mudstone: 100%	r.m. is mottled and has slicks

1960-1970	red mudstone: 100%	r.m. has slicks
1970-1980	red mudstone: 100%	r.m. has slicks
1980-1990	red mudstone: 100%	
1990-2000		missing section
2000-2010	red mudstone: 100%	r.m. is calc.
2010-2020	red mudstone: 100%	
2020-2300		missing section
2300-2310	calc. mudstone: 20% micrite: 80%	
2310-2320	micrite: 100%	pyrite present
2320-2330	micrite: 100%	sparry calcite replaced fossils

Appendix B-6.

Cuttings observations table:

Wyoming 714

depth	composition (%)	notes
1300-1310	wh. ss.: <5% gray mudstone: 15% calc. mudstone: 70% micrite: 10%	c.m. is silty
1310-1320	calc. mudstone: <10% micrite: >90%	fossils present (bivalves?)
1320-1330	calc. mudstone: <10% micrite: >90%	fossils present (bivalves and ostracods?)
1330-1340	micrite: 100%	fossils present (bivalves and ostracods?)
1340-1350	red mudstone: 100%	r.m. is slightly calcareous
1350-1360	red mudstone: 100%	r.m. is calcareous
1360-1370	red mudstone: 100%	r.m. is slightly calcareous and mottled
1370-1380	red mudstone: <5% wh. ss.: 15% lg/wh. ss.: 30% gray mudstone: 40% calc. mudstone: 10%	wh. ss. Is calcite cemented
1380-1390	red mudstone: 100%	r.m. is slightly calcareous, mottled, and has root traces
1390-1400	red mudstone: 5% lg/wh. ss.: 5% gray mudstone: 90%	r.m. is more brown than red
1400-1410	red mudstone: <5% gray mudstone: 85% calc. mudstone: 10%	r.m. is more brown than red
1410-1420	red mudstone: <5% gray mudstone: 60% calc. mudstone: 35%	
1420-1430	gray mudstone: 40% calc. mudstone: 60%	c.m. is silty
1430-1440	gray mudstone: 40% calc. mudstone: 60%	

1440- 1450	red mudstone: 5% wh. ss.: 5% lg/wh. ss.: 60% gray mudstone: 30%	
1450- 1460	red mudstone: 5% lg/wh. ss.: 60% gray mudstone: 35%	
1460- 1470	red mudstone: 95% gray mudstone: 5%	r.m. is very calcareous and slightly mottled
1470- 1480	red mudstone: 100%	r.m. is very calcareous and slightly mottled
1480- 1490	red mudstone: 100%	r.m. is calcareous
1490- 1500	red mudstone: >95% gray mudstone: <5%	black, organic debris present in r.m. r.m. is calcareous
1500- 1510	red mudstone: <5% lg/wh. ss.: 15% gray mudstone: 80%	
1510- 1520	red mudstone: 100%	
1520- 1530	red mudstone: <5% lg/wh. ss.: 10% gray mudstone: 85%	
1530- 1540	red mudstone: <5% wh. ss.: <5% lg/wh. ss.: 80% gray mudstone: 5%	
1540- 1550	red mudstone: 100%	r.m. is calcareous
1550- 1560	red mudstone: 95% gray mudstone: 5%	r.m. is calcareous
1560- 1570	red mudstone: 100%	r.m. is very calcareous
1570- 1580	red mudstone: 100%	
1580- 1590	red mudstone: 100%	
1590- 1600	red mudstone: 100%	
1600- 1610	red mudstone: <5% lg/wh. ss.: 10% gray mudstone: 85%	
1610- 1620	red mudstone: 50% gray mudstone: 50%	coaly material in g.m. r.m. has mottling
1620- 1630	red mudstone: 35% gray mudstone: 65%	r.m. has mottling
1630- 1640	red mudstone: 30% gray mudstone: 65% calc. mudstone: 5%	r.m. has mottling

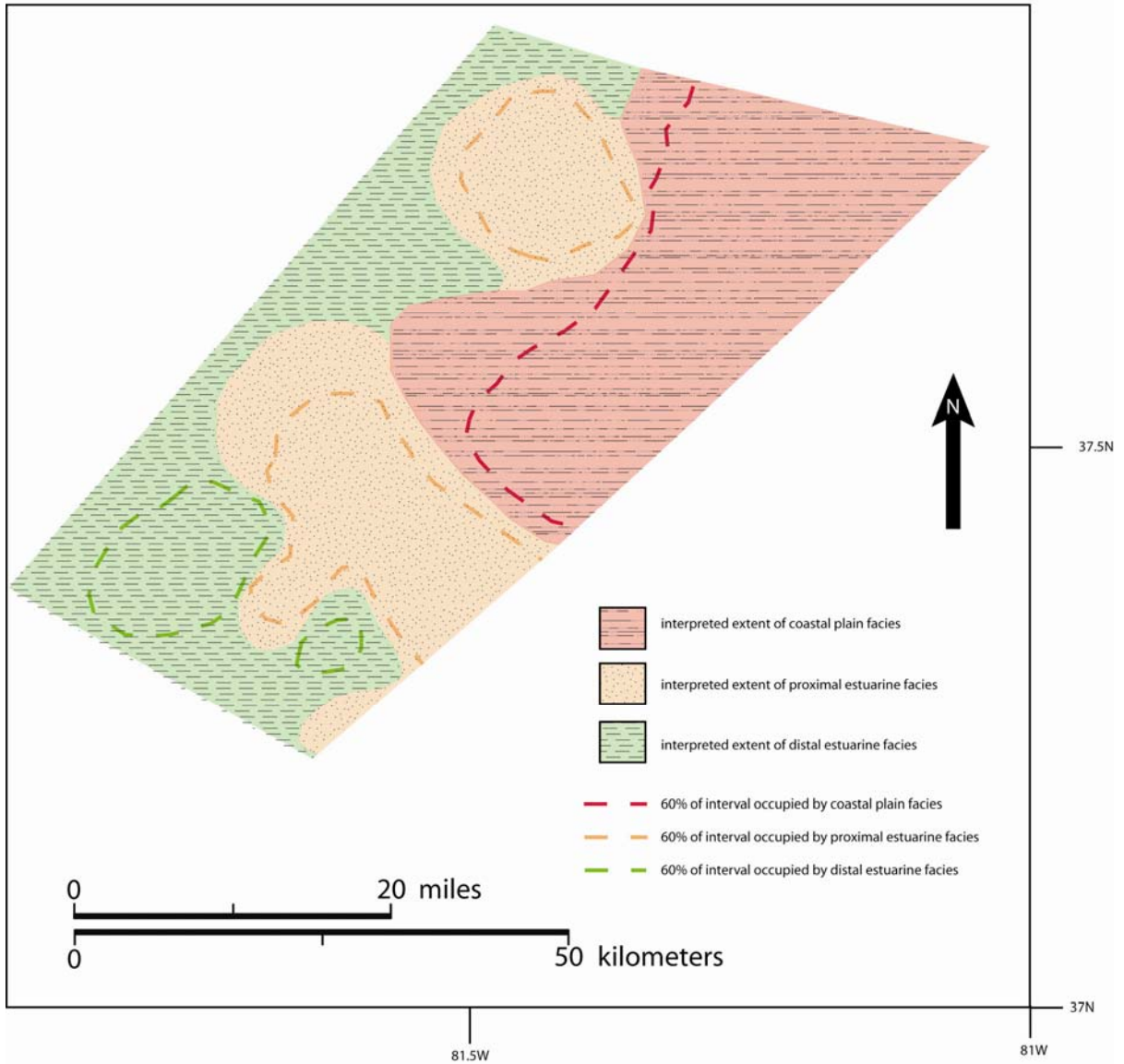
1640- 1650	red mudstone: 5% gray mudstone: 75% calc. mudstone: 20%	pyrite present
1650- 1660	red mudstone: <5% gray mudstone: 15% calc. mudstone: 80%	c.m. has significant amounts of pyrite and black debris
1660- 1670	red mudstone: 15% gray mudstone: 75% calc. mudstone: 10%	
1670- 1680	red mudstone: 15% gray mudstone: 80% calc. mudstone: 10% skel. wh. ls: 5%	
1680- 1690	gray mudstone: 75% calc. mudstone: 20% skel. wh. ls: 5%	
1690- 1700	lg/wh. ss.: 10% gray mudstone: 90%	
1700- 1710	lg/wh. ss.: 5% gray mudstone: 95%	
1710- 1720	lg/wh. ss.: 5% gray mudstone: 95%	
1720- 1730	lg/wh. ss.: 10% gray mudstone: 90%	
1730- 1740	lg/wh. ss.: 40% gray mudstone: 60%	
1740- 1750	red mudstone: <5% br. sand: 15% gray mudstone: 80%	
1750- 1760	gray mudstone: 100%	
1760- 1770	lg/wh. ss.: 40% gray mudstone: 60%	lg/wh. ss. is vf pyrite present
1770- 1780	lg/wh. ss.: 70% gray mudstone: 30%	lg/wh. ss. is vf pyrite present
1780- 1790	lg/wh. ss.: 15% gray mudstone: 85%	lg/wh. ss. is vf
1790- 1800	lg/wh. ss.: 5% gray mudstone: 95%	lg/wh. ss. is vf
1800- 1810	lg/wh. ss.: 15% gray mudstone: 85%	lg/wh. ss. is vf
1810- 1820	lg/wh. ss.: 60% gray mudstone: 40%	lg/wh. ss. is vf pyrite present
1820- 1830	lg/wh. ss.: 5% gray mudstone: 95%	
1830- 1840	lg/wh. ss.: <5% gray mudstone: >95%	
1840-	gray mudstone:	

1850	100%	
1850-1860	lg/wh. ss.: 30%	
1860	gray mudstone: 70%	
1860-1870	lg/wh. ss.: 60%	
1870	gray mudstone: 40%	
1870-1880	lg/wh. ss.: 10%	
1880	gray mudstone: 90%	
1880-1890	gray mudstone: 100%	
1890-1900	lg/wh. ss.: 5%	
1900	gray mudstone: 95%	
1900-1910	lg/wh. ss.: 85%	
1910	gray mudstone: 15%	
1910-1920	red mudstone: <10% wh. ss.: 60% gray mudstone: 30%	wh. ss is 100% quartz and very fragmented->calcite cemented (?)
1920-1930	red mudstone: <10% wh. ss.: 60% gray mudstone: 30%	wh. ss is 100% quartz
1930-1940	wh. ss.: 95% gray mudstone: <5%	wh. ss is 100% quartz
1940-1950	wh. ss.: 95% gray mudstone: <5%	wh. ss is 100% quartz
1950-1960	red mudstone: 100%	slicks present
1960-1970	red mudstone: 100%	slicks present
1970-1980	red mudstone: 100%	slicks and ped structures present
1980-1990	lg/wh. ss.: 10% gray mudstone: 80% calc. mudstone: 10%	
1990-2000	gray mudstone: 95% calc. mudstone: 5%	
2000-2010	red mudstone: 5% br. sand.: 90% gray mudstone: 5%	
2010-2020	gray mudstone: 100%	significant portions of black debris->terrestrial om?
2020-2030	wh. ss.: 80% gray mudstone: 20%	wh. ss. is calcite cemented
2030-2040	br. sand: 85% wh. ss.: 5% gray mudstone: 5% micrite: 5%	wh. ss. is calcite cemented micrite may be incorporated into wh. ss.
2040-2050	br. sand: 90% gray mudstone: 5% calc. mudstone: 5%	wh. ss. is calcite cemented br. sand has opaque fragments (plagioclase?)
2050-2060	micrite: 100%	

2060-2070	calc. mudstone: 80% micrite: 20%	
2070-2080	calc. mudstone: 90% micrite: 10%	
2080-2090	calc. mudstone: 60% micrite: 40%	
2090-2100	calc. mudstone: 90% micrite: 10%	calcite produces sulfur smell during rxn with HCl
2100-2110	calc. mudstone: 80% micrite: 20%	
2110-2120	calc. mudstone: 60% micrite: 40%	calcite produces sulfur smell during rxn with HCl
2120-2130	calc. mudstone: 100%	calcite produces sulfur smell during rxn with HCl
2130-2140	calc. mudstone: 80% micrite: 20%	
2140-2150	calc. mudstone: 80% micrite: 20%	
2150-2160	calc. mudstone: 70% micrite: 30%	pyrite present
2160-2170	calc. mudstone: 70% micrite: 30%	
2170-2180	calc. mudstone: 90% micrite: 10%	calcite produces sulfur smell during rxn with HCl
2180-2190	calc. mudstone: 90% micrite: 10%	sparry replaced fossils present
2190-2200		missing section
2200-2210	calc. mudstone: 80% micrite: 20%	sparry replaced fossils present
2210-2220	calc. mudstone: 80% micrite: 20%	sparry replaced fossils present
2220-2230	calc. mudstone: 95% micrite: <5%	sparry replaced fossils present pyrite present

Appendix C.

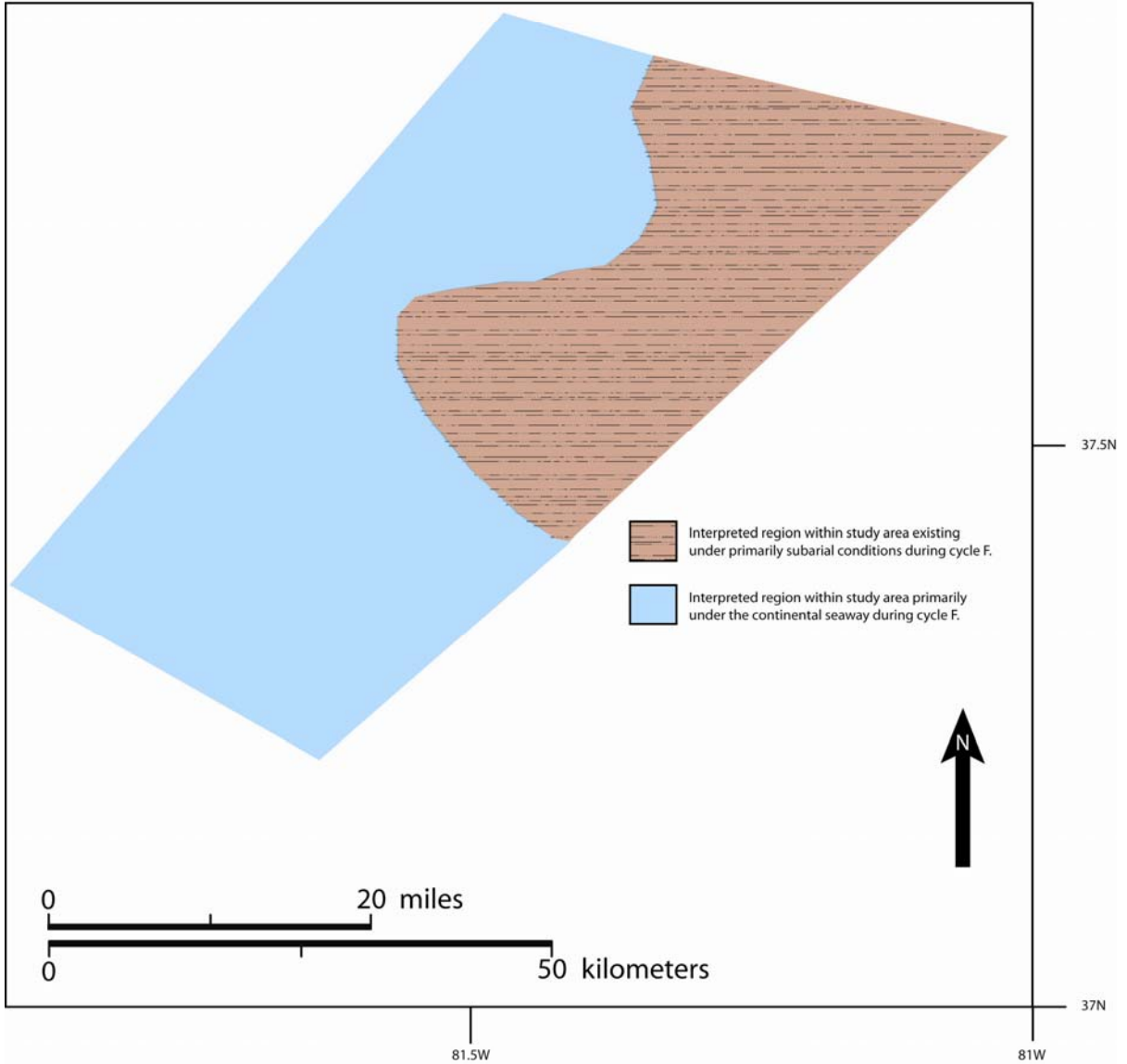
Facies distribution map of study interval: cycle F



Facies map of cycle F was generated by calculating regions that contained 60 %, or more of a particular facies, and showing those areas within the appropriate dashed lines. The rest of the facies map was interpreted using the best estimate of predominate facies in between zones of 60% facies concentrations.

Appendix D.

Paleoshorline during cycle F



A paleoshoreline map was generated using the boundary between coastal plain facies and marginal marine facies from facies map of cycle F.

Appendix E (description).

This figure displays the observed lithologies versus the wire-line log (when available), and shows the generated interpreted lithology. For a description of lithologies see table 1.

Appendix F-1 (description).

Outcrop A was measured along interstate 64, north of the New River in WV. A majority of the Stony Gap Sandstone measured is below the onramp to I-64. The top of this outcrop exposes a lacustrine limestone interpreted as the flooding surface separating cycle B and C, and the high energy facies above the sequence boundary in cycle C. Note the incised fluvial channel above the Stony Gap Sandstone and the incised valley fill of cycle C. The incision of these fluvial channels took advantage of the natural dynamics of the system during a period of allocyclically controlled, low accommodation. For latitude and longitude coordinates see data location table.

Appendix F-2 (description).

Outcrop B was measured along interstate 64, off of the Green Sulfur Springs exit in WV. For latitude and longitude coordinates see data location table. This outcrop exposes the a lacustrine limestone, interpreted as the flooding surface separating cycle B and C, and the high energy facies above the sequence boundary in cycle C. The incision of the fluvial channel above the incised valley fill of cycle C suggests that the natural dynamics of the system took advantage of the period of allocyclically controlled, low accommodation. For latitude and longitude coordinates see data location table.

Appendix F-3 (description).

Outcrop C was measured along interstate 64 north of outcrop B. For latitude and longitude coordinates see data location table. This outcrop exposes the contact between the Little Stone Gap Limestone and flood gleyed paleosols of the lower Hinton below. Note well developed paleosol at contact. For latitude and longitude coordinates see data location table.

Appendix F-4 (description).

Outcrop D exposes from the top of the Stony Gap Sandstone, to slightly above the flooding event associated with the boundary of cycle B and C. Note the multiple horizons on well developed paleosols and deep channel in the regressive phase of cycle B. For latitude and longitude coordinates see data location table.

Appendix G-1(description).

Cross-section 11 was generated using gamma ray wire-line logs and cuttings. Cross-section 11 trends NW/SE, and displays an overall progradation of depositional environments throughout the study interval. Eight regionally significant flooding surfaces and three localized flooding surfaces in the SW portion of the cross-section are identified. Two of the localized flooding surfaces are also identified in portions of cross-section 22, and are interpreted to have resulted from autogenic processes.

Appendix G-2(description).

Cross-section 11 was generated using gamma ray wire-line logs and cuttings. Cross-section 11 trends NW/SE, and displays an overall progradation of depositional environments throughout the study interval. Eight regionally significant flooding surfaces are identified.

Appendix G-3(description).

Cross-section 21 was generated using gamma ray wire-line logs, cuttings, and outcrop measurements. Cross-section 21 trends NE/SW, and displays an overall progradation of depositional environments throughout the study interval, but also shows that the greatest concentration of basinward facies occurs around the intersection with cross-section line 11. This is attributed to the presence of a paleotopographic low in that region. This figure does not show measured section D, which can be found correlated in cross-section in the appendix. Eight regionally significant flooding surfaces are identified. Identification of flooding surfaces in wire-line logs in the NE portion of the cross-section (and study interval) is very difficult due to the overwhelming presence of coastal plain facies.

Appendix G-4(description).

Cross-section 22 was generated using gamma ray wire-line logs, cuttings, and outcrop measurements. Cross-section 22 trends NE/SW, and displays an overall progradation of depositional environments throughout the study interval. Eight regionally significant flooding surfaces and two localized flooding surfaces in the SW portion of the cross-section are identified. The localized flooding surfaces are also identified in portions of cross-section 11, and are interpreted to have resulted from autogenic processes. Identification of flooding surfaces in wire-line logs in the NE portion of the cross-section (and study interval) is very difficult due to the overwhelming presence of coastal plain facies. The SW portion of x-section 22 displays the greatest magnitude of incision, at all four sequence boundaries, throughout the entire study interval. This is most likely due to a major fluvial system running through that location during the late Chesterian.